Early intervention in a mouse model of childhood obesity: effects on brown adipose tissue function

Jaclyn S. Lerea

Submitted in partial fulfillment of the
requirements for the degree of
Doctor of Philosophy
under the Executive Committee
of the Graduate School of Arts and Sciences

Columbia University
2016

ABSTRACT

Early intervention in a mouse model of childhood obesity: effects on brown adipose tissue function

Jaclyn S. Lerea

Due to the high childhood obesity rates within the United States, it is necessary to develop efficacious strategies to combat childhood obesity. To explore whether early intervention can produce lasting metabolic improvements, we used a mouse model of genetically-induced hypothalamic leptin resistance ($Lepr^{Nkx2.1}$knockout, hereby known as KO) that exhibits early-onset hyperphagia and obesity. We found that KO mice exhibit reduced capacity of the brown adipose tissue (as seen by disorganized mitochondrial structure). Brown adipose tissue capacity can be restored by paired-feeding in the peri-weaning period, leading to persistent improvements in later adiposity even after restriction ends. These studies lead us to investigate the maturation process of brown adipose tissue in the peri-weaning period. We found that brown adipose tissue expansion between 2 to 3 weeks of age is accompanied by a reduced thermogenic capacity in control mice, as determined by protein levels of uncoupling protein 1 and disorganization of the mitochondrial cristae. Thermogenic function was restored by 5 weeks of age, as demonstrated by a peak of uncoupling protein 1, in control mice but not KO mice. Paired-feeding of KO mice in the peri-weaning period rescued this peak at 5 weeks of age. These studies elucidate a critical period when brown adipose tissue expansion is followed by activation. The magnitude of brown adipose tissue activation at this time might be predictive of future obesity and metabolic rate, highlighting a potential therapeutic time window in which to intervene in pediatric obesity.

Table of Contents

LIST OF FIGURES ..... **vi**

LIST OF TABLES ..... **xi**

LIST OF ABBREVIATIONS ..... **xii**

DEDICATION ..... **xvii**

Chapter 1: Background Overview **1**

Part I: Epidemiology of Childhood Obesity **1**

Obesity prevalence within the United States 1

Etiology of childhood obesity 1

(i) "Catch-up growth" 2

(ii) Adiposity rebound 3

(iii) Peak height velocity 4

Part II: Current Efforts to Combat Pediatric Obesity in Humans **4**

Reason for implementing early intervention 4

Early intervention in humans 4

(i) Maternal control of food intake 4

(ii) Community-based intervention programs targeting pediatric obesity 5

(iii) Age as a predictor of success 7

(iv) Length of intervention 8

Summary for early intervention efforts in children 9

Part III: Interventions in Mouse Models of Obesity **9**

Existing mouse models of obesity 10

Litter size manipulation 10

Diet-induced obesity (DIO)-susceptible rats 10

Genetic models manipulating leptin signaling 11

(i) Global leptin/leptin receptor deficient models 12

(ii) Other models with targeted disruption of leptin-mediated pathways 12

(iii) CCK1-receptor knockout model 13

Summary of intervention in rodent models of early-onset obesity 14

Part IV: Thermogenesis: Brown Adipose Tissue Function and Regulation 17

Thermogenesis 17

Thermoregulation of brown adipose tissue 18

BAT development 19

(i) Growth factors and neuroendocrine control of BAT neonatal development 21

(ii) Leptin and BAT development 23

Central regulation of adult BAT 23

(i) Leptin effects on SNS control of BAT 26

Peripheral regulation of BAT activation 26

(i) Liver secreted factors 26

(ii) Heart-secreted BAT activating factors 28

(ii) BAT autocrine regulation of thermogenesis 28

Part V: Modulation of BAT Capacity and Activity 28

Thyroid hormone 30

Caloric restriction and cold acclimation 30

Rearing temperature 31

High fat diet 31

Part VI: BAT relevance in humans 32

Brown adipose tissue presence in humans 32

Brown adipose tissue in response to cold in humans 33

Age and BMI correlation to brown adipose tissue activity 34

Brown adipose tissue activity during the transition from childhood to adulthood 35

Part VII: Summary 36

REFERENCES 37

Chapter 2: Reducing Adiposity in a Critical Developmental Window has Lasting Benefits in Mice 55

Part I: Manuscript 55

Abstract 55

Introduction 56

Methods 58

Results 63

Discussion 70

Acknowledgements 74

Figures and Tables 75

Supplemental Figures 85

Part II: Concluding Remarks 90

REFERENCES 91

Chapter 3: Influences of BAT Development Start in the Peri-weaning Period 98

Part I: Current Data 98

Introduction 98

Methods 102

Results in progress 105

Discussion 111

Part II: Outstanding Issues 117

Part III: Future Outlook 118

Acknowledgements 118

Figures 119

Supplemental Figures 126

REFERENCES 131

Chapter 4: Concluding Remarks and Future Directions 136

Part I: Generalizability of lessons learned from rodent models of early intervention 136

Part II: Defining the developmental window to establish thermoregulatory circuits 137

Concluding Remarks 137

Future Directions 139

(i) Cold tolerance 139

(ii) Fasting-induced torpor 140

Part III: The role of IGF-1 in BAT development 141

Concluding Remarks 141

Future Directions 142

(i) Mitochondrial structure 142

(ii) Mitochondrial consolidation and activation initiated by paired-feeding 142

(iii) Mitochondrial structure vs. activation 143

Part IV: Concluding Remarks 143

Figures 145

REFERENCES 146

Appendix I: Organ Contribution to Increased Energy Expenditure in KO-PF Mice ..... .150

Pituitary and hypothalamus 151

White adipose tissue 153

Skeletal muscle 157

Liver 158

Brown adipose tissue 161

Plasma catecholamine levels 167

REFERENCES 167

Appendix II: The Epigastric Depot as a Source of Brown Adipose Tissue in Humans 168

Introduction 168

Methods 169

Results 170

Visceral adipose tissue 170

Epigastric adipose tissue 171

Infant adipose tissue 172

Lap band removal 172

Discrepancies in the data 172

Mitochondrial structure from adipose tissue 173

Discussion 173

Future Directions 174

Figures and Tables 175

REFERENCES 184

LIST OF FIGURES

Figure 1.1: Adiposity rebound curves 3

Figure 1.2: Thermogenic regulation of brown adipose tissue 20

Figure 1.3: Hypothalamic influences of sympathetic regulation of BAT 25

Figure 1.4: Peripheral activators of BAT 27

Figure 1.5: Brown adipose tissue capacity and activity 29

Figure 1.6: Peak of BAT activity in adolescents 35

Figure 2.1: Experimental groups 75

Figure 2.2: Decreased energy expenditure in adult Lep^{HYP}KOs (KO) following weight loss 76

Figure 2.3: Paired-feeding results in increased energy expenditure due to improved BAT function 77

Figure 2.4: Improvements in energy expenditure and BAT morphology persist into adulthood 79

Figure 2.5: Paired-feeding of KO mice at an early age results in persistent changes in body weight and adiposity. 81

Figure 2.6: Caloric restriction at any age improves BAT mitochondrial structure 82

Figure 2.7: There is a critical time period in which to intervene 83

Figure 2.8: Working hypothesis to explain temporal differences in the metabolic response of obese KO mice to weight loss 84

Supplemental Figure 2.1: Paired-feeding of female KO mice at an early age results in persistent changes in body weight and adiposity 85

Supplemental Figure 2.2: Lasting impact of paired-feeding on serum leptin levels. 86

Supplemental Figure 2.3: Improvements in glucose homeostasis during paired-feeding are not maintained 87

Supplemental Figure 2.4: Serum fT3 levels decrease with age 88

Supplemental Figure 2.5: No change in sympathetic marker tyrosine hydroxylase during paired-feeding 89

Figure 3.1: 2 to 3 weeks is a time of reduced BAT capacity in control mice 119

Figure 3.2: BAT expansion occurs from 2 to 3 weeks of age in control mice 120

Figure 3.3: Peak in BAT thermogenic and mitochondrial genes at 5 weeks of age in control mice. 121

Figure 3.4: Serum IGF-1 does not track with growth rate 122

Figure 3.5: BAT *Igf-1* is upregulated between 2-5 weeks of age in control mice 123

Figure 3.6: KO-AL mice do not exhibit a peak in BAT thermogenic function 124

Figure 3.7: Paired-feeding rescues thermogenic activation in BAT at 5 weeks of age . 125

Supplemental Figure 3.1: Unchanged mitochondrial related genes across different ages in control mice 126

Supplemental Figure 3.2: Serum T3 and BAT *deiodinase 2* expression levels are unchanged during the early peri-weaning period 127

Supplemental Figure 3.3: . Serum IGF-1 follows a similar pattern in female wild type and male AL-KO mice, but is blunted in KO-PF during the peri-weaning period 128

Supplemental Figure 3.4: 3 week control and KO mice have similar mitochondrial structure 129

Supplemental Figure 3.5: Reduced BAT *Mfn2* expression from 2 to 3 weeks of age ... 130

Figure 4.1: Fasting elicits a greater decrease in serum T3 in KO-AL than control mice 145

Appendix Figure 1.1: Pituitary *Dio2* and *TSHb* do not differ between PF and AL mice at 10 and 20 weeks of age 151

Appendix Figure 1.2: Hypothalamus gene expression at 10 and 20 week of age between paired-feeding and *ad libitum* KO does not differ 152

Appendix Figure 1.3: Increased energy expenditure is not due to browning of inguinal fat 154

Appendix Figure 1.4: Increased energy expenditure is not due to browning of gonadal fat 155

Appendix Figure 1.5: *Hsl* is WAT is not changed by paired-feeding 156

Appendix Figure 1.6: Skeletal muscle *Ucp3* (Uncoupling protein 3) does not contribute to increased energy expenditure in KO-PF mice at 10 weeks of age 157

Appendix Figure 1.7: Liver gene expression 159

Appendix Figure 1.8: Bile acid conversion pathway 160

Appendix Figure 1.9: BAT FGF21 signaling is not increased in PF-KO mice 162

Appendix Figure 1.10: Adrenergic receptors are unchanged in BAT of KO-AL versus KO-PF 163

Appendix Figure 1.11: BAT Natriuretic peptide receptors and bone morphogenic protein receptors are unchanged 164

Appendix Figure 1.12: BAT hormone sensitive lipase and lipoprotein lipase are unchanged in KO-AL versus KO-PF 165

Appendix Figure 1.13: A subset of mitochondrial genes are not upregulated in KO-PF mice compared to KO-AL 166

Appendix Figure 1.14: Norepinephrine is normalized at 10 weeks of age in KO-PF mice 167

Appendix Figure 2.1: Gene expression analysis of visceral adipose tissue from obese patients. 178

Appendix Figure 2.2: Gene expression analysis of visceral adipose tissue from a lean patient 179

Appendix Figure 2.3: Gene expression analysis of the falciform ligament from both an obese and lean patient 179

Appendix Figure 2.4: Gene expression analysis of the epigastric depot from obese patients 180

Appendix Figure 2.5: Intra-patient variation in gene expression analysis of epigastric tissue 181

Appendix Figure 2.6: Gene expression analysis of the adipose depots from infants 182

Appendix Figure 2.7: Gene expression from epigastric adipose depot after laparoscopic band removal 183

LIST OF TABLES

Table 1.1: Mouse models of early-onset obesity 16

Table 1.2: Intervention strategy on BAT capacity and activity in obese rodents with and without norepinephrine 32

Supplemental Table 2.1: qPCR primers..... 90

Appendix Table 2.1: Demographic of patient population 175

Appendix Table 2.2: Good correlation between gene expression and UCP1 IHC within samples 176

Appendix Table 2.3: Poor correlation between gene expression and UCP1 IHC within samples 177

LIST OF ABBREVIATIONS

(in alphabetical order)

α-MSH	α-melanocyte-stimulating hormone
AgRP	Agouti-related peptide
AL	Ad libitum
AR	Adiposity rebound
ARC	Arcuate nucleus
ARH	Arcuate nucleus of the hypothalamus
ATP	Adenosine triphosphate
β_3-AR	β_3-adrenergic receptor
BAT	Brown adipose tissue
BMI	Body mass index
BMI-SDS	Body mass index standard deviation score
BMP8B	Bone morphogenic protein 8b
BMP8BR	Bone morphogenic protein 8b receptor
BMR	Basal metabolic rate
cAMP	Cyclic adenosine monophosphate
cBAT	Classical BAT
CCK1	Cholecystokinin 1
CI	Confidence interval
CNS	Central nervous system
CON	Control

COXIV	Cytochrome C oxidase IV
CPT1b	Carnitine palmitoyltransferase 1b
CR	Caloric restriction
CT	Computed tomography
CYP	Cytochrome p450
D2KO	Deiodinase 2 knockout
DIO rat	Diet-induced obese rat
DIO1	Deiodinase 1
DIO2	Deiodinase 2
DMH	Dorsal medial hypothalamus
DR	Diet resistant
EE	Energy expenditure
EM	Electron microscopy
ERRα	Estrogen related receptor α
FDG	^{18}F-fluorodeoxyglucose
FGF	Fibroblast growth factor
fT3	Free Triiodothyronine
fT4	Free Thyroxine
gFAT	Gonadal fat
HFD	High fat diet
HPT axis	hypothalamic-pituitary-thyroid axis
HSL	Hormone sensitive lipase
iBAT	interscapular brown adipose tissue

ICV	Intracerebroventricular
iFAT	Inguinal fat
IGF-1	Insulin-like growth factor 1
IGF-1R	Insulin-like growth factor 1 receptor
IGF-2	Insulin-like growth factor 2
IGFBP	Insulin-like growth factor binding protein
IHC	Immunohistochemistry
IR	Insulin receptor
KLB	β-Klotho
KO	Knockout
Lepr	Leptin receptor
LH	Lateral hypothalamus
MAPK	Mitogen-activated protein kinase
MC3R	Melanocortin-3 receptor
MC4R	Melanocortin-4 receptor
MFN2	Mitofusin 2
MYF5	Myogenic factor 5
NE	Norepinephrine
NGF	Nerve growth factor
NP	Natriuretic peptide
NPR	Natriuretic peptide receptor
NPY	Neuropeptide Y
NTS	Nucleus tractus Solitarii

OLETF rat	Otsuka Long-Evans Tokushima Fatty rat
OR	Odds ratio
P	Postnatal day
PET	Positron emission tomography
PF	Pair-fed
PGC1α	Peroxisome proliferator-activated receptor gamma coactivator 1 alpha
PHV	Peak height velocity
PKA	Protein kinase A
POA	Preoptic area
POMC	Pro-opiomelanocortin
PRDM16	PR domain containing 16
PRLR	Prolactin receptor
PVH	Paraventricular nucleus of the hypothalamus
REE	Resting energy expenditure
rRPA	Rostral raphe pallidus
SNS	Sympathetic nervous system
STAT3	Signal transducer and activator of transcription 3
$t_{1/2}$	Half-life
T3	Triiodothyronine
T4	Thyroxine
TAM	Tamoxifen
TH	Tyrosine hydroxylase
UCP1	Uncoupling protein 1

UCP3	Uncoupling protein 3
VMH	Ventral medial nucleus of the hypothalamus
VTA	Ventral tegmental area
WAT	White adipose tissue

DEDICATION

This work is dedicated to my loving family. To my dad, Ken Lerea, who has always been supportive of everything I do and who has been instrumental to my success. To my fiancé, Bradford Antes, who has given me continuous support throughout this entire process.

This work is dedicated in loving memory of my mother, Connie Lerea.

CHAPTER 1: Background Overview

Part I: Epidemiology of Childhood Obesity

Obesity prevalence within the United States

Based on the 2011-2012 census, 34.9% of the adult population is obese, with over 66% of the population being either obese or overweight (1). The high prevalence of obesity during this timeframe is not limited to adults, as roughly 17% of children and adolescents are obese (2). The high prevalence of childhood obesity may underlie the increased rates of early-onset obesity-associated comorbidities, such as type 2 diabetes, pulmonary and cardiovascular disorders, gastrointestinal disorders, and metabolic syndrome (3-7). In an effort to battle the rise in childhood obesity and early-onset comorbidities, there has been an increase in obesity prevention programs geared towards adolescents. If treated early, the metabolic abnormalities (i.e. blood pressure and lipid profiles) can resolve (5, 8) and result in long lasting improvements.

Etiology of childhood obesity

In order to identify the age at which intervention programs would be most effective, it is helpful to first consider when patterns of increased body weight in childhood might be established. One way to approach this issue is to determine the age at which increased body mass index (BMI) and body weight during childhood are highly predictive of later adiposity. Obesity at a very young age (1-2 years of age) is not predictive of becoming obese in young adulthood (odds ratio (OR) of 1.3, 95% confidence interval (CI) 0.6-3.0) (9), whereas children who are obese at 5 years of age are 4-5 times more likely to maintain their obesity into eighth grade (10, 11). If obese by 10-

14 years of age, there is a 75% prevalence of staying obese into young adulthood (21-29 years of age) (OR of 28.3, CI 15.0-53.5) (9). These findings support the idea that increased BMI during early childhood leads to an increase in relative risk for obesity in adulthood (9, 12).

While body weight during childhood is increasingly correlated with adult obesity, a high birth weight *per se* is not predictive of obesity in adulthood (9, 13, 14), as a heavier birth weight tracks with increased lean mass as opposed to fat mass (13). Similarly, body weight in infants 1-2 years old does not correlate with later adiposity (9, 12). However, three distinct patterns of growth in early childhood have been linked to later obesity risk: (i) rapid "catch-up" growth (13), (ii) early adiposity rebound (AR) (15), and (iii) the age of onset of peak height velocity (PHV) (7).

(i) "Catch-up" growth. This pattern of growth refers to the rapid weight gain after birth that often occurs in small for gestational age babies that received insufficient nutrition during fetal development (13, 16). This rapid weight gain within the first 1-2 years of life, as opposed to low birth weight *per se*, appears to be associated with later obesity (13, 16, 17). These findings are supported by outcomes from several studies demonstrating that increased "catch-up" growth within the first few months of age is correlated with later adiposity (18-20). "Catch-up" growth within the first year after birth coincides with the normal period of rapid adipose tissue expansion, which promotes increased BMI (21). The rate of "catch-up" growth is also inversely associated with rates of energy expenditure (EE) in infants born to obese mothers (22), raising the possibility that early deficits in EE can contribute to later body weight gain.

(ii) Adiposity rebound. After the first year of life, the rate of adipose tissue deposition declines as the child continues to grow in height, leading to steady reductions in BMI over the next several years (21). The point at which body fat begins to increase again is called the adiposity rebound (AR) (21, 23, 24) (AR is illustrated in Figure 1.1). The average AR occurs at 6 years of age (21, 23, 24). Children with an AR at 3 years of age are more likely to be obese by 21 years than those with an AR around 6 years of age (24). This correlation has been shown to be independent of parental obesity and BMI at the onset of AR (23). It is important to note that a child with increased BMI and a later AR will most likely stay obese as an adult (24), however most children with an early AR tend to have a normal BMI to start, and begin to increase body fat after AR begins (24). Early AR is associated with increased rate of maturity (24), and therefore "catch-up growth" and timing of AR are not necessarily related.

Figure 1.1. Adiposity Rebound Curves. X axis represents BMI (kg/m^2). Solid line represents early AR, dashed line represents late AR. AR; Adiposity rebound. Graph adapted from information derived from Rolland-Cachera MF, Deheeger M, Maillot M, Bellisle F. *Int J Obes*. (2006). Reference (24).

(iii) Peak height velocity (PHV). PHV is defined as the time period of maximal growth rate (25). PHV occurs on average at 11.5 years of age in girls and 13.5 years of age in boys (26). Early-onset PHV is correlated with increased BMI and central adiposity (27), as well as metabolic syndrome in boys (7). Early AR is often associated with an earlier PHV (28). Therefore, obesity risk associated with PHV could also reflect earlier growth-related processes. Blunting the rapid increase in body weight gain during AR represents a promising target for childhood obesity interventions (16, 20).

Part II: Current Efforts to Combat Pediatric Obesity in Humans

Reason for implementing early intervention

Weight loss is associated with changes in sympathetic nervous system (SNS) tone (29), subsequently driving the decreased EE that promotes weight regain (29, 30). This phenomenon is also seen in adolescence, where lifestyle intervention results in a similar compensatory metabolic phenotype as seen in adults (31-33). These observations support the idea that body fat baselines are established at an early age, prior to puberty. Thus, interventions in teens are likely to face the same obstacles as in adults.

Early intervention in humans

Efforts to combat childhood obesity are increasingly focused on younger ages. Results from several different types of intervention are summarized below.

(i) Maternal control of food intake. One of the simplest types of interventions is when a mother restricts the amount of food she will give to her young child during the first few years of life. Maternal restriction of solid food during infancy, as well as restriction between 3-5 years of age, can influence later weight gain in females, as

children become disinhibited (34, 35) (as measured by food consumption in the absence of an appetite (35, 36)). The level of disinhibition is correlated with the magnitude of restriction (36). Conversely, pressure to eat more at this young age was associated with restrictive eating behavior later in life, resulting in reduced body weight (34). Therefore, strategies to combat childhood obesity in young girls that involve caloric restriction may backfire due to undesired effects on the development of brain circuits regulating motivated aspects of feeding behavior.

(ii) Community-based intervention programs targeting pediatric obesity. A growing number of programs involving school-based, community-based and home-based intervention have been implemented to reduce the prevalence of childhood obesity (37-39). These programs have included increased physical activity, dietary restriction, and behavioral counseling/education, alone or in combination (40). The High Five for Kids and LEAP 2 randomized control trails evaluated behavioral modification obesity prevention programs, using educational material given to the family and children and/or motivational interviewing of the family members, for children 2-10 years of age across different clinical practice groups (41, 42). These intervention trials resulted in no improvements in BMI, as the physical activity amount and nutritional choices did not change (41, 42). This is reflected in the fact that 77.2% of children in the intervention group remained obese/overweight 12 months post-intervention in the LEAP 2 trial compared to the 82.6% of the control group remaining obese (difference of -5.4%, 95% CI; -15.5, 4.6. p=.29) (42). Similarly, the High Five intervention trial participants only had changes in BMI of -0.21 kg/m^2 (95% CI; -0.05, 0.07. p=.15) compared to the control group 12 months post-intervention (41). When stratified by gender, there was a modest,

but significant difference in BMI in young girls (-.38; 95% CI; -0.73, -0.03. *p*=.03), which could be an artifact of overall family awareness of body weight or healthier lifestyles leading to further adherence to intervention (41). These findings suggest that education alone is not enough to result in improvements in obesity related outcomes.

One meta-analysis of intervention programs implemented in children between the ages of 5 and 16 years old showed that physical activity impacted percent body fat (-.4%; 95% CI; -0.7, -0.1. *p*=.05, effect size; 9/369) without changes in BMI (43). Other meta-analyses of physical activity intervention programs yielded inconsistent findings within the cohorts tested (-0.5%; 95% CI; -0.7, -0.3. *p*=.81, effect size 6/358) (44). Differences could be due to the discrepancies in amount of physical activity, as there is a high correlation between the amount of exercise per week and the reductions in percent body fat (43). Although it seems that physical activity could reduce adiposity during this time window in overweight and obese children, the evidence for long-term improvements in body weight, BMI, and central obesity in adulthood has been inconclusive (43).

A meta-analysis of interventions involving only caloric restriction showed that it is ineffective in preventing future obesity (BMI change of -0.22; 95% CI -0.56, 0.22, NS) (44). Combination therapy of physical activity and caloric intervention, however, resulted in BMI reduction, especially when there was parental involvement (BMI change of -0.64; 95% CI -0.88, -0.39, *p* value not reported) (44). This is in contrast with a meta-analysis performed by Peirson *et al.* (2015) who found that classroom-based intervention geared towards individual children resulted in significant changes in BMI compared to those with parental involvement (*p*=.007 between the two groups) (individual focus BMI change -0.9; 95% CI -1.27,-0.53. *p*<.001; Family focus BMI change -0.34; 95% CI -0.52,

-0.16. p= <.001), yet there was still a significance in both subgroups of intervention type (8). Regardless of the individual versus family focus, Peirson *et al.* (2015) is in agreement with previous meta-analysis results, reporting that reductions in BMI as a result of exercise and diet (-1.09; 95% CI -1.84,-0.34. p<.001) are greater than when compared to diet (-0.36; 95% CI -0.65, -0.06. p=.27) and exercise (-.43; 95% CI -0.65,-0.21. p=N/A) alone (8). Unfortunately, many of these studies did not look at follow-up beyond the intervention. Given the increased cost of healthcare for childhood obesity, it is important to determine the most cost-effective treatment (45). Even reductions of 1% in BMI during childhood can make an impact on overall healthcare costs (46).

(iii) Age as a predictor of success. Several groups examined whether age is a predictor of success in BMI reduction following weight loss intervention (47, 48). Although there was no significant correlation of age at which intervention is implemented and success of intervention, there was a trend towards increased effectiveness when intervention was implemented in children 8-10 years of age or younger (44, 49, 50). In a separate study in 1291 children ranging from 8.5-13.5 years of age, it was found that extremely obese children who were less than 10 years of age had a greater BMI standard deviation score (SDS) (adjusted for child's age and gender) (BMI-SDS) reduction (-0.24 ± 0.38) than those over 10 years of age (-0.05 ± 0.30), which lasted 1 year post-intervention (49). Similarly, an outpatient lifestyle intervention program conducted in 663 obese children aged 4-16 years old found that intervention in younger obese children resulted in the greatest reduction in BMI-SDS (50). Children 4-7 years old had the highest rate of BMI-SDS reduction (-0.44±.04), followed by 8-10 year olds (-0.37±.05) and 11-12 year olds (-0.26±.05) during intervention (50). However, 8-10 year olds had

the lowest reduction in BMI-SDS 4 years post-intervention (-0.30±.05) compared to 4-7 year olds (-0.50±.04) or 11-12 year olds (-.038±.05) (50). This discrepancy can be explained by the onset of puberty that occurs within this age group (50). The poorest prognosis for intervention success was in children aged 13-16 years old (-0.21±.06 immediately post-intervention, -0.27±.05 4 years post-intervention) (50), consistent with the fact that obesity at 10-14 years of age is associated with increased relative risk of becoming obese in adulthood (9).

Further supporting the idea of a critical time window for intervention around 10 years of age was a study conducted in Sweden using a one-year intervention approach in children 8-13 years of age. The study found that the one-year intervention program resulted in differential effects on weight maintenance; a subset of children regained the lost weight while others did not (51). Weight maintenance versus regain was associated with changes in thyroid hormone (51), providing a possible biomarker of weight loss success in children. Unfortunately, these studies did not look at EE changes in the two subgroups, nor did they correlate the successful outcomes to age. Therefore, it seems that intervention implemented before 10 years of age produces promising results in obesity related outcomes, whereas intervention later than 10 years of age does not produce significant effects. Further work is needed to determine whether age of intervention truly correlates with sustained improvements in obesity related outcomes.

(iv) Length of intervention. Several meta-analyses examined the impact of the length of intervention and its efficacy on obesity outcomes. Interventions lasting 3 months did not produce sustained reductions in BMI 9 months later (8), while those lasting more than 4 months were more promising (39, 47). In a study examining longer-

term endpoints, year-long interventions resulted in better outcomes 4 years later (50). Because most interventions are implemented for less than 6 months (8), inadequate duration of these programs could contribute to their limited efficacy.

Summary of early intervention efforts in children

The wide variety of programs designed to combat childhood obesity have not produced significant changes in the prevalence of adolescent nor adult obesity rates within the cohorts tested (2, 39). The decreased efficacy of these programs suggests that current efforts implemented for obesity prevention are not working because they are either being implemented at the wrong age, in the wrong way, or for the wrong duration of time.

Part III: Intervention in Mouse Models of Obesity

Thus far, interventions in mouse models of obesity have been focused on intervention during adulthood. Food restriction in adult rats has been shown to result in decreased EE driven by reductions in norepinephrine (NE) output, the primary neurotransmitter of the SNS (52-54). Therefore, reduced EE drives weight regain in food-restricted adult rodents (52-55), similar to what is seen in adult humans. Caloric restriction in young animals, however, primarily impacts linear growth, leading to reduced tissue deposition as opposed to altered EE (55). Although reductions in growth may not be desirable, this provides evidence that intervention of increased body weight elicits differential age-dependent responses.

Existing mouse models of obesity

Several groups have developed rodent models of early-onset obesity to assess the influence of age or means of lifestyle intervention (via both caloric restriction and/or exercise) on obesity-related outcomes.

1. Litter size manipulation. Overnutrition during the suckling period in rats, achieved by reducing the size of the litter, programs lasting increases in food intake and body weight (56). Caloric restriction from 3-12 weeks of age in rats reared in a small litter size produced long lasting improvements in adult body weight (56). However, this effect was lost when caloric restriction was implemented from only 3-6 weeks or 9-12 weeks of age (56). Moreover, caloric restriction from 9-12 weeks of age resulted in rebound hyperphagia in response to resumption of *ad libitum* feeding, leading to increased weight gain (56). This study provides evidence that there is a developmental window in the postnatal period where prolonged caloric restriction can produce beneficial outcomes. However, the major limitation to this approach is that the effect size is often modest, and in mice, differences in body weight tend to diminish over time.

2. Diet-induced obesity (DIO)-susceptible rats. Barry Levin's lab generated strains of rats that are preferentially sensitive or resistant to weight gain on a high fat diet (HFD). In response to HFD feeding, some Sprague-Dawley rats gained an abundance of weight (DIO-sensitive), while others in the same cohort did not (DIO-resistant, DR) (57). By intercrossing DIO-sensitive and DR rats, they produced strains that reliably exhibited a pre-programmed response to HFD. After many generations of intercrosses, DIO-

sensitive rats exhibited normal body weights on chow, but would rapidly gain weight when fed a HFD (58, 59). The weight gain exhibited by the DIO-susceptible rats was a result of increased caloric intake compared to the DR rats (58).

The effects of early intervention from weaning (at 3 weeks of age) involving caloric restriction vs. exercise were compared. The impact of restricting the caloric intake of HFD-fed DIO-susceptible rats by 15% from 3-9 weeks of age did not have any lasting impact on weight gain when rats were allowed to resume *ad libitum* feeding (60). Conversely, 3 weeks of post-weaning exercise resulted in reduced body weight and adiposity of DIO-susceptible rats even 10 weeks after the cessation of exercise, largely due to the lack of caloric compensation that usually accompanies exercise (61). Early exercise intervention was also reported to increase leptin sensitivity in the hypothalamus, while caloric restriction did not (61). While this model is useful in studying prevention of adult obesity, it is not a model for intervention methods of early-onset obesity as mice become obese later. Additionally, continuous HFD feeding come with developmental consequences, such as permanent changes in the circuits regulating the neuronal reward pathway (62).

3. Genetic models manipulating leptin signaling. Genetics manipulations have also produced early-onset obesity in rodent models. The best-studied examples of genetically-induced obesity involve deficits in leptin signaling. Leptin, a hormone found in proportional levels to adipose tissue (63) (as reviewed in (64)), is secreted by adipose tissue and regulates fat deposition and energy homeostasis (63-65).

(i) Global leptin/leptin receptor deficient models. Leptin is known to regulate energy homeostasis through its effects on metabolism and appetite, and models of functional leptin receptor deficiencies (*db/db* mice/Zucker (*fa/fa)* rats) and leptin protein deficiencies (*ob/ob* mice) are hyperphagic and hypometabolic, resulting in increased fat deposition (66-68). Paired-feeding of *db/db* mice to the intake of controls has been shown to lead to decreased body weight compared to never-restricted *db/db,* yet their body weight remained elevated compared to lean controls (69). Similarly, early caloric restriction in Zucker (*fa/fa*) rats reduced body weight, but adiposity levels remained comparable to obese Zucker rats that had never been restricted (70). In addition, *ob/ob* mice preferentially maintained increased adiposity in the face of reduced body weight when subjected to caloric restriction (71-74). Taken together, these findings suggest that models involving global leptin signaling deficiency are not suitable for studying early intervention.

(ii) Other models with targeted disruption of leptin-mediated pathways. The action of leptin on energy homeostasis is regulated through signal transducer and activator of transcription 3 (*Stat3*) (75). A mutation in the leptin receptor (Lepr) isoform b in which tyrosine 1138, a docking site necessary for *Stat3* activation, is replaced with a serine residue (*s/s* mouse) leads to robust early-onset obesity caused by a dysregulation of metabolic control (75). Paired-feeding of *s/s* mice from 3-8 weeks of age failed to correct the increased fat deposition in these mice, regardless of a decreased body weight (69).

Pro-opiomelanocortin (POMC) processing produces signal through the melanocortin-4 receptor (MC4R) to modulate energy homeostasis. While global deficiencies in both POMC and MC4R cause obesity, the onset of obesity is delayed (76-

79). In contrast to the MC4R knockout (KO) mice, mice lacking another melanocortin receptor (MC3R) are only mildly obese and the onset of obesity is further delayed (80). Malcolm Lowe's group demonstrated that knocking out the POMC in the arcuate nucleus of the hypothalamus (ARH) (arc*Pomc*$^{-/-}$) caused hyperphagia and body weight gain, with noticeable obesity at 5 weeks of age (81). In arc*Pomc*$^{-/-}$ mice, rescue of *Pomc* expression with a tamoxifen (TAM)-inducible *cre* recombinase normalized food intake at any age, but the effect on body weight was less effective when induced after postnatal day (P)60, and even less effective when induced after P180 (81). Paired-feeding before the induction of TAM resulted in a full rescue of body weight when POMC in the ARH was restored, regardless of age at which restoration occurred (81). These data support a role for early intervention in the peri-weaning period in which body weight baselines are being established.

(iii) CCK1-receptor knockout model. There are other hormonal factors aside from leptin that regulate food intake and body weight. For example, cholecystokinin-1 (CCK1) is another satiety factor. The Otsuka Long-Evans Tokushima Fatty (OLETF) rat lacks the CCK1-receptor resulting in hyperphagia starting at birth, leading to obesity (82-86). Interestingly, the CCK1-receptor KO mouse model does not exhibit hyperphagia and does not become obese (87) and thus is not a model used for obesity. The difference between the mouse and rat model of CCK1-receptor deficiency could be attributed to the difference in CCK1-receptor distribution, specifically in the brain (88).

Similar to the DIO-susceptible model, acute exercise in male OLETF rats from weaning until P45 resulted in long-lasting improvements in body weight and adiposity, even 45 days after their running wheel was locked (wheel-lock), without compensatory

increased food intake (86). Moreover, exercise implemented at a later age and longer period of time (8 -14 weeks of age) also produced long lasting effects on fat mass in male OLETF rats (89). Female OLETF rats did not respond to exercise in the same way, suggesting a sexual dimorphic role of exercise in attenuation of obesity in the OLETF model (86). However, differing from the DIO rat model, acute early paired-feeding from P23-P45 resulted in long lasting reductions of fat mass in male OLETF rats (85). Similar to what was seen in response to exercise, there was a sexual dimorphic response to early caloric restriction, as female OLETF rats did not have long-lasting improvements in fat mass in response to acute early food restriction (84). Interestingly, food intake was still permanently altered in these female mice, suggesting CCK1-receptor involvement in body weight might be a result of other mechanisms besides food intake in females (84). Caloric restriction in the male OLETF rat resulted in normalized NPY and POMC in the arcuate nucleus (ARC), which increases leptin sensitivity (90). These changes might persist once early caloric restriction ends, contributing to the long-term reductions in food intake once paired-feeding ends (84, 85). Consistent with observations in humans, this study highlights the need to evaluate the impacts of early intervention in both genders.

Summary of intervention in rodent models of early-onset obesity (Table 1.1)

Of the limited number of early-onset obesity rodent models, few of these models are suitable for early intervention studies. The DIO mouse and rat (58, 91, 92), POMC KO (77, 79), and MC4R KO (76, 78) models do not become obese until after 5 weeks of age, too late to study early intervention. Weight-reduced leptin deficient models do not decrease adiposity in the same way as other models (69-74). Additionally, some models

display a sexual dimorphic response to caloric restriction, such is the case in the OLETF rat model (84, 85). Similar to the OLETF male rats, early intervention in rats reared in a small litter size resulted in persistent reductions in body weight gain (56). Taken together, further work is needed to determine the best model and method for early intervention studies.

Early exercise can also influence future body weight gain by influencing energy expenditure, while simultaneously affecting leptin sensitivity. Subsequently, early exercise has been shown to lead to changes in metabolic rate without compensatory increases in food intake in both the OLETF and DIO-susceptible rats. Although Schroeder *et al.* (2010) documented changes in food intake of the OLETF rat in response to caloric restriction and/or exercise, the significance in food intake is only present at certain time points and not across the recovery period (85, 86). Therefore, the changes seen in body weight post-intervention might be caused by changes in EE as opposed to reprogramming of food intake. Long-lasting changes in thermogenesis leading to increased EE have not yet been looked at as mechanisms of prolonged weight loss interventions, yet there has been supporting evidence that early weight gain results in long lasting reductions in thermogenesis resulting from abnormalities in brown adipose tissue (BAT) (93). Further work is needed in order to elucidate how body weight baselines become established, and whether it can be regulated by changes in thermogenic baselines.

Rodent model	Onset of obesity	Early caloric intervention of models of early-onset obesity
DIO-Susceptible rat and DIO mouse	Body weight increased >5 weeks on chow; % Body fat; NS on chow (58, 91,92)	
Mc4r KO mouse	Obesity starts >5 weeks (76, 78)	
Pomc KO mouse	Obesity starts >5 weeks (77, 79)	
OLETF mouse	Not obese (87)	
ob/ob mouse	Obese by 3 weeks (66)	Predisposition to keep increased % body fat in the face of weight loss (71-74)
db/db mouse, Zucker *fa/fa* rat	Obese by 3 weeks (67, 68)	Zucker; Increase body fat (70) Db/db; Increased body weight compared to controls when pair-fed (69).
s/s mouse	Obese by 3 weeks (75)	Increased fat deposition in the face of decreased BW (69)
OLETF Rat	Obese by 3 weeks (85, 86)	Reduced fat mass Absence of compensatory hyperphagia (85)
Small Litter Size manipulation	Obese by 3 weeks (56, 93)	Long-lasting improvements in body weight (56)

Table 1.1: Mouse models of early-onset obesity. DIO-susceptible, *Mc4r* KO, *Pomc* KO, and OLETF mouse models become obese too late to be considered for models of childhood obesity (gray shaded boxes). *Ob/ob, db/db, s/s* mice, and Zucker *fa/fa* rats, do not respond normally to caloric restriction (red font). The OLETF rat and the small litter size manipulation are two models that succeed in long-term reductions of adiposity in response to caloric restriction (Light blue shaded boxes). BW (Body weight). DIO (Diet-induced obese). *Pomc*; Pro-opiomelanocortin. *Mc3r/Mc4r*; Melanocortin-3/4 receptor. OLETF; Otsuka Long-Evans Tokushima Fatty.

Part IV: Thermogenesis: Brown Adipose Tissue Function and Regulation

Thermogenesis

Adaptive thermogenesis is the protective mechanism by which an organism regulates body temperature and energy balance in response to external temperature (i.e. cold) and diet (94-97). The two main types of thermogenic mechanisms are shivering, controlled by the skeletal muscle, and non-shivering (adaptive) thermogenesis, controlled primarily through the BAT (98). Additionally, diet-induced thermogenesis (via diet action onto BAT) and behavioral thermogenesis (huddling of young animals) contribute to thermogenesis of a rodent.

BAT is the main thermogenic organ in the rodent (93), and it is characterized by being mitochondria-rich and multilocular in structure (containing an abundance of small lipid droplets) (93, 99, 100), making it distinct from white adipose tissue (WAT), which is unilocular with few mitochondria (100). BAT is developmentally distinct from WAT and is derived from the myogenic precursor myogenic factor 5 (*Myf5*), and the upregulation of PR domain containing 16 (*Prdm16*) expression differentiates *Myf5* containing pre-adipocytes to BAT instead of muscle (100-102). The mitochondrion of the BAT is the key site of its thermogenic action (94, 103) via uncoupling protein 1 (UCP1) located on the cristae (99, 103-106). UCP1 uncouples the proton gradient from adenosine triphosphate (ATP) production to release energy in the form of heat (94, 103), and is essential for cold-induced non-shivering thermogenesis (107, 108). Genetic models of obesity have impaired mitochondrial structure and function, resulting in impaired thermogenesis (109), thus making them cold intolerant (109). Small litter size, known to drive increased body weight gain in rodents, also leads to reductions in

thermogenesis as seen by reduced UCP1 in response to cold (93). Therefore, obesity is partially mediated by an inability to properly regulate adaptive thermogenesis.

Thermoregulation of brown adipose (Figure 1.2)

The SNS activates BAT through secretion of NE, which acts through the β_3-adrenergic receptor (β_3-AR) to upregulate UCP1 via a cyclic adenosine monophosphate/protein kinase A (cAMP-PKA)-dependent mechanism (97, 110). Knocking out β-adrenergic receptors leads to a reduced thermogenic effect of NE in rodents (101). In UCP1 KO mice, NE is unable to elicit a thermogenic response, suggesting the effect of NE on non-shivering thermogenesis is through a UCP1-dependent pathway (97, 108). Moreover, inactivation of β-hydroxylase to diminish endogenous epinephrine and NE results in mice that are cold intolerant and unable to mount a UCP1 response during cold exposure (111), providing evidence that cold-induced thermogenesis is dependent on NE-induced UCP1 activation (111). Cold and diet-induced thermogenesis activate BAT thermogenesis via similar mechanisms through the SNS in the rodent (112).

Thyroid hormone is necessary for BAT thermogenic function, and acts synergistically with the SNS to upregulate *Ucp1* gene expression (113, 114). Hypothyroid rats are cold intolerant, which can be rescued upon thyroid hormone treatment (115). Additionally, hypothyroid rats are unable to mount a thermogenic response to NE (113, 114) highlighting the permissive role of thyroid hormone on SNS-induced thermogenesis. Thyroxine (T4) is transported into the brown adipocyte and is converted into the active thyroid hormone, 3,3',5-triiodothyronine (T3), by deiodinase 2

(DIO2) (113). NE stimulates the cAMP-PKA pathway to lead to increased *Dio2* upregulation and the conversion of T4 to T3 (116). T3, either produced by DIO2 or transported into BAT from serum, can influence mitochondrial *Ucp1* expression, as well as the production of cAMP (114). It has been shown that brown adipocytes isolated from hypothyroid rats had reduced capacity to generate NE-mediated cAMP compared to euthyroid rats (114). This further supports the idea that that there is an interplay between thyroid hormones and the SNS in order to produce maximal BAT activation. Additionally, mice lacking DIO2 (D2KO) become obese at thermoneutrality but not at room temperature (113, 117). The lack of obesity at room temperature in D2KO mice is a result of compensatory upregulation of SNS tone onto BAT, which is then blunted at thermoneutral conditions (113).

BAT development

BAT is highly vascularized and innervated (93, 94, 97, 99), and its thermogenic output is regulated by the SNS (94, 97, 101, 118). Formation of the BAT depot does not rely on SNS activity, as BAT is fully formed in neonates before SNS activity is detected (119-121). At birth, the mitochondria of the BAT have dense lipid filled inclusions that disappear within 1-2 days (122). There is a rise in postnatal *Ucp1* expression in BAT within the first 24 hours of life (123), which coincides with the disappearance of lipid filled inclusions of the mitochondria. Postnatal induction of *Ucp1* is abolished when neonates are reared in thermoneutral conditions, indicating that the early *Ucp1* upregulation in neonates is in response to the cold stress of the environment (123). In

sheep, it has been found that there is a surge in NE around the time of birth, which could influence BAT activation further (124).

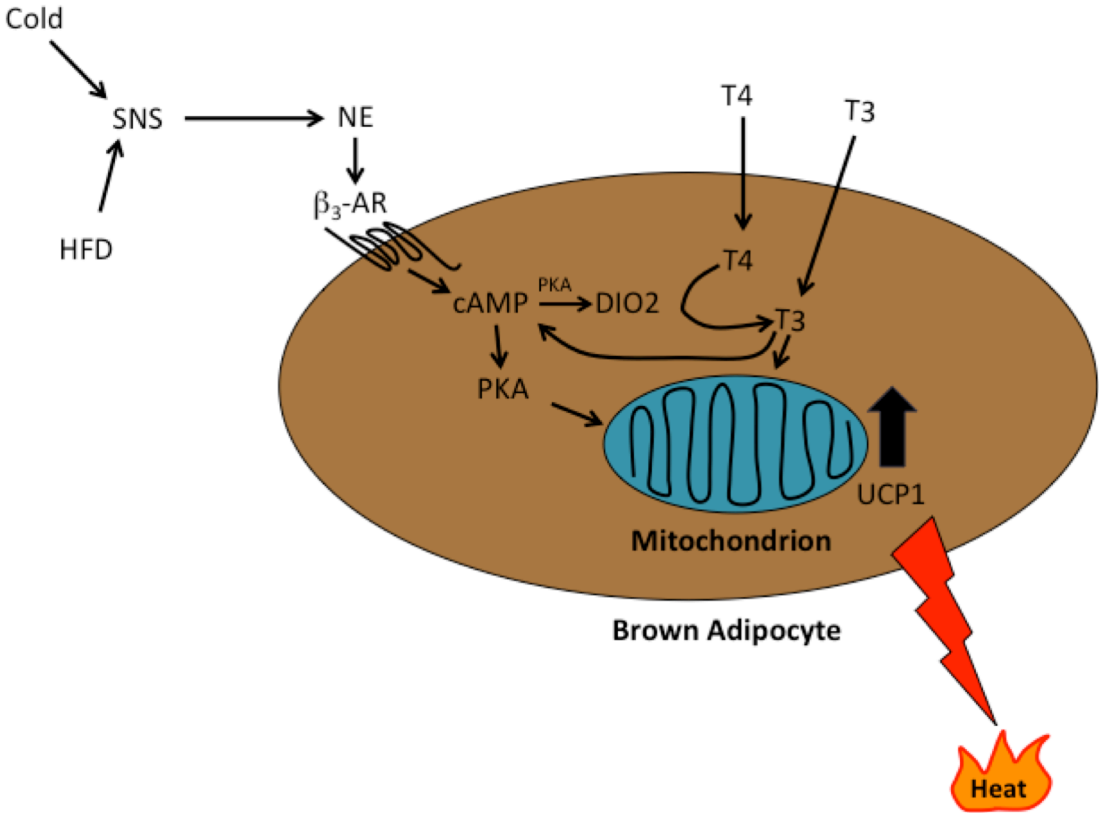

Figure 1.2. Thermogenic regulation of brown adipose tissue. HFD and cold stimulate the SNS to release NE. NE acts on the β-AR receptors to activate mitochondrial UCP1 in a cAMP-PKA-dependent mechanism. Additionally, T4 can be transported into BAT. cAMP can upregulate *Dio2* to convert T4 into its active form, T3, to influence UCP1. Upregulation of *Ucp1* releases energy in the form of heat. T3 can also contribute to the generation of cAMP. Abbreviations: HFD; high fat diet. NE; norepinephrine. β_3-AR; β_3-adrenergic receptor. cAMP; cyclic adenosine monophosphate. PKA; protein kinase A. T4; Thyroxine. T3; 3,3',5-Triiodothyronine. DIO2; deiodinase 2. UCP1; Uncoupling protein 1. Adapted from de Jesus LA, Carvalho SD, Ribeiro MO, Schneider M, Kim SW, Harney JW, et al. *J Clin Invest*. (2001). Reference (211).

BAT is innervated by the SNS at two different locations, the parenchyma and the blood vessels (120, 125). Immunosympathectomy (preventing sympathetic outgrowth) of

rodent BAT from P0-5 does not eliminate parenchymal innervation of BAT, indicating that BAT SNS innervation into the parenchyma is developed prior to birth (120). Outgrowth of projections from the sympathetic ganglia onto the BAT depot can be detected at P2 (120). Sympathetic projections penetrate into BAT by traveling along blood vessels, which is largely completed by P10 (120). Sympathetic axons branch and expand to occupy the parenchyma, reaching adult levels by P21 (weaning) (120).

(i) Growth factors and neuroendocrine control of BAT neonatal development. The BAT depot forms during gestation, but is not active until birth. Following parturition, BAT activity is "unmasked" through the actions of secreted factors, and not neuronal signals. Prolactin, which is secreted by the anterior pituitary to stimulate mammary gland development and lactation, is critical to the differentiation and growth of BAT during gestation and the early postnatal period (126, 127). Prolactin receptors (PRLR) are highly expressed in neonatal BAT, and PRLR KO mice have severely decreased BAT mass at birth, reduced *Ucp1* mRNA and protein levels, and morphological abnormalities in BAT mitochondria, resulting in severe cold intolerance (127). Prolactin works in concert with insulin-like growth factor 2 (IGF-2) to control BAT differentiation at birth (127). IGF-2 is not necessary for further growth of the depot, as IGF-2 declines within several weeks of birth (127).

BAT DIO2 is important during the late gestational/early postnatal period (128). Hypothyroid dams (and subsequently developing fetuses) exhibit decreased BAT *Ucp1* gene expression in utero, and the sharp increase of *Ucp1* within 24 hours post-birth is blunted (129). Moreover, DIO2 is important during development, and when knocked out during differentiation, it leads to defective maturation of the brown adipocytes (130).

This suggests that a normal thyroid environment is needed for proper thermogenic capacity of BAT (129). Therefore, thyroid hormones play a crucial role for the functionality of the BAT during gestation and the early postnatal period, and it has the ability to increase *Ucp1* in a thermoneutral condition (such as *in utero*) (131). Additionally, T3 has been hypothesized to play a role in the expansion of the BAT depot during fetal development (121).

BAT development is also under the trophic control of growth factors. Insulin-like growth factor 1 (IGF-1) is important for organ differentiation of fetal BAT (119, 132), and its receptor (IGF-1R) increases during BAT differentiation (121). IGF-1 in conjunction with T3 could aid in the expansion of BAT in the absence of NE during fetal development (121). Nerve growth factor (NGF) is important for sympathetic innervation (132) and BAT proliferation (133) and is under inhibitory control of NE (132). NGF is inversely correlated to SNS tone onto BAT (119), and thus decreased SNS tone results in increased BAT NGF (132). Consistent with these findings, obese mice have increased BAT NGF levels compared to lean controls (132), most likely due to a compensatory mechanism for the decreased SNS tone in obese mice. In contrast, cold, which is known to increase sympathetic tone, lowers BAT NGF levels (119). Therefore, NGF might be a compensatory mechanism of sympathetic innervation when SNS tone is low (132).

Fibroblast growth factors (FGF) are also important in BAT growth and development. FGF-16 stimulates BAT proliferation during gestation (100), while FGF-15 plays a role in BAT expansion and thermogenic capacity (100). Similarly, FGF-21 becomes present within 48 hours after birth and influences increases in BAT capacity

(134). FGF-2 is also important in the recruitment and hypertrophy of BAT in response to cold (135).

(ii) Leptin and BAT development. Leptin does not seem to be required for BAT development during gestation (136), however it has a crucial differential role in BAT proliferation and thermogenesis during the early postnatal period (137, 138). In the postnatal period, serum leptin levels, primarily secreted from BAT (139) are elevated (139, 140), with a peak in levels at P10 (137, 140). Interestingly, BAT leptin levels are inversely correlated with SNS activity onto BAT, and neonates reared in thermoneutral conditions exhibit increased circulating leptin (139). Moreover, leptin administration in the early postnatal period reduces BAT UCP1 in sheep (141), and thyroid hormones in rats (142). The SNS tone onto BAT is influenced by leptin (94, 136, 143-147), and early leptin-treatment (P4-P14) to *ob/ob* mice results in enhanced cold tolerance (138). Increased activity in thermogenic circuits during the first few postnatal weeks can permanently program improvements in thermoregulation in *ob/ob* mice (138).

Central regulation of adult BAT (Figure 1.3)

BAT is regulated by various regions within the hypothalamus, including the paraventricular nucleus (PVH), preoptic area (POA), arcuate nucleus (ARH), ventral medial nucleus (VMH), dorsal medial hypothalamus (DMH), and lateral hypothalamus (LH), as well as extrahypothalamic regions, such as the nucleus tractus solitarii (NTS) (148) or ventral tegmental area (VTA) (149). The LH synthesizes the neuropeptide orexin, and orexinergic neurons can project to the orexin receptors in the rostral raphe pallidus (rRPA) to amplify sympathetic activity onto BAT (150). Conversely, the PVN

contains inhibitory neuronal influence over BAT activation through the rRPA (148, 151), and provides a control mechanism that is under the influence of nutritional and metabolic regulation. PVH control of BAT thermogenesis is mediated in part by the ARH, and both NPY and POMC have influence on the thermogenic control of BAT via the PVH (152, 153). Moreover, central nervous system (CNS) injections of NPY increase adiposity, even when mice are being pair-fed, suggesting that NPY influences EE (153) independent of food intake. Infusion of MTII (an MC4R agonist) into the PVH has been shown to increase BAT thermogenesis (152, 154, 155). Therefore, the NPY and POMC neuronal projections from the ARH to the PVH influence BAT thermogenesis (152, 153). Recent studies have also implicated agouti-related peptide (AgRP) in the regulation of BAT through projections to the anterior bed nucleus of the stria terminalis (156).

Retrograde labeling of BAT using pseudo rabies virus has implicated the POA of the hypothalamus as an important regulator of BAT thermoregulation (97, 157). Thermosensory receptors on the skin send signals through the spinal dorsal horn to activate the parabrachial nucleus projections to the POA (148). The POA exerts inputs onto the DMH, which is the primary brain region influencing BAT thermogenesis in response to temperature (152, 158). The thermoregulatory control of the DMH onto BAT is mediated through the rRPA (148, 152, 159). Subsequently, blocking the DMH prevents SNS-mediated BAT activation (160). Additionally, the rRPA region is necessary in the thermosensory control of BAT, as de-activation of the rRPA results in reduced body temperature (148). The VMH also receives inputs from the POA that regulates BAT thermogenesis, and cooling and warming the cold-sensing neurons and the warm-sensing neurons respectively activates and deactivates BAT, through inhibitory

outputs onto the VMH (97, 161). Lesions of the VMH lead to atrophy of BAT (97), and suppression of the ability for acute cold (97, 162) or cooling of the POA to stimulate BAT (97, 161).

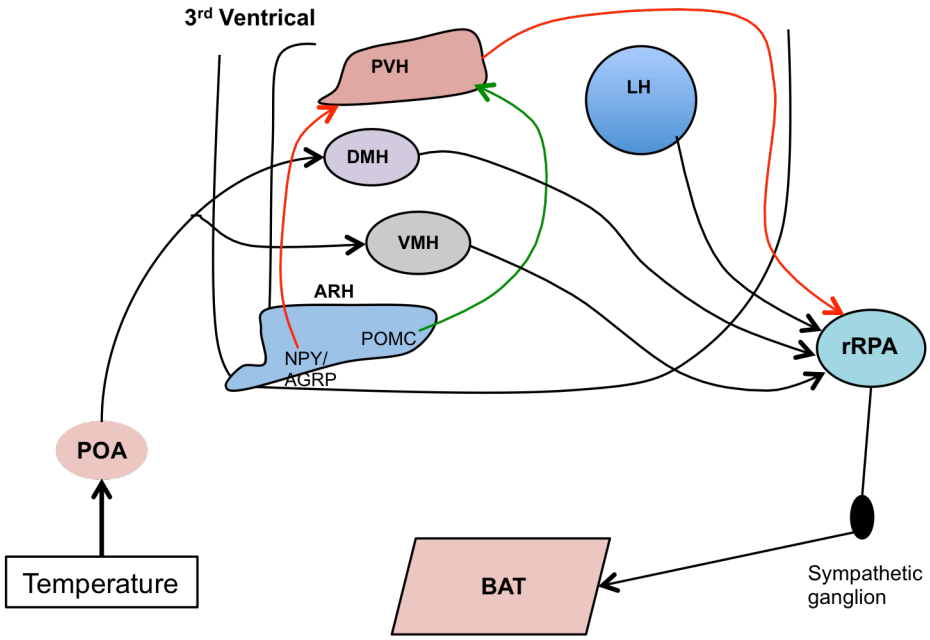

Figure 1.3. Hypothalamic influences of sympathetic regulation of BAT. Temperature influences the temperature sensing neurons in the POA to stimulate hypothalamic nuclei to influence BAT thermogenesis mediated by the rRPA. The ARH mediates PVN inhibitory control of the rRPA through action of NPY/AgRP and POMC neurons. The POA projects to the DMH and VMH to act on the rRPA to influence BAT thermogenesis. The rRPA signals to BAT through the sympathetic ganglion. Abbreviations: POA; preoptic area. NPY/AGRP: neuropeptide Y/agouti-related peptide. ARH; arcuate nucleus of the hypothalamus. VMH; ventral medial nucleus of hypothalamus. DMH; dorsal medial hypothalamus. PVH; periventricular nucleus of hypothalamus. LH; lateral hypothalamus. rRPA; rostral raphe pallidus. BAT; brown adipose tissue. Figure adapted from Zhang W , Bi S. *Front Endocrinol (Lausanne)*. [Internet] (2015). Reference (212).

(i) Leptin effects on SNS control of BAT. In adulthood, leptin infusion can elicit a thermogenic response and intracerebroventricular (ICV) injections of leptin into the VMH results in increased SNS tone onto BAT (163). It is thought that leptin-mediated SNS tone is mediated through the melanocortin system in adulthood, as some studies have indicated that MC4R KO mice are unable to elicit a thermogenic response upon peripheral leptin injection (145). Additionally, while leptin ICV injection increases BAT UCP1 in control mice, co-administration with SHU9119, an α-melanocortin stimulating hormone (α-MSH) inhibitor, has been shown to inhibit leptin-induced thermogenesis (144). There have been contradictory reports as to whether SHU9119 co-administration inhibits leptin's effect on BAT UCP1 (146), which could be due to different experimental conditions. Additionally, although MC4R KO mice are cold intolerant, further supporting the role of MC4R in thermoregulation, prolonged cold exposure results in increased cold tolerance (152). Therefore, there are compensatory mechanisms by which melanocortin-dependent thermogenesis is regulated (152).

Peripheral regulation of BAT activation (Figure 1.4)

(i) Liver secreted factors. BAT can also be activated through stimuli in the periphery, especially the liver (164). FGF21, primarily secreted by the liver, regulates energy and glucose homeostasis, and exogenous FGF21 results in weight loss effects (165-167). Interestingly, models of obesity exhibit relatively high levels of circulating FGF21, supporting the hypothesis that obesity might be a state of FGF21 resistance (166, 167). BAT can also secrete its own FGF21 to upregulate BAT thermogenesis (168).

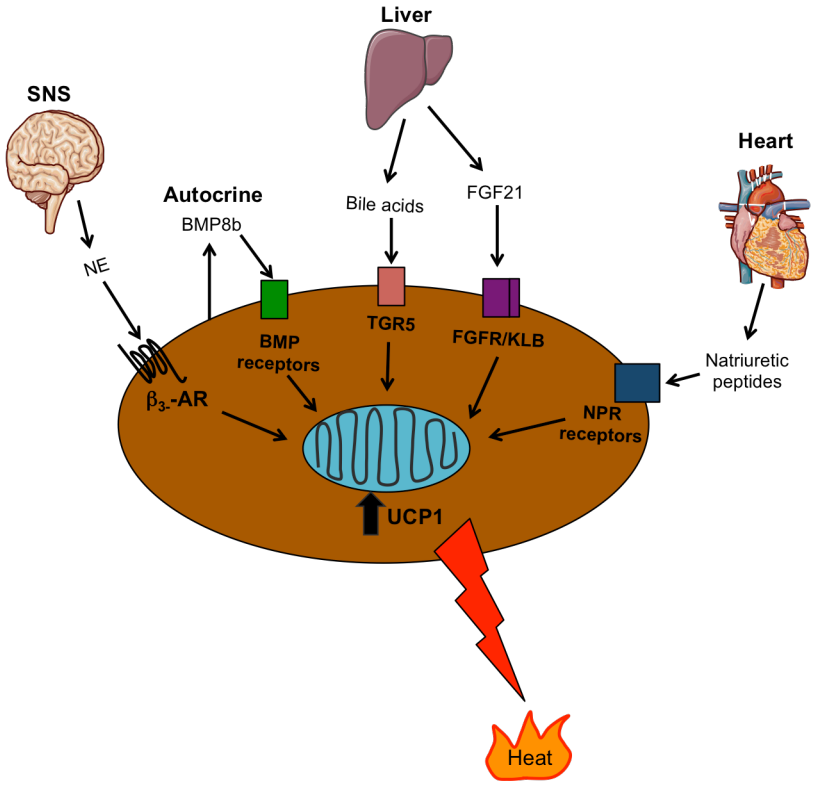

Figure 1.4. Peripheral activators of BAT. NE from the SNS acts through the β_3-AR. BAT produces BMP8b that acts on its BAT receptors to increase thermogenesis. The liver secretes bile acids and FGF21 that interacts with TGR5 and FGFR/KLB respectively. The heart produces natriuretic peptides that also influence thermogenesis. Abbreviations: SNS; sympathetic nervous system. NE; norepinephrine. β_3-AR; β_3 adrenergic receptor. BMP; bone morphogenic protein. FGFR; fibroblast growth factor receptor. KLB; β-klotho. FGF21; fibroblast growth factor. NPR; natriuretic peptide receptor. UCP1; uncoupling protein 1. Figure adapted from Villarroya, F, Vidal-Puig, A. *Cell Metabolism*. (2013). Reference (164).

Bile acids are another factor released from the liver that can drive BAT thermogenesis (164). Bile acids activate BAT via the TGR5 receptor in a mitogen-activated protein kinase (MAPK) dependent pathway, through its action on DIO2 (subsequently converting T4 to T3) (169). Synthesis of T3 within the BAT results in BAT thermogenesis (164). Rodents fed a HFD supplemented with bile acids leads to significantly less weight gain, with increased oxygen consumption, compared to HFD consumption alone (169).

(ii). Heart-secreted BAT activating factors. Two other organs implicated in BAT regulation are the heart and the BAT itself. The heart produces hormones called natriuretic peptides (NP) that can act through the BAT natriuretic peptide receptor (NPR) to stimulate BAT thermogenesis (164). Rodents lacking the clearance receptor for NPs have enhanced activation of BAT in conjunction with reduced body fat deposition (164).

(iii) BAT autocrine regulation of thermogenesis. The BAT makes bone morphogenic protein 8b (BMP8b), a growth factor, that can act on itself through its receptor (BMP8bR) to enhance thermogenesis (170). BMP8b is correlated with nutritional status, and KO models of BMP8b result in decreased EE, are temperature sensitive, and exhibit increased weight gain in the presence of HFD (170). BMP8b can also have CNS-dependent effects on sympathetic control of BAT thermogenesis (170).

Taken together, there are a number of organs that can contribute to BAT activation via hormones and growth factors that they secrete. Some of these secreted factors have been used as therapeutic strategies to enhance BAT activation, but more work is needed in order to elucidate which mechanism might have the most beneficial impact.

Part V: Modulation of BAT Capacity and Activity (Table 1.2)

The SNS innervates BAT via the stellate ganglion; these projections are critical for cold-induced thermogenesis (97, 118, 171, 172). Exogenous NE administration can override a ganglionic blockade (118), by acting directly on β_3-ARs on BAT. The rate of

NE turnover has been used as a surrogate for BAT activity, while response to exogenous NE has been used as a surrogate for BAT capacity (how well the BAT can respond to stimulation) (97). Both capacity and activation are required to maximize BAT function (97) (Figure 1.5). Models of obesity have lower thermogenic capacity, demonstrated by distorted BAT mitochondria (Figure 1.5) and inability to respond to exogenous NE (109, 173, 174), as well as being cold intolerant (173). Additionally, obese models have decreased SNS tone onto BAT, as defined by reduced NE turnover (175, 176). Decreased BAT capacity and activity precede obesity in these models (176, 177), consistent with the idea that deficits in BAT thermogenic responses contribute to the subsequent development of obesity (178). Moreover, it has been shown that treatment with a β_3-AR agonist between 8-16 days of age restores thermogenic capacity of BAT in obese rodents, further indicating that decreased BAT capacity was impaired due to impairments in SNS activity (179).

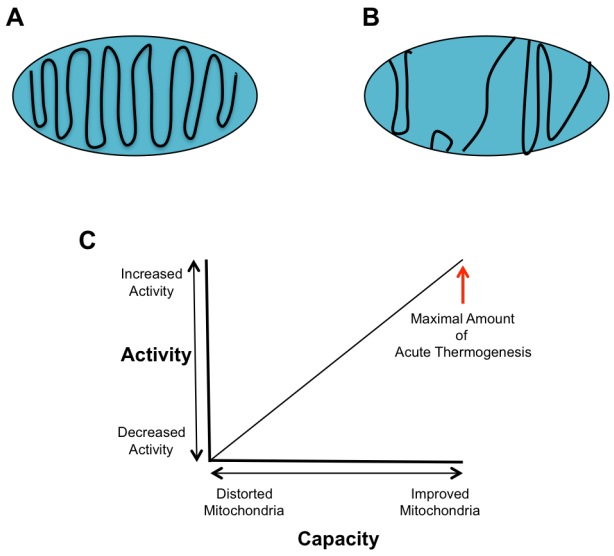

Figure 1.5. Brown adipose tissue capacity and activity. A) Mitochondria of lean rodents with tightly packed cristae. B) Mitochondria of obese rodent with disrupted cristae. C) Relationship between capacity of mitochondria and its activity to acute stimuli to mount a thermogenic response. Figure adapted from Cannon B, Nedergaard J. *Physiol Rev*. (2004). Reference (97).

Thyroid hormone

T4 can influence BAT capacity by restoring mitochondrial structure (174), yet can not directly activate BAT (97, 174). There is an interaction between T4 and NE in BAT activation and in response to stimuli, such as cold (114). Although genetically obese mice do not exhibit increased thermogenesis upon treatment with T4, treatment with T4 elicits an improved response to exogenous NE and cold (174), supporting a permissive role for T4 in improving BAT capacity to respond to endogenous/exogenous stimuli (97, 174).

Caloric restriction and cold acclimation

There are several other factors that influence BAT capacity. Although caloric restriction reduces metabolic rate through mechanisms stated earlier, it has beneficial impacts on BAT capacity. Caloric restriction results in enhanced response to exogenous NE in obese mice (180) due to increased binding capacity of the mitochondria (181). Similarly, cold acclimation can induce a thermogenic response (173). Although obese rodents do not respond favorably to acute 4°C stimulus and are cold intolerant, gradual acclimation to cold is able to restore mitochondrial structure and capacity to respond to exogenous NE (173, 182, 183), as well as to increase NE turnover in BAT of obese mice (184). Additionally, cold is reported to upregulate *Dio2* in lean rodents (185). This upregulation is blunted in *ob/ob* mice, consistent with the idea that cold intolerance in these mice is, in part, due to impaired *Dio2* (185).

Rearing temperature

Rearing temperature can have long lasting implications on metabolic status of an animal. Rearing rats in cold temperatures increases SNS innervation in BAT (171, 186), and increases NE content (171) compared to rats reared in warm temperatures, suggesting that early exposure to BAT-activating environments have neuroregulatory influences on BAT. Pups reared at cold temperatures also have long-lasting improvements in cold tolerance (186). Conversely, warm temperatures decrease NE turnover and content leading to reduced BAT activity (171, 184), as well as the ability to respond to exogenous NE (182). Interestingly, although rodents reared at 18°C have increased SNS innervation along with increased BAT NE turnover and UCP1 levels, they have increased predisposition to gain weight on a HFD compared to mice raised at 30°C (186). Increased body weight gain could be due to hyper-innervation of the BAT, reducing sensitivity to thermogenic stimuli (186).

High fat diet

Interestingly, a HFD can stimulate a thermogenic response of BAT known as diet-induced thermogenesis (96, 97, 187, 188). Diet induced thermogenesis is mediated in a UCP1-dependent manner (187). HFD feeding increases depots of BAT and elicits structural changes of BAT similar to that of adaptation to cold (96, 177). Additionally, HFD increases UCP1 protein levels (187) leading to increased EE (96). HFD also increases NE turnover, similar to that seen in cold exposure (101). Similarly, rats fed a HFD exhibited an even more robust increase in rectal and interscapular temperature when injected with NE (96), further supporting the fact that HFD not only activates the BAT,

but improves its capacity to respond to stimuli. This effect of HFD is not lost in genetically obese mice, as HFD feeding in *ob/ob* mice results in increased SNS activity in BAT, capacity of BAT to respond to NE, and improvements in cold tolerance (188). The effect of HFD is a compensatory mechanism to combat increased caloric consumption.

Intervention	**BAT capacity**	**BAT activity**	**BAT activity + NE**
Caloric Restriction	Increased (180, 181)	Decreased (52-54)	Increase (180)
T4	Increased (174)	Unchanged (97, 174)	Increased (174)
Cold	Increased (184)	Unchanged (173)	Increased (173)
HFD	Increased (96)	Increased (96, 97, 187, 188)	Increased (96)

Table 1.2. **Intervention strategy on BAT capacity and activity in obese rodents with and without norepinephrine.** Caloric restriction improves BAT capacity to respond to exogenous NE. T4 has a similar effect. Obese rodents are cold-intolerant, but cold increases BAT capacity to respond to exogenous NE. HFD increases BAT capacity and activation, further increasing activity in response to NE.
Abbreviations: NE: norepinephrine. HFD: high fat diet. T4: Thyroxine.

Part VI: BAT Relevance in Humans

Brown adipose tissue presence humans

The classical BAT depot (interscapular BAT, iBAT) relevant to rodents is also extremely active in humans during infancy (189). IBAT activity declines with age (189), contributing to the old dogma that human BAT was only relevant during infancy, and not in adulthood (as discussed in (190, 191)). This hypothesis has been debunked, as BAT was determined to be the cause of many false positive ^{18}F-flurodeoxyglucose (FDG) positron-emission tomography (PET) uptake studies routinely performed in cancer patients (191, 192). Adipose tissue is known to be the site of glucose uptake via its glucose transporter (GLUT4), and thus metabolically active tissue will result in increased

glucose uptake, and thus an increased FDG uptake (191). Further analysis of false positive readings indicated that glucose uptake is further exacerbated by cold (190, 193-195), indicative of BAT activation. Differing from what is found in infants (and rodents), the main depot in BAT in the adult is found in the supraclavicular region (196). Histological (190, 193) and molecular (190) analysis of the adipose tissue in the supraclavicular region confirmed BAT identity, with increased innervation by the SNS and increased expression of UCP1 (197).

Metabolically active adipose tissue comes in two types, the classical BAT (cBAT) and beige/"brite" adipose tissue. Beige adipose tissue is *Myf5* negative, and is generated from mature WAT that can become metabolically active and expresses UCP1 and other thermogenic markers (as reviewed in (198)). Although it is widely agreed upon that infant BAT is of cBAT origin (199), many of the BAT depots found in adults are thought to be of beige fat origin as opposed to the cBAT seen in rodents (200).

Brown adipose tissue in response to cold in humans

Although BAT activity is not present in all individuals at thermoneutral conditions, BAT can be stimulated upon cold exposure (190, 193-195, 201), leading to increased EE (193, 202). Because human BAT is responsive to cold, non-shivering thermogenesis is hypothesized to be relevant to humans (193). Moreover, cold exposure coincides with reductions in temperature of non-BAT regions, along with increased temperature of supraclavicular BAT, further indicating BAT activation in response to cold stimulation (203). Similar to what is found in rodents, human BAT can also be activated by adrenergic stimulation (204), yet this is has been shown to only be effective

in lean individuals (204). Additionally, the adrenergic stimulatory findings contradict other studies that found cold, but not ephedrine (an adrenergic stimulus), stimulates increased BAT activity (204, 205). Variations in BMI/weight, age, gender, and environmental temperature can influence the discrepancies found in these studies.

Age and BMI correlation to brown adipose tissue activity

There are many factors that influence BAT activation in humans. BAT activity is correlated with age; younger individuals have increased cold-induced BAT activation compared to older individuals (193, 195, 202). Additionally, BAT activity has been shown to be inversely correlated to BMI (201, 206), and the number of BAT-positive islands found within white fat is correlated with leanness (197), thus reduced BAT activity could drive obesity. Conversely, other groups have demonstrated obese individuals can elicit BAT activity during cold exposure (195, 202), similar to the cold-induced response seen in lean subjects (195). These findings might suggest that beige adipose tissue or BAT can be recruited upon cold exposure when performed in young healthy individuals, independent of BMI (195). Interestingly, weight loss induced by laparoscopic gastric banding surgery results in increased BAT responsiveness to cold (207), similar to the BAT capacity improvements of caloric restriction in rodent models (180). Discrepancies in amounts of BAT activation detected in lean versus obese individuals in response to cold could be due to differences of temperatures within studies (uniform vs. personalized cooling methods) as well as the age of the individuals (197, 202). Increased BAT activity has been associated with decreased cardiovascular disease

independent of age and BMI (208), raising the possibility that human BAT might contribute to cardiometabolic status of an individual and not just body weight.

Brown adipose tissue activity during the transition from childhood to adulthood

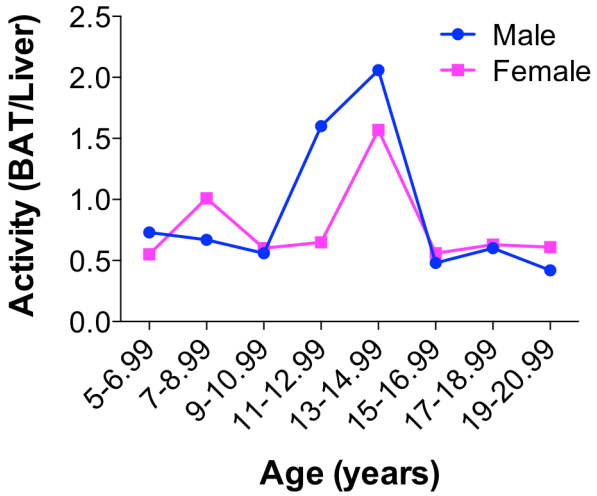

Figure 1.6. Peak of BAT activity in adolescents. BAT activity normalized to liver activity. Blue bar represents male, pink bar represents female. Figure was generated using data from Drubach LA, Palmer EL, Conolly LP, Baker A, Zurakowski D, Cypess AM. *J Pediatr*. (2011). Reference (209).

There is a peak in BAT activation during adolescence (Figure 1.6), which is dampened in obese children (209). BAT activity can be correlated with EE, and therefore the peak of activity during adolescents is a time of elevated EE. This might be a potential mechanism by which basal metabolic rate is established during the pubertal time period. Obesity might be associated with reduced BAT capacity and activation at room temperature, as shown by the lack of response to ephedrine (204), but BAT capacity might be improved upon cold stimulus (195). While ephedrine use is not recommended to treat obesity due to its adverse side effects (i.e. increased blood pressure) (204), this study in combination with studies including cold stimuli suggest BAT might still be a therapeutic organ to combat obesity.

Part VII: Summary

Although there have been some studies showing that early intervention can result in lasting effects on body weight, the mechanism behind this outcome remains unclear. By understanding the mechanistic drivers by which early intervention might reprogram adiposity baselines, we might be able to determine more efficacious strategies to combat childhood obesity in humans. The first goal of this thesis was to determine whether early intervention in a mouse model of early-onset obesity would produce long lasting effects on adiposity. We addressed this question using a mouse model of early-onset obesity generated by the lab, the *Nkx2.1-Cre* (*Lepr*$^{Nkx2.1}$KO), which lacks the leptin receptor in most of the hypothalamus. The resulting mice exhibit hyperphagia, reduced EE, and obesity (210). The *Lepr*$^{Nkx2.1}$KO mouse, which exhibits increased body fat at weaning, differs from the other models of leptin deficiency in that its adiposity stabilizes between 8-12 weeks of age (210). Adiposity stabilization suggests that there is a critical developmental window in which adiposity set points are being established. We hypothesized that intervention in this time window is not accompanied by the decreased EE that typically accompanies caloric intervention in adults.

REFERENCES

1. Ogden CL, Carroll MD, Kit BK, Flegal KM. Prevalence of obesity among adults: United States, 2011-2012. NCHS Data Brief. 2013;131:1-8.

2. Ogden CL, Carroll MD, Kit BK, Flegal KM. Prevalence of childhood and adult obesity in the United States, 2011-2012. JAMA. 2014;311(8):806-14.

3. Daniels SR. The consequences of childhood overweight and obesity. Future Child. 2006;16(1):47-67.

4. Craig LC, Love J, Ratcliffe B, McNeill G. Overweight and cardiovascular risk factors in 4- to 18-year-olds. Obes Facts. 2008;1(5):237-42.

5. Knip M, Nuutinen O. Long-term effects of weight reduction on serum lipids and plasma insulin in obese children. Am J Clin Nutr. 1993;57(4):490-3.

6. Sabo RT, Yen MS, Daniels S, Sun SS. Associations between childhood body size, composition, blood pressure and adult cardiac structure: the Fels Longitudinal Study. PLoS One [Internet]. 2014; 9(9):[e106333 p.].

7. Sun SS, Sima AP, Himes JH. Retarded tempo of physiological development in childhood delays the onset of the metabolic syndrome in adulthood. Ann Nutr Metab. 2014;65(2-3):175-83.

8. Peirson L, Fitzpatrick-Lewis D, Morrison K, Warren R, Usman Ali M, Raina P. Treatment of overweight and obesity in children and youth: a systematic review and meta-analysis. CMAJ Open. 2015;3(1):E35-E46.

9. Whitaker RC, Wright JA, Pepe MS, Seidel KD, Dietz WH. Predicting obesity in young adulthood from childhood and parental obesity. New England Journal of Medicine. 1997;337(13):869-73.

10. Cunningham SA, Kramer MR, Narayan KM. Incidence of childhood obesity in the United States. New England Journal of Medicine. 2014;370(5):403-11.

11. Nader PR, O'Brien M, Houts R, Bradley R, Belsky J, Crosnoe R, et al. Identifying risk for obesity in early childhood. Pediatrics. 2006;118(3).

12. Sachdev HS, Fall CH, Osmond C, Lakshmy R, Dey Biswas SK, Leary SD, et al. Anthropometric indicators of body composition in young adults: relation to size at birth and serial measurements of body mass index in childhood in the New Delhi birth cohort. Am J Clin Nutr. 2005;82(2):456-66.

13. Ong KK. Size at birth, postnatal growth and risk of obesity. Horm Res. 2006;65(Suppl 3).

14. Gardner DS, Hosking J, Metcalf BS, Jeffery AN, Voss LD, Wilkin TJ. Contribution of early weight gain to childhood overweight and metabolic health: a longitudinal study (EarlyBird 36). Pediatrics. 2009;123(1):e67-73.

15. Taylor RW, Williams SM, Carter PJ, Goulding A, Gerrard DF, Taylor BJ. Changes in fat mass and fat-free mass during the adiposity rebound: FLAME study. Int J Pedatr Obes [Internet]. 2011; 6(2-2):[e243-e51 pp.].

16. Ekelund U, Ong KK, Linné Y, Neovius M, Brage S, Dunger DB, et al. Association of weight gain in infancy and early childhood with metabolic risk in young adults. J Clin Endocrinol Metab. 2007;92(1):98-103.

17. Wells JC, Chomtho S, Fewtrell MS. Programming of body composition by early growth and nutrition. Proc Nutr Soc. 2007;66(3):423-34.

18. Mook-Kanamori DO, Durmuş B, Sovio U, Hofman A, Raat H, Steegers EA, et al. Fetal and infant growth and the risk of obesity during early childhood: the Generation R Study. Eur J Endocrinol. 2011;165(4):623-30.

19. Leunissen RW, Kerkhof GF, Stijnen T, Hokken-Koelega A. Timing and tempo of first-year rapid growth in relation to cardiovascular and metabolic risk profile in early adulthood. JAMA. 2009;301(21):2234-42.

20. Taveras EM, Rifas-Shiman SL, Sherry B, Oken E, Haines J, Kleinman K, et al. Crossing growth percentiles in infancy and risk of obesity in childhood. Arch Pediatr Adolesc Med. 2011;165(11):993-8.

21. Rolland-Cachera MF, Deheeger M, Bellisle F, Sempé M, Guilloud-Bataille M, Patois E. Adiposity rebound in children: a simple indicator for predicting obesity. Am J Clin Nutr. 1984;39(1):129-35.

22. Roberts SB, Savage J, Coward WA, Chew B, Lucas A. Energy expenditure and intake in infants born to lean and overweight mothers. The New England Journal of Medicine. 1988;318(8):461-6.

23. Whitaker RC, Pepe MS, Wright JA, Seidel KD, Dietz WH. Early adiposity rebound and the risk of adult obesity. Pediatrics. 1998;101(3):E5.

24. Rolland-Cachera MF, Deheeger M, Maillot M, Bellisle F. Early adiposity rebound: causes and consequences for obesity in children and adults. Int J Obes (Lond). 2006;Suppl 4:S11-S7.
25. Aksglaede L, Olsen LW, Sørensen TI, Juul A. Forty years trends in timing of pubertal growth spurt in 157,000 Danish school children. PLoS One. 2008;3(7):e2728.

26. Abbassi V. Growth and normal puberty. Pediatrics. 1998;102(2 pt 3):507-11.

27. Kindblom JM, Lorentzon M, Norjavaara E, Lönn L, Brandberg J, Angelhed JE, et al. Pubertal timing is an independent predictor of central adiposity in young adult males: the Gothenburg osteoporosis and obesity determinants study. Diabetes. 2006;3047-3052.

28. Ohlsson C, Lorentzon M, Norjavaara E, Kindblom JM. Age at adiposity rebound is associated with fat mass in young adult males-the GOOD study. PLoS One. 2012;7(11):e49404. Epub Nov 14 2012.

29. Rosenbaum M, Hirsch J, Murphy E, Leibel RL. Effects of changes in body weight on carbohydrate metabolism, catecholamine excretion, and thyroid function. Am J Clin Nutr. 2000;71(6):1421-32.

30. Leibel RL, Rosenbaum M, Hirsch J. Changes in energy expenditure resulting from altered body weight. New England Journal of Medicine. 1995;332(10):621-8.

31. Lazzer S, Boirie Y, Montaurier C, Vernet J, Meyer M, Vermorel M. A weight reduction program preserves fat-free mass but not metabolic rate in obese adolescents. Obes Res. 2004;12(2):233-40.

32. Kiortsis DN, Durack I, Turpin G. Effects of a low-calorie diet on resting metabolic rate and serum tri-iodothyronine levels in obese children. Eur J Pediatr. 1999;158(6):446-50.

33. Vermorel M, Lazzer S, Bitar A, Ribeyre J, Montaurier C, Fellmann N, et al. Contributing factors and variability of energy expenditure in non-obese, obese, and post-obese adolescents. Reprod Nutr Dev. 2005;45(2):129-42.

34. Farrow CV, Blissett J. Controlling feeding practices: cause or consequence of early child weight? Pediatrics. 2008;121(1):e164-e9.

35. Fisher JO, Birch LL. Restricting access to foods and children's eating. Appetite. 1999;32(3):405-19.

36. Birch LL, Fisher JO, Davison KK. Learning to overeat: maternal use of restrictive feeding practices promotes girls' eating in the absence of hunger. Am J Clin Nutr. 2003;78(2):215-20.

37. Khan LK, Sobush K, Keener D, Goodman K, Lowry A, Kakietek J, et al. Recommended community strategies and measurements to prevent obesity in the United States. MMWR Recomm Rep. 2009;58(RR-7):1-26.

38. Barlow SE. Expert committee recommendations regarding the prevention, assessment, and treatment of child and adolescent overweight and obesity: summary report. Pediatrics. 2007;120(Suppl 4):S164-S92.

39. Kamath CC, Vickers KS, Ehrlich A, McGovern L, Johnson J, Singhal V, et al. Clinical review: behavioral interventions to prevent childhood obesity: a systematic review and metaanalyses of randomized trials. J Clin Endocrinol Metab. 2008;93(12):4606-15.

40. Wang Y, Wu Y, Wilson RF, Bleich S, Cheskin L, Weston C, et al. Childhood Obesity Prevention Programs: Comparative Effectiveness Review and Meta-Analysis. AHRQ Comparative Effectiveness Reviews [Internet]. 2013; 13-EHC081-EF.

41. Taveras EM, Gortmaker SL, Hohman KH, Horan CM, Kleinman KP, Mitchell K, et al. Randomized controlled trial to improve primary care to prevent and manage childhood obesity: the High Five for Kids study. Arch Pediatr Adolesc Med. 2011;165(8):714-22.

42. Wake M, Baur LA, Gerner B, Gibbons K, Gold L, Gunn J, et al. Outcomes and costs of primary care surveillance and intervention for overweight or obese children: the LEAP 2 randomised controlled trial. BMJ. 2009;B3308.

43. Kelley GA, Kelley KS. Effects of exercise in the treatment of overweight and obese children and adolescents: a systematic review of meta-analyses. J Obes [Internet]. 2013.

44. McGovern L, Johnson JN, Paulo R, Hettinger A, Singhal V, Kamath C, et al. Clinical review: treatment of pediatric obesity: a systematic review and meta-analysis of randomized trials. J Clin Endocrinol Metab. 2008;93(12):4600-5.

45. Cawley J. The economics of childhood obesity. Health Aff (Millwood). 2010;29(3):364-71.

46. Trasande L. How much should we invest in preventing childhood obesity? Health Aff (Millwood). 2010;29(3):372-8.

47. Danielsson P, Kowalski J, Ekblom Ö, Marcus C. Response of severely obese children and adolescents to behavioral treatment. Arch Pediatr Adolesc Med. 2012;166(12):1103-8.

48. Danielsson P, Svensson V, Kowalski J, Nyberg G, Ekblom O, Marcus C. Importance of age for 3-year continuous behavioral obesity treatment success and dropout rate. Obes Facts. 2012;5(1):34-44.

49. Knop C, Singer V, Uysal Y, Schaefer A, Wolters B, Reinehr T. Extremely obese children respond better than extremely obese adolescents to lifestyle interventions. Pediatr Obes. 2015;10(1).

50. Reinehr T, Kleber M, Lass N, Toschke AM. Body mass index patterns over 5 y in obese children motivated to participate in a 1-y lifestyle intervention: age as a predictor of long-term success. Am J Clin Nutr. 2010;91(5):1165-71.

51. Wolters B, Lass N, Reinehr T. TSH and free triiodothyronine concentrations are associated with weight loss in a lifestyle intervention and weight regain afterwards in obese children. Eur J Endocrinol. 2013;168(3):323-9.

52. Oscai LB. Evidence that body size does not determine voluntary food intake in the rat. Am J Physiol. 1980;238(4):E318-E21.

53. MacLean PS, Higgins JA, Johnson GC, Fleming-Elder BK, Donahoo WT, Melanson EL, et al. Enhanced metabolic efficiency contributes to weight regain after weight loss in obesity-prone rats. Am J Physiol Regul Integr Comp Physiol. 2004;287(6):R1306-R15.

54. Levin BE, Dunn-Meynell AA. Defense of body weight against chronic caloric restriction in obesity-prone and -resistant rats. Am J Physiol. 2000;278(1):R231-R7.

55. Mohan PF, Rao BS. Adaptation to underfeeding in growing rats. Effect of energy restriction at two dietary protein levels on growth, feed efficiency, basal metabolism and body composition. J Nutr. 1983;113(1):79-85.

56. Widdowson EM, McCance RA. The effect of finite periods of undernutrition at different ages on the composition and subsequent development of the rat. Proc R Soc Lond B Biol Sci. 1963;158:329-42.

57. Levin BE, Dunn-Meynell AA, Balkan B, Keesey RE. Selective breeding for diet-induced obesity and resistance in Sprague-Dawley rats. Am J Physiol. 1997;273(2 pt 2):R275-R30.

58. Ricci MR, Levin BE. Ontogeny of diet-induced obesity in selectively bred Sprague-Dawley rats. Am J Physiol Regul Integr Comp Physiol. 2003;285(3):R610-R8.

59. Levin BE, Keesey RE. Defense of differing body weight set points in diet-induced obese and resistant rats. Am J Physiol. 1998;274(2 pt 2):R412-R9.

60. Patterson CM, Dunn-Meynell AA, Levin BE. Three weeks of early-onset exercise prolongs obesity resistance in DIO rats after exercise cessation. Am J Physiol Regul Integr Comp Physiol. 2008;294(2):R290-301.

61. Patterson CM, Bouret SG, Dunn-Meynell AA, Levin BE. Three weeks of postweaning exercise in DIO rats produces prolonged increases in central leptin sensitivity and signaling. Am Physiol Regul Integr Comp Physiol. 2009;296:R537-R48.

62. Johnson PM, Kenny PJ. Dopamine D2 receptors in addiction-like reward dysfunction and compulsive eating in obese rats. Nat Neurosci. 2010;13(5):635-41.

63. Zhang Y, Proenca R, Maffei M, Barone M, Leopold L, Friedman JM. Positional cloning of the mouse *obese* gene and its human homoglogue. Nature. 1994;372:425-32.

64. Friedman JM, Halaas JL. Leptin and the regulation of body weight in mammals. Nature. 1998;395(6704):763-70.

65. Bates SH, Myers MG, Jr. The role of leptin receptor signaling in feeding and neuroendocrine function. Trends endocrinol metab. 2003;14(10):447-52.

66. Pelleymounter MA, Cullen MJ, Baker MB, Hecht R, Winters D, Boone T, et al. Effects of the obese gene product on body weight regulation in ob/ob mice. Science. 1995;269(5223):540-3.

67. Chua SC, Jr , Chung WK, Wu-Peng XS, Zhang Y, Liu SM, Tartaglia L, et al. Phenotypes of mouse diabetes and rat fatty due to mutations in the OB (leptin) receptor. Science. 1996;271(5251):994-6.

68. Chen D, Wang MW. Development and application of rodent models for type 2 diabetes. Diabetes Obes Metab. 2005;7(4):307-17.

69. Bates SH, Kulkarni RN, Seifert M, Myers MG, Jr. Roles for leptin receptor/STAT3-dependent and -independent signals in the regulation of glucose homeostasis. Cell Metabolism. 2005;1(3):169-78.

70. Cleary MP, Vasselli JR, Greenwood MR. Development of obesity in Zucker obese (fafa) rat in absence of hyperphagia. Am J Physiol. 1980;238(3):E284-E92.

71. Alonso LG, Maren TH. Effect of food restriction on body composition of hereditary obese mice. Am J Physiol. 1955;183(2):284-90.

72. Chlouverakis C. Effect of caloric restriction on body weight loss and body fat utilization in obese hyperglycemic mice (Obob). Metabolism. 1972;21(1):10-7.
73. Dubuc PU. Effects of limited food intake on the obese-hyperglycemic syndrome. Am J Physiol. 1976;230(6):1474-9.

74. Dubuc PU, Cahn PJ, Willish P. The effects of exercise and food restriction on obesity and diabetes in young ob/ob mice. Int J Obes. 1984;8(3):271-8.

75. Bates SH, Stearns WH, Dundon TA, Schubert M, Tso AW, Wang Y, et al. STAT3 signalling is required for leptin regulation of energy balance but not reproduction. Nature. 2003;421(6925):856-9.

76. Huszar D, Lynch CA, Fairchild-Huntress V, Dunmore JH, Fang Q, Berkemeier LR, et al. Targeted disruption of the melanocortin-4 receptor results in obesity in mice. Cell. 1997;88(1):131-41.

77. Yaswen L, Diehl N, Brennan MB, Hochgeschwender U. Obesity in the mouse model of pro-opiomelanocortin deficiency responds to peripheral melanocortin. Nature Medicine. 1999;5:1066-70.

78. Weide K, Christ N, Moar KM, Arens J, Hinney A, Mercer JG, et al. Hyperphagia, not hypometabolism, causes early onset obesity in melanocortin-4 receptor knockout mice. Physiol Genomics. 2003;13(1):47-56.

79. Balthasar N, Coppari R, McMinn J, Liu SM, Lee CE, Tang V, et al. Leptin receptor signaling in POMC neurons is required for normal body weight homeostasis. Neuron. 2004;42(6):983-91.

80. Chen AS, Marsh DJ, Trumbauer ME, Frazier EG, Guan XM, Yu H, et al. Inactivation of the mouse melanocortin-3 receptor results in increased fat mass and reduced lean body mass. Nat Genet. 2000;26(1):97-102.

81. Bumaschny VF, Yamashita M, Casas-Cordero R, Otero-Corchón V, de Souza FS, Rubinstein M, et al. Obesity-programmed mice are rescued by early genetic intervention. J Clin Invest. 2012;122(11):4203-12.

82. Nakamura H, Kihara Y, Tashiro M, Kanagawa K, Shirohara H, Yamamoto M, et al. Defects of cholecystokinin (CCK)-A receptor gene expression and CCK-A receptor-mediated biological functions in Otsuka Long-Evans Tokushima Fatty (OLETF) rats. J Gastroenterol. 1998;33(5):702-9.

83. Schroeder M, Zagoory-Sharon O, Lavi-Avnon Y, Moran TH, Weller A. Weight gain and maternal behavior in CCK1 deficient rats. Physiol Behav. 2006;89(3):402-9.

84. Schroeder M, Gelber V, Moran TH, Weller A. Long-term obesity levels in female OLETF rats following time-specific post-weaning food restriction. Horm Behav. 2010;58(5):844-53.

85. Schroeder M, Moran TH, Weller A. Attenuation of obesity by early-life food restriction in genetically hyperphagic male OLETF rats: peripheral mechanisms. Hormones and behavior. 2010;57(4-5):455-62.

86. Schroeder M, Shbiro L, Gelber V, Weller A. Post-weaning voluntary exercise exerts long-term moderation of adiposity in males but not in females in an animal model of early-onset obesity. Hormones and behavior. 2010;57:496-505.

87. Kopin AS, Mathes WF, McBride EW, Nguyen M, Al-Haider W, Schmitz F, et al. The cholecystokinin-A receptor mediates inhibition of food intake yet is not essential for the maintenance of body weight. Journal of Clinical Investigation. 1999;103(3):383-91.

88. Moran TH. Unraveling the obesity of OLETF rats. Physiol Behav. 2008;94(1):71-8.

89. Bi S, Scott KA, Hyun J, Ladenheim EE, Moran TH. Running wheel activity prevents hyperphagia and obesity in Otsuka long-evans Tokushima Fatty rats: role of hypothalamic signaling. Endocrinology. 2005;146(4):1676-85.

90. Bi S, Ladenheim EE, Schwartz GJ, Moran TH. A role for NPY overexpression in the dorsomedial hypothalamus in hyperphagia and obesity of OLETF rats. Am J Physiol Regul Integr Comp Physiol. 2001;281(1):R254-R60.

91. Surwit RS, Kuhn CM, Cochrane C, McCubbin JA, Feinglos MN. Diet-induced type II diabetes in C57BL/6J mice. Diabetes. 1988;37(9):1163-57.

92. Lin S, Thomas TC, Storlien LH, Huang XF. Development of high fat diet-induced obesity and leptin resistance in C57Bl/6J mice. Int J Obes Relat Metab Disord. 2000;24:639-46.

93. Xiao XQ, Williams SM, Grayson BE, Glavas MM, Cowley MA, Smith MS, et al. Excess weight gain during the early postnatal period is associated with permanent reprogramming of brown adipose tissue adaptive thermogenesis. Endocrinology. 2007;148(9):4150-9.

94. Lowell BB, Spiegelman BM. Towards a molecular understanding of adaptive thermogenesis. Nature. 2000;404:652-60.

95. Foster DO, Frydman ML. Tissue distribution of cold-induced thermogenesis in conscious warm- or cold-acclimated rats reevaluated from changes in tissue blood flow: the dominant role of brown adipose tissue in the replacement of shivering by nonshivering thermogenesis. Can J Physiol Pharmacol. 1979;57(3):257-70.

96. Rothwell NJ, Stock MJ. A role for brown adipose tissue in diet-induced thermogenesis. Nature. 1979;281(5726):31-5.
97. Cannon B, Nedergaard J. Brown Adipose Tissue: Function and Physiological Significance. Physiol Rev. 2004;84:277-359.

98. Banet M, Hensel H, Liebermann H. The central control of shivering and non-shivering thermogenesis in the rat. J Physiol. 1978;283(569-584).

99. Himms-Hagen J. Brown adipose tissue thermogenesis and obesity. Prog Lipid Res. 1989;28:67-115.

100. Seale P, Kajimura S, Spiegelman BM. Transcriptional control of brown adipocyte development and physiological function--of mice and men. Genes Devel. 2009;23(7):788-97.

101. Richard D, Carpentier AC, Doré G, Ouellet V, Picard F. Determinants of brown adipocyte development and thermogenesis. Int J Obes (Lond). 2010;34(Suppl 2):S59-66.

102. Seale P, Bjork B, Yang W, Kajimura S, Chin S, Kuang S, et al. PRDM16 controls a brown fat/skeletal muscle switch. Nature. 2008;454(7207):961-7.

103. Nicholls DG, Locke RM. Thermogenic Mechanisms in Brown Fat. Physiol Rev. 1984;64(1):1-64.

104. Cadrin M, Tolszczuk M, Guy J, Pelletier G, Freeman KB, Bukowiecki LJ. Immunohistochemical identification of the uncoupling protein in rat brown adipose tissue. J Histochem Cytochem. 1985;33(2):150-4.

105. Cinti S, Zancanaro C, Sbarbati A, Cicolini M, Vogel P, Ricquier D, et al. Immunoelectron microscopical identification of the uncoupling protein in brown adipose tissue mitochondria. Biol Cell. 1989;67(3):359-62.

106. Cannon B, Hedin A, Nedergaard J. Exclusive occurrence of thermogenin antigen in brown adipose tissue. FEBS Letters. 1982;150(1):129-32.

107. Enerbäck S, Jacobsson A, Simpson EM, Guerra C, Yamashita H, Harper ME, et al. Mice lacking mitochondrial uncoupling protein are cold-sensitive but not obese. Nature. 1997;387(6628):90-4.

108. Golozoubova V, Hohtola E, Matthias A, Jacobsson A, Cannon B, Nedergaard J. Only UCP1 can mediate adaptive nonshivering thermogenesis in the cold. FASEB J. 2001;15(11):2048-50.

109. Trayhurn P, James WP. Thermoregulation and non-shivering thermogenesis in the genetically obese (ob/ob) mouse. Pfluegers Arch. 1978;373:189-93.

110. Cao W, Medvedev AV, Daniel KW, Collins S. beta-Adrenergic activation of p38 MAP kinase in adipocytes: cAMP induction of the uncoupling protein 1 (UCP1) gene requires p38 MAP kinase. Journal of Biological Chemistry. 2001;276(29):27077-82.

111. Thomas SA, Palmiter RD. Thermoregulatory and metabolic phenotypes of mice lacking noradrenaline and adrenaline. Nature. 1997;387(6628):94-7.

112. Young JB, Saville E, Rothwell NJ, Stock MJ, Landsberg L. Effect of diet and cold exposure on norepinephrine turnover in brown adipose tissue of the rat. J Clin Invest. 1982;69(5):1061-71.

113. McAninch EA, Bianco AC. Thyroid hormone signaling in energy homeostasis and energy metabolism. Ann N Y Acad Sci. 2014;1311:77-87.

114. Carvalho SD, Bianco AC, Silva JE. Effects of hypothyroidism on brown adipose tissue adenylyl cyclase activity. Endocrinology. 1996;137(12):5519-29.

115. Bianco AC, Silva JE. Intracellular conversion of thyroxine to triiodothyronine is required for the optimal thermogenic function of brown adipose tissue. J Clin Invest. 1987;79(1):295-300.

116. Silva JE, Larsen PR. Adrenergic activation of triiodothyronine production in brown adipose tissue. Nature. 1983;305(5936):712-3.

117. Castillo M, Hall JA, Correa-Medina M, Ueta C, Kang HW, Cohen DE, et al. Disruption of thyroid hormone activation in type 2 deiodinase knockout mice causes obesity with glucose intolerance and liver steatosis only at thermoneutrality. Diabetes. 2011;60(4):1082-9.

118. Hsieh AC, Carlson LD, Gray G. Role of the sympathetic nervous system in the control of chemical regulation of heat production. Am J Physiol. 1957;190(2):257-1.

119. Nisoli E, Tonello C, Carruba MO. Nerve growth factor, beta3-adrenoceptor and uncoupling protein 1 expression in rat brown fat during postnatal development. Neurosci Lett. 1998;246(1):5-8.

120. Derry DM, Daniel H. Sympathetic nerve development in the brown adipose tissue of the rat. Can J Physiol Pharmacol. 1970;48(3):160-8.

121. Teruel T, Valverde AM, Alvarez A, Benito M, Lorenzo M. Differentiation of rat brown adipocytes during late foetal development: role of insulin-like growth factor I. Biochem J. 1995;310(pt 3):771-6.

122. Suter ER, Stäubli W. An ultrastructural histochemical study of brown adipose tissue from neonatal rats. J Histochem Cytochem. 1970;18(2):100-6.

123. Obregón MJ, Jacobsson A, Kirchgessner T, Schotz MC, Cannon B, Nedergaard J. Postnatal recruitment of brown adipose tissue is induced by the cold stress experienced by the pups. An analysis of mRNA levels for thermogenin and lipoprotein lipase. Biochem J. 1989;259(2):341-6.

124. Eliot RJ, Klein AH, Glatz TH, Nathanielsz PW, Fisher DA. Plasma norepinephrine, epinephrine, and dopamine concentrations in maternal and fetal sheep during spontaneous parturition and in premature sheep during cortisol-induced parturition. Endocrinology. 1981;108(5):1678-82.

125. Derry DM, Schönbaum E, Steiner G. Two sympathetic nerve supplies to brown adipose tissue of the rat. Can J Physiol Pharmacol. 1969;47(1):57-63.

126. Carré N, Binart N. Prolactin and adipose tissue. Biochimie. 2014;97(16-21).

127. Viengchareun S, Servel N, Fève B, Freemark M, Lombès M, Binart N. Prolactin receptor signaling is essential for perinatal brown adipocyte function: a role for insulin-like growth factor-2. PLoS One. 2008;3(2):e1535.

128. Obregón MJ, Ruiz de Oña C, Hernandez A, Calvo R, Escobar del Rey F, Morreale de Escobar G. Thyroid hormones and 5'-deiodinase in rat brown adipose tissue during fetal life. Am J Physiol. 1989;257(5 pt 1):E625-E31.

129. Obregon MJ, Pitamber R, Jacobsson A, Nedergaard J, Cannon B. Euthyroid status is essential for the perinatal increase in thermogenin mRNA in brown adipose tissue of rat pups. Biochem Biophys Res Commun. 1987;148(1):9-14.

130. Hall JA, Ribich S, Christoffolete MA, Simovic G, Correa-Medina M, Patti ME, et al. Absence of thyroid hormone activation during development underlies a permanent defect in adaptive thermogenesis. Endocrinology. 2010;151(9):4573-82.

131. Obregón MJ. Thyroid Hormone and Adipocyte Differentiation. Thyroid. 2008;18(2):185-95.

132. Nisoli E, Tonello C, Benarese M, Liberini P, Carruba MO. Expression of nerve growth factor in brown adipose tissue: implications for thermogenesis and obesity. Endocrinology. 1996;237(2):495-503.

133. Néchad M, Ruka E, Thibault J. Production of nerve growth factor by brown fat in culture: relation with the in vivo developmental stage of the tissue. Comp Biochem Physiol Comp Physiol. 1994;107(2):381-8.

134. Hondares E, Rosell M, Gonzalez FJ, Giralt M, Iglesias R, Villarroya F. Hepatic FGF21 expression is induced at birth via PPARalpha in response to milk intake and contributes to thermogenic activation of neonatal brown fat. Cell Metabolism. 2010;11(3):206-12.

135. Yamashita H, Sato Y, Kizaki T, Oh S, Nagasawa J, Ohno H. Basic fibroblast growth factor (bFGF) contributes to the enlargement of brown adipose tissue during cold acclimation. Pflugers Arch. 1994;428(3-4):352-6.

136. Zeltser LM. Developmental influences on circuits programming susceptibility to obesity. Front Neuroendocrinol. 2015;39:17-27.

137. Frontini A, Bertolotti P, Tonello C, Valerio A, Nisoli E, Cinti S, et al. Leptin-dependent STAT3 phosphorylation in postnatal mouse hypothalamus. Brain Res. 2008;1215:105-15.

138. Bouyer K, Simerly RB. Neonatal leptin exposure specifies innervation of presympathetic hypothalamic neurons and improves the metabolic status of leptin-deficient mice. J Neurosci. 2013;33(2):840-51.

139. Zhang Y, Hufnagel C, Eiden S, Guo KY, Diaz PA, Leibel R, et al. Mechanisms for LEPR-mediated regulation of leptin expression in brown and white adipocytes in rat pups. Physiol Genomics. 2001;4(3):189-99.

140. Mistry AM, Swick A, Romsos DR. Leptin alters metabolic rates before acquisition of its anorectic effect in developing neonatal mice. Am J Physiol. 1999;277(3 pt 2):R742-7.

141. Mostyn A, Bispham J, Pearce S, Evens Y, Raver N, Keisler DH, et al. Differential effects of leptin on thermoregulation and uncoupling protein abundance in the neonatal lamb. FASEB J. 2002;16(11):1438-40.

142. Toste FP, Alves SB, Dutra SC, Bonomo IT, Lisboa PC, Moura EG, et al. Temporal evaluation of the thyroid function of rats programmed by leptin treatment on the neonatal period. Horm Metab Res. 2006;38(12):827-31.

143. Collins S, Kuhn CM, Petro AE, Swick AG, Chrunyk BA, Surwit RS. Role of leptin in fat regulation. Nature. 1996;380(6576):677.

144. Satoh N, Ogawa Y, Katsuura G, Numata Y, Masuzaki H, Yoshimasa Y, et al. Satiety effect and sympathetic activation of leptin are mediated by hypothalamic melanocortin system. Neurosci Lett. 1988;249(2-3):107-10.

145. Ste Marie L, Miura GI, Marsh DJ, Yagaloff K, Palmiter RD. A metabolic defect promotes obesity in mice lacking melanocortin-4 receptors. Proc Natl Acad Sci USA. 2000;97(22):12339-44.

146. Haynes WG, Morgan DA, Djalali A, Sivitz WI, Mark AL. Interactions between the melanocortin system and leptin in control of sympathetic nerve traffic. Hypertension. 1999;33(1 pt 2):542-7.

147. Haynes WG, Morgan DA, Walsh SA, Mark AL, Sivitz WI. Receptor-mediated regional sympathetic nerve activation by leptin. Journal of Clinical Investigation. 1997;100(2):270-8.

148. Tupone D, Madden CJ, Morrison SF. Autonomic regulation of brown adipose tissue thermogenesis in health and disease: potential clinical applications for altering BAT thermogenesis. Front Neurosci [Internet]. 2014; 8(14):[1-13 pp.].

149. Caron E, Sachot C, Prevot V, Bouret SG. Distribution of leptin-sensitive cells in the postnatal and adult mouse brain. J Comp Neurol. 2010;518(4):459-76.

150. Tupone D, Madden CJ, Cano G, Morrison SF. An orexinergic projection from perifornical hypothalamus to raphe pallidus increases rat brown adipose tissue thermogenesis. J Neurosci. 2011;31(44):15944-55.

151. Madden CJ, Morrison SF. Neurons in the paraventricular nucleus of the hypothalamus inhibit sympathetic outflow to brown adipose tissue. Am J Physiol Regul Integr Comp Physiol. 2009;296(3):R831-R43.

152. Labbé SM, Caron A, Lanfray D, Monge-Rofarello B, Bartness TJ, Richard D. Hypothalamic control of brown adipose tissue thermogenesis. Front Syst Neurosci. 2015;9(150):1-13.

153. Shi YC, Lau J, Lin Z, Zhang H, Zhai L, Sperk G, et al. Arcuate NPY controls sympathetic output and BAT function via a relay of tyrosine hydroxylase neurons in the PVN. Cell Metabolism. 2013;17(2):236-48.

154. Bartness TJ, Vaughan CH, Song CK. Sympathetic and sensory innervation of brown adipose tissue. Int J Obes (Lond). 2010;34(Suppl 1):S36-S42.

155. Song CK, Vaughan CH, Keen-Rhinehart E, Harris RB, Richard D, Bartness TJ. Melanocortin-4 receptor mRNA expressed in sympathetic outflow neurons to brown adipose tissue: neuroanatomical and functional evidence. Am J Physiol Regul Integr Comp Physiol. 2008;295(2):R417-28.

156. Steculorum SM, Ruud J, Karakasilioti I, Backes H, Engström R, L. , Timper K, et al. AgRP Neurons Control Systemic Insulin Sensitivity via Myostatin Expression in Brown Adipose Tissue. Cell. 2016;165(1):125-38.

157. Satinoff E, Valentino D, Teitelbaum P. Thermoregulatory cold-defense deficits in rats with preoptic/anterior hypothalamic lesions. Brain Res Bull. 1976;1(6):553-65.

158. Zhang Y, Kerman IA, Laque A, Nguyen P, Faouzi M, Louis GW, et al. Leptin-receptor-expressing neurons in the dorsomedial hypothalamus and median preoptic area regulate sympathetic brown adipose tissue circuits. J Neurosci. 2011;31(5):1873-84.

159. Rezai-Zadeh K, Münzberg H. Integration of sensory information via central thermoregulatory leptin targets. Physiol Behav. 2013;121:49-55.

160. Enriori PJ, Sinnayah P, Simonds SE, Garcia Rudaz C, Cowley MA. Leptin action in the dorsomedial hypothalamus increases sympathetic tone to brown adipose tissue in spite of systemic leptin resistance. J Neurosci. 2011;31(34):1289-97.

161. Chen XM, Hosono T, Yoda T, Fukuda Y, Kanosue K. Efferent projection from the preoptic area for the control of non-shivering thermogenesis in rats. J Physiol. 1998;512(pt 3):883-92.

162. Niijima A, Rohner-Jeanrenaud F, Jeanrenaud B. Role of ventromedial hypothalamus on sympathetic efferents of brown adipose tissue. Am J Physiol. 1984;247(4 pt 2):R650-R4.

163. Minokoshi Y, Haque MS, Shimazu T. Microinjection of leptin into the ventromedial hypothalamus increases glucose uptake in peripheral tissues in rats. Diabetes. 1999;48(2):287-91.

164. Villarroya F, Vidal-Puig A. Beyond the sympathetic tone: the new brown fat activators. Cell Metabolism. 2013;17(5):638-43.

165. Markan KR, Naber MC, Ameka MK, Anderegg MD, Mangelsdorf DJ, Kliewer SA, et al. Circulating FGF21 is liver derived and enhances glucose uptake during refeeding and overfeeding. Diabetes. 2014;63(12):4057-63.

166. Fisher FM, Chui PC, Antonellis PJ, Bina HA, Kharitonenkov A, Flier JS, et al. Obesity is a fibroblast growth factor 21 (FGF21)-resistant state. Diabetes. 2010;59(11):2781-9.

167. Mraz M, Bartlova M, Lacinova Z, Michalsky D, Kasalicky M, Haluzikova D, et al. Serum concentrations and tissue expression of a novel endocrine regulator fibroblast growth factor-21 in patients with type 2 diabetes and obesity. Clin Endocrinol (Oxf). 2009;71(3):369-75.

168. Chartoumpekis DV, Habeos IG, Ziros PG, Psyrogiannis AI, Kyriazopoulou VE, Papavassiliou AG. Brown adipose tissue responds to cold and adrenergic stimulation by induction of FGF21. Molecular Medicine. 2011;17(7-8):736-40.

169. Watanabe M, Houten SM, Mataki C, Christoffolete MA, Kim BW, Sato H, et al. Bile acids induce energy expenditure by promoting intracellular thyroid hormone activation. Nature. 2006;439(7075):484-9.

170. Whittle AJ, Carobbio S, Martins L, Slawik M, Hondares E, Vázquez MJ, et al. BMP8B increases brown adipose tissue thermogenesis through both central and peripheral actions. Cell. 2012;149(4):871-85.

171. Morrison SF, Ramamurthy S, Young JB. Reduced rearing temperature augments responses in sympathetic outflow to brown adipose tissue. J Neurosci. 2000;20(24):9264-71.

172. Oldfield BJ, Giles ME, Watson A, Anderson C, Colvill LM, McKinley MJ. The neurochemical characterisation of hypothalamic pathways projecting polysynaptically to brown adipose tissue in the rat. Neuroscience. 2002;110(3):515-26.

173. Hogan S, Himms-Hagen J. Abnormal brown adipose tissue in obese mice (*ob/ob*): response to acclimation to cold. Am J Physiol. 1980;239:E301-E9.

174. Hogan S, Himms-Hagen J. Abnormal brown adipose tissue in genetically obese mice (*ob/ob*): effect of thyroxine. Am J Physiol. 1981;241(6):E436-E43.

175. Young JB, Landsberg L. Diminished sympathetic nervous system activity in genetically obese (ob/ob) mouse. Am J Physiol. 1983;245(2):E148-E54.

176. Knehans AW, Romsos DR. Norepinephrine turnover in obese (ob/ob) mice: effects of age, fasting, and acute cold. Am J Physiol. 1983;244(6):E567-E74.

177. Hull D, Vinter J. The development of cold-induced thermogenesis and the structure of brown adipocyte mitochondria in genetically-obese (ob/ob) mice. Br J Nutr. 1984;52(1):33-9.

178. Bazin R, Eteve D, Lavau M. Evidence for decreased GDP binding to brown-adipose-tissue mitochondria of obese Zucker (fa/fa) rats in the very first days of life. Biochem J. 1984;221(1):241-5.

179. Charon C, Dupuy F, Marie V, Bazin R. Effect of the beta-adrenoceptor agonist BRL-35135 on development of obesity in suckling Zucker (fa/fa) rats. Am J Physiol. 1995;268(6 pt 1):E1039-E45.

180. Himms-Hagen J. Food restriction increases torpor and improves brown adipose tissue thermogenesis in ob/ob mice. Am J Physiol. 1985;248(5 pt 1):E531-E9.

181. Batt RA, Tyler DD, Sutton CM. Influence of restricted food intake on brown adipose tissue function in genetically obese mice (genotype, ob/ob). Biochim Biophys Acta. 1985;838(229-235).

182. Hsieh AC, Carlson LD. Role of adrenaline and noradrenaline in chemical regulation of heat production. Am J Physiol. 1957;190(2):243-6.

183. Seydoux J, Assimacopoulos-Jeannet F, Jeanrenaud B, Girardier L. Alterations of brown adipose tissue in genetically obese (ob/ob) mice. I. Demonstration of loss of metabolic response to nerve stimulation and catecholamines and its partial recovery after fasting or cold adaptation. Endocrinology. 1982;110(2):432-8.

184. Knehans AW, Romsos DR. Reduced norepinephrine turnover in brown adipose tissue of ob/ob mice. Am J Physiol. 1982;242(4):E253-E61.

185. Kates AL, Himms-Hagen J. Defective cold-induced stimulation of thyroxine 5'-deiodinase in brown adipose tissue of the genetically obese (ob/ob) mouse. Biochem Biophys Res Commun. 1985;130(1):188-93.

186. Young JB, Weiss J, Boufath N. Effects of rearing temperature on sympathoadrenal activity in young adult rats. Am J Physiol Regul Integr Comp Physiol. 2002;283(5):R1198-R209.

187. Feldmann HM, Golozoubova V, Cannon B, Nedergaard J. UCP1 ablation induces obesity and abolishes diet-induced thermogenesis in mice exempt from thermal stress by living at thermoneutrality. Cell Metabolism. 2009;9(2):203-9.

188. Himms-Hagen J, Hogan S, Zaror-Behrens G. Increased brown adipose tissue thermogenesis in obese (ob/ob) mice fed a palatable diet. Am J Physiol. 1986;230(3 pt 1):E274-E81.

189. Heaton JM. The distribution of brown adipose tissue in the human. J Anat. 1972;112(Pt 1):35-9.

190. Virtanen KA, Lidell ME, Orava J, Heglind M, Westergren R, Niemi T, et al. Functional brown adipose tissue in healthy adults. New England Journal of Medicine. 2009;360(15):1518-25.

191. Yeung HW, Grewal RK, Gonen M, Schöder H, Larson SM. Patterns of (18)F-FDG uptake in adipose tissue and muscle: a potential source of false-positives for PET. J Nucl Med. 2003;44(11):1789-96.

192. Cohade C, Osman M, Pannu HK, Wahl RL. Uptake in supraclavicular area fat ("USA-Fat"): description on 18F-FDG PET/CT. J Nucl Med. 2003;44(2):170-6.

193. Yoneshiro T, Aita S, Matsushita M, Kameya T, Nakada K, Kawai Y, et al. Brown adipose tissue, whole-body energy expenditure, and thermogenesis in healthy adult men. Obesity (Silver Spring). 2011;19(1):13-6.

194. Saito M, Okamatsu-Ogura Y, Matsushita M, Watanabe K, Yoneshiro T, Nio-Kobayashi J, et al. High incidence of metabolically active brown adipose tissue in healthy adult humans: effects of cold exposure and adiposity. Diabetes. 2009;58(7):1526-31.

195. Hanssen MJ, van der Lans AA, Brans B, Hoeks J, Jardon KM, Schaart G, et al. Short-term cold acclimation recruits brown adipose tissue in obese humans. Diabetes. 2015;[Epub ahead of print].

196. Vosselman MJ, van Marken Lichtenbelt WD, Schrauwen P. Energy dissipation in brown adipose tissue: from mice to men. Mol Cell Endocrinol. 2013;379(1-2):43-50.

197. Zingaretti MC, Crosta F, Vitali A, Guerrieri M, Frontini A, Cannon B, et al. The presence of UCP1 demonstrates that metabolically active adipose tissue in the neck of adult humans truly represents brown adipose tissue. FASEB J. 2009;23(9):3113-20.

198. Harms M, Seale P. Brown and beige fat: development, function and therapeutic potential. Nature Medicine. 2013;19(10):1252-63.

199. Lidell ME, Betz MJ, Dahlqvist Leinhard O, Heglind M, Elander L, Slawik M, et al. Evidence for two types of brown adipose tissue in humans. Nat Med. 2013;19(5):631-4.

200. Sharp LZ, Shinoda K, Ohno H, Scheel DW, Tomoda E, Ruiz L, et al. Human BAT possesses molecular signatures that resemble beige/brite cells. PLoS One [Internet]. 2012; 7(11):[e49452 p.].

201. van Marken Lichtenbelt WD, Vanhommerig JW, Smulders NM, Drossaerts JM, Kemerink GJ, Bouvy ND, et al. Cold-activated brown adipose tissue in healthy men. New England Journal of Medicine. 2009;360(15):1500-8.

202. Bahler L, Verberne HJ, Admiraal W, Stok WJ, Soeters MR, Hoekstra JB, et al. Differences in Sympathetic Nervous Stimulation of Brown Adipose tissue between the young and old and the lean and obese. J Nucl Med. 2015;[epub ahead of print].

203. van der Lans AA, Vosselman MJ, Hanssen MJ, Brans B, van Marken Lichtenbelt WD. Supraclavicular skin temperature and BAT activity in lean healthy adults. J Physiol Sci. 2016;66(1):77-83.

204. Carey AL, Formosa MF, Van Every B, Bertovic D, Eikelis N, Lambert GW, et al. Ephedrine activates brown adipose tissue in lean but not obese humans. Diabetologia. 2013;56(1):147-55.

205. Cypess AM, Chen YC, Sze C, Wang K, English J, Chan O, et al. Cold but not sympathomimetics activates human brown adipose tissue in vivo. Proc Natl Acad Sci USA. 2012;109(25):10001-5.

206. Cypess AM, Lehman S, Williams G, Tal I, Rodman D, Goldfine AB, et al. Identification and importance of brown adipose tissue in adult humans. New England Journal of Medicine. 2009;360(15):1509-17.

207. Vijgen GH, Bouvy ND, Teule GJ, Brans B, Hoeks J, Schrauwen P, et al. Increase in brown adipose tissue activity after weight loss in morbidly obese subjects. J Clin Endocrinol Metab. 2012;97(7):E1229-E33.

208. Takx R, Ishai A, Truong QA, MacNabb MH, Scherrer-Crosbie M, Tawakol A. Supraclavicular Brown adipose tissue FDG uptake and cardiovascular disease. J Nucl Med. 2016;[Epub ahead of print].

209. Drubach LA, Palmer EL, Connolly LP, Baker A, Zurakowski D, Cypess AM. Pediatric brown adipose tissue: detection, epidemiology, and differences from adults. J Pediatr. 2011;159(6):939-44.

210. Ring LE, Zeltser LM. Disruption of hypothalamic leptin signaling in mice leads to early-onset obesity, but physiological adaptations in mature animals stabilize adiposity levels. J Clin Invest. 2010;120(8):2931-41.

211. de Jesus LA, Carvalho SD, Ribeiro MO, Schneider M, Kim SW, Harney JW, et al. The type 2 iodothyronine deiodinase is essential for adaptive thermogenesis in brown adipose tissue. J Clin Invest. 2001;108(9):1379-85.

212. Zhang W, Bi S. Hypothalamic Regulation of Brown Adipose Tissue Thermogenesis and Energy Homeostasis. Front Endocrinol (Lausanne) [Internet]. 2015; 6(136).

CHAPTER 2: Reducing Adiposity in a Critical Developmental Window has Lasting Benefits in Mice

Part I: Manuscript

This chapter has been published in *Endocrinology*, 2016. 157(2); p. 666-678.

Jaclyn S. Lerea, Laurence E. Ring, Rim Hassouna, Angie C.N. Chong, Klara Szigeti-Buck, Tamas L. Horvath, Lori M. Zeltser

ABSTRACT

While most adults can lose weight by dieting, a well-characterized compensatory decrease in energy expenditure promotes weight regain more than 90% of the time. Using mice with impaired hypothalamic leptin signaling as a model of early-onset hyperphagia and obesity, we explored whether this unfavorable response to weight loss could be circumvented by early intervention. Early-onset obesity was associated with impairments in the structure and function of brown adipose tissue (BAT) mitochondria, which were ameliorated by weight loss at any age. Whereas decreased sympathetic tone in weight-reduced adults resulted in net reductions in BAT thermogenesis and energy expenditure that promoted rapid weight regain, this was not the case when dietary interventions were initiated at weaning. Enhanced energy expenditure persisted even after mice were allowed to resume over-eating, leading to lasting reductions in adiposity. These findings reveal a time window when dietary interventions can produce metabolic improvements that are stably maintained.

INTRODUCTION

Approximately 17% of U.S. children and adolescents are obese (1). As childhood obesity increases the risk of developing diabetes and cardiovascular disease (2), there is an urgent need to combat this epidemic. Many of the co-morbidities associated with obesity can be forestalled by maintaining even a modest degree of body weight loss (3, 4). Unfortunately, programs aimed at preventing childhood obesity involving "common sense" behavioral modifications to diet and/or physical activity have not produced significant improvements in body mass index (BMI) (5, 6). The contribution of resting energy expenditure (REE) to the risk of obesity and/or efficacy of intervention strategies in children has largely been ignored. This is a major oversight, since modest (4-7%) reductions in basal metabolic rate have been linked to increased risk of weight gain in non-dieting subjects (7) and are thought to promote regain in the weight-reduced state (8, 9).

There are two lines of evidence to suggest that there are discrete development periods when the "rules" of energy balance as defined in adults do not apply. First, a model that accurately predicts REE in young children and adults is consistently ~7% too low when applied to teens (10). Second, weight loss in young children is not necessarily followed by a compensatory decrease in free triiodothyronine (fT3), the active form of thyroid hormone that is often used as a surrogate measurement for basal metabolic rate (11). Moreover, the failure to exhibit a compensatory decrease in fT3 correlates with successful weight loss maintenance in young obese children (11). These observations

raise the possibility that there is a window of opportunity for weight loss interventions in young children without the compensatory decrease in REE that promotes regain.

A major obstacle to studying whether early interventions can produce sustained improvements in obesity-related outcomes in pre-clinical rodent models is the ability to generate obese animals before puberty is initiated at 4-5 weeks of age (12). We developed a mouse model of genetically-induced early-onset hyperphagia and obesity with the goal of identifying drivers of childhood obesity that respond to early intervention. Mice with genetically-induced hypothalamic leptin resistance (*Nkx2.1-Cre;Lepr*$^{flox/flox}$ mice, hereafter referred to as KOs) are hyperphagic and exhibit increased adiposity from weaning at 3 weeks of age (13). We used this model to explore whether a reduction in adiposity before puberty is not accompanied by a compensatory decrease in energy expenditure, and if true, whether early improvements in obesity-related outcomes are long-lasting.

METHODS

Mouse husbandry. All mouse protocols were overseen and approved by the Columbia University Medical Center Institutional Animal Care and Use Committee. Mice were maintained in a temperature (22+/- 1˚C) and light controlled (12 hours light: 12 hours dark) barrier facility. Unless otherwise indicated, mice were singly housed from weaning and had *ad libitum* access to chow (13.2% energy from fat, 5053* PicoLab Rodent Diet 20) and autoclaved drinking water.

Generation of Lepr^{HYP}KO mice. To disrupt LepRb signaling in the hypothalamus, mice homozygous for the floxed allele of *Lepr* (FVB.BKS(D)-*Lepr^{db}* provided by S. Chua, Albert Einstein College of Medicine) (14) were crossed with the *Nkx2.1-Cre* driver line (C57BL/6J-Tg(Nkx2.1-Cre)2Sand/J provided by S. Anderson, Weill Cornell Medical College) (15). F1 heterozygotes (*Nkx2.1-Cre;Lepr$^{fl/+}$*) were intercrossed to create an F2 generation of *Lepr$^{Nkx2.1}$*KO mice and Lepr$^{fl/fl}$ control mice. Mice were tail-tipped at 18-20 days of age and genotyped using PCR on genomic DNA using the following primers:

Cre 5'-GCGGTCTGGCAGTAAAAACTATC-3' (forward);

Cre 5'-GTGAAACAGCATTGCTGTCACTT-3' (reverse);

Lepr 5'-GTCTGATTTGATAGATGGTCTT-3' (forward);

Lepr 5'-AGAATGAAAAAGTTGTTTTGGGA-3' (forward);

Lepr 5'-ACAGGCTTGAGAACATGAACAC-3' (reverse).

Paired-feeding paradigm. Mice were weaned at 3weeks and chow was provided in custom-made stainless steel feeding baskets that minimized spillage (Dieter Wenzel; Detmold, Germany). Food intake was measured daily by weighing the baskets. Pair-fed

(PF) groups were provided with the same amount of food consumed by controls the day before (1/3 of the amount in the morning and 2/3 at night). Adiposity levels at weaning were used as a guide to ensure that *ad libitum* and pair-fed groups would be evenly matched. For the adult caloric restriction (CR) challenge, 13 week old mice that had been previously fed *ad libitum* were restricted by 64-75% to achieve a 15% weight loss over a 2-week period, after which point they were either released to *ad libitum* feeding or sacrificed (KO-adult CR group, Figure 2.1). In other cohorts, paired-feeding was initiated either at 3 weeks or at 5 weeks of age and maintained until sacrifice at 10 weeks of age (PF^{3wk} and PF^{5wk} groups, respectively, Figure 2.1). Some cohorts of males and females that were PF from 3 weeks were released to *ad libitum* feeding at 10 weeks and sacrificed at 18-20wks (8-10wks after release to *ad libitum* feeding)(KO-PF→AL groups, Figure 2.1). Mice were excluded from the study if they could not properly eat out of the feeding baskets. Experimenters were not blinded to experimental groups of animals.

***In vivo* measurements.** Mice were weighed 3 times per week. Body composition was assessed on a weekly or bi-weekly basis using nuclear magnetic resonance imaging (Minispec, Bruker). Naso-anal length was measured on anesthetized animals (4% isoflurane) biweekly. Starting at 9wks and 17wks of age, oxygen consumption, carbon dioxide production, food intake and locomotor activity were measured simultaneously for a week using a 16-cage, Indirect Calorimetry System combined with Feeding Monitor and TSE ActiMot system (TSE-Systems). Metabolic cage data were obtained from KO-adult CR mice over 10 days. Measurements from the first 24h were discarded. Resting energy expenditure was calculated by averaging heat of each individual mouse when their locomotor activity was <10 total beam breaks (x and y directions combined) per minute.

Preservation of brown adipose tissue. On the day before sacrifice, mice were subjected to an overnight fast at room temperature. On the morning of sacrifice, mice were anesthetized using 2.5% Avertin (0.02mL/g i.p.) before undergoing a terminal bleed (serum) and cervical dislocation. Brown adipose tissue was collected and portions were preserved in the following ways: All Protect (for gene expression)(Qiagen), in Z-fix (for histology) or in 4% paraformaldehyde, 0.08% gluteraldehyde for 4 hours and then overnight in 4% paraformaldehyde (for electron microscopy (EM)). Tissues for EM were transferred to 0.1M phosphate buffer the following day and sent to Yale University for processing. Samples used for tyrosine hydroxylase protein quantification were flash frozen in liquid nitrogen and stored in -80˚C freezer until used.

Brown adipose tissue morphology. Z-fixed brown adipose tissue was paraffin-embedded and 5μm sections were stained with hemotoxylin and eosin (H&E). Images were acquired at 10x and 20x magnification using a Nikon Eclipse 80i equipped with a Retiga EXi camera. Lipid droplet size and number were calculated using Image J software (NIH). At least 2 images per mouse and at least 3 mice per group were analyzed.

Electron microscopy analysis of brown adipose tissue. Brown adipose tissue samples were fixed in 4% paraformaldehyde, 0.1% glutaraldehyde in 0.1M phosphate buffer (PB, pH 7.3) for 1h. They were washed several times in PB followed by post-fix in 1% OsO_4 for 30min, then dehydrated through increasing concentrations of alcohol (the 70% ethanol contained 1% uranyl acetate) followed by propylene oxide. Samples were embedded in Durcupan and then sectioned (70 nm) using a Leica Ultracut ultramicrotome. The sections were placed on formvar coated grids and examined under

an FEI BioTwin electron microscope equipped with an AMT XR16 camera. Pictures were taken at a direct magnification of 4800x.

Brown adipose tissue gene expression. We isolated total RNA using the RNeasy Universal Mini kit (Qiagen) and synthesized cDNA using Transcriptor First Strand cDNA Synthesis kit (Roche). We used a LightCycler 480 SYBR Green I Master System (Roche) in quantitative PCR experiments. We normalized the expression of target genes against *b-actin*. Primer sequences are provided in Supplemental Table 2.1.

Measurement of glucose, leptin, free T3 and free T4. All blood samples were collected between 10am and 12pm. Fasting blood samples were obtained from mice following 16h of fasting with *ad libitum* access to drinking water. Blood was collected by orbital sinus puncture in isoflurane-anesthetized mice. The blood was allowed to clot for 1h and then centrifuged at 3000g for 15min. Serum was decanted and stored at -20˚C until used in leptin (Millipore) or fT3/fT4 analysis (Leinco Technology, Inc) ELISAs, per the manufacturer's protocol. Whole blood for glucose levels were taken via tail-nick on unanaesthetized mice and measured using a glucometer with disposable test strips (Abbott). A "HI" reading was given a value of 501mg/dl. Glucose tolerance tests (2g/kg, i.p. D-glucose) were administered at 5wks after an overnight fast. Whole blood glucose was assayed via tail nick at baseline, and 30, 60, 90, and 120 minutes after injection.

Protein analysis: Brown adipose tissue proteins were extracted in RIPA buffer (ThermoFisher Scientific) with the addition of protease and phosphatase inhibitors (ThermoFisher Scientific). Protein quantification was performed via the Pierce BCA protein assay kit (ThermoFisher Scientific). Western blotting was performed using 30μg

of protein from each sample, and polyacrylamide gel electrophoresis was performed using a 10% Tris-glycine gel. Tyrosine hydroxylase was detected using tyrosine hydroxylase antibody (Millipore) normalized to b-actin (Abcam), both primary antibodies were incubated at 4˚C overnight. Fluorescent secondary antibodies were used (Rockland, LI-COR) for fluorescent imaging such that each primary antibody was detected in a different channel. Fluorescence was measured via Odyssey v3.0 imaging program.

Statistical Analysis: Data are presented as group mean ± SEM. Pilot experiments were used to determine initial statistical power. Power analysis was performed post-hoc for subsequent experimental data. We performed statistical comparisons between 2 groups using an equality of variance test, and then performing Student's or Welch's t-test accordingly. We performed statistical comparisons between multiple groups using a one-way ANOVA, followed Fisher's PLSD post-hoc analysis. Data using percentages were transformed using arcsine transformation, before performing a one-way ANOVA and post-hoc test. We considered a P value of 0.05 or less to be statistically significant. Statistical significance was determined using StatView statistical software.

RESULTS

Compensatory decrease in energy expenditure in weight-reduced adult KOs

We first assessed the response of mature KOs to a 15% reduction in body weight, a condition known to elicit a compensatory decrease in energy expenditure in humans and rodents (8, 16). To this end, we compared energy expenditure in 13-week-old male KOs at baseline and after weight loss was achieved by restricting caloric intake by 25-35% for a 2 week period (Figure 2.2A). All weight-reduced KOs exhibited lower resting energy expenditure (REE) (Figure 2.2B), which likely contributed to rapid weight regain following release to *ad libitum* feeding (Figure 2.2A). The 33.4% decrease in REE was also reflected in a 46.5% decrease in the expression of uncoupling protein 1 (*Ucp1*) mRNA in brown adipose tissue (BAT), the mitochondrial protein responsible for thermogenesis in this organ (17, 18) (Figure 2.2C). Decreased energy expenditure was not associated with a change in expression levels of the mRNA encoding deiodinase 2 (Dio2*)* in BAT, which can enhance adrenergic stimulation of *Ucp1* expression by converting the inactive form of thyroid hormone (thyroxine - T4) to the active form (triiodothyronine -T3) (19) (Figure 2.2C).

Young KOs increase energy expenditure after caloric restriction due to improved BAT function

Next we examined whether weight loss achieved by caloric restriction at a young age might not be accompanied by the compensatory decrease in energy expenditure that is always seen in adults. KO males were pair-fed to the intake of control littermates (CON) from weaning at 3 weeks through 10 weeks of age, corresponding to a ~36% reduction in

daily caloric intake (KO-PF^{3wk} group in Figure 2.1). To compare energy expenditure in pair-fed (KO-PF^{3wk}) and *ad libitum*-fed (KO-AL) KOs at 10 weeks of age, we first generated a regression equation relating REE, as measured by indirect calorimetry (TSE Systems), to fat mass and lean mass in KO-ALs. We then calculated differences in REE, or "residuals", between the two groups by comparing the actual energy expenditure in KO-PF^{3wk} to predicted values of KO-ALs (20-22).

In contrast to what we observed in weight-reduced adults, KO-PF^{3wk} males at 10 weeks expended 37.8% more energy than predicted for a KO-AL of the same body composition (Figure 2.3A). This increase was not accompanied by increased locomotor activity (Figure 2.3B). Next we measured circulating concentrations of free T3 (fT3), the active form of thyroid hormone that usually correlates closely with basal metabolic rate in rodents (23) and its prohormone, fT4. To minimize confounding effects of different feeding patterns on thyroid hormone levels in PF and AL mice, measurements were taken after an overnight fast. While serum concentrations of fT4 were similar in the two groups, levels of fT3 were 37% higher in KO-PF^{3wk} males (Figure 2.3C). These observations support the idea that there is a period of time in young animals when weight loss is not inextricably followed by a compensatory decrease in energy expenditure.

Decreased oxygen consumption of BAT in LepR-deficient mice and rats (*db/db* and *fa/fa*, respectively) is associated with an increase in unilocular adipocytes at the expense of multilocular adipocytes and reduced expression of the thermogenic gene *Ucp1* (24, 25). Thus, we examined whether increased energy expenditure of KO-PF^{3wk} mice is

accompanied by improvements in these endpoints. Whereas BAT of 10 week-old controls was largely comprised of multilocular adipocytes with small lipid droplets (<200μm^2) (Figure 2.3E), KO-AL mice had 73.7% fewer small lipid droplets, and a corresponding increase in medium (201-1000μm^2) and large (>1000μm^2) lipid droplets (Figure 2.3F, H-J). At the end of the PF period, the BAT of KO-PF^{3wk} mice contained fewer medium-sized lipid droplets and a trend toward more small-sized droplets (Figure 2.3G, H-J). The shift toward a more multilocular organization of BAT in KO-PF^{3wk} mice was accompanied by increased expression of *Ucp1* (131%, p<0.01) and *Dio2* (138%, N.S.)(Figure 2.3D). These observations are consistent with the idea that improved BAT structure due to restricted feeding underlies the increased *Ucp1* expression and energy expenditure of KO-PF^{3wk} mice.

Persistent increases in energy expenditure and reduced adiposity

As changes in the activity of thermogenic circuits in the peri-weaning period lead to persistent increases in thermogenic capacity (26, 27), we examined whether improved BAT function and increased rates of REE in KO-PF^{3wk} males could be stably maintained. To this end, we assessed body composition, metabolic and BAT phenotypes in KO-PF^{3wk} males that were released to *ad libitum* feeding from 10-20 weeks of age (KO-PF→AL group in Figure 2.1). REE of KO-PF→AL males was 15.3% higher than KO-AL littermates at 20 weeks (Figure 2.4A) and was not due to increased locomotor activity (Figure 2.4B). Similarly, serum levels of fT3 were 41% higher in KO-PF→AL mice, while circulating concentrations of fT4 were not significantly different (Figure 2.4C).

Consistent with previous reports (28), the number of small multilocular adipocytes was stable from 10-20 weeks in all groups (Figure 2.4E-H). In KO-AL mice, there was a trend toward an increase in the number of large lipid droplets at the expense of medium droplets (1059 medium vs. 80 large at 10 weeks; 748 medium vs. 87 large at 20 weeks)(Figure 2.4I-J). Conversely, the number of large droplets was significantly lower in KO-PF→AL mice at 20 weeks (Figure 2.4J). In parallel with persistent effects of early PF on BAT morphology, expression of thermogenic genes trended higher in BAT of PF→AL mice (increases of 68.3% in *Ucp1* and 84.3% in *Dio2*), although these differences did not reach significance (Figure 2.4D). These findings are reminiscent of reports that interventions in young leptin-deficient *ob/ob* mice programmed lasting improvements in BAT morphology and thermoregulatory activity (29).

We next assessed whether lasting increases in REE due to caloric restriction from a young age were also reflected in improved obesity-related endpoints in KO-PF→AL mice at 20 weeks in both males (Figure 2.5) and females (Supplemental Figure 2.1). In response to reduced caloric intake, KO-PF^{3wk} mice initially defended the same elevated levels of adiposity as seen in KO-ALs at the expense of lean mass deposition (Figure 2.5A-C, Supplemental Figure 2.1A-C), similar to observations in LepR-deficient mice and rats (30, 31). In contrast to pair-fed global LepR knockouts, the adiposity of KO-PF^{3wk} males and females diverged from KO-AL littermates at 6 weeks of age and were stably maintained, such that they were 18.9% lower at the end of PF in males (Figure 2.5A) and 14.9% lower at the end of PF in females (Supplemental Figure 2.1A).

After release to *ad libitum* feeding, KO-PF→AL mice rapidly increased food intake, reaching KO-AL levels within 1 week of *ad libitum* feeding (Figure 2.5). Increased food intake was immediately followed by increases in lean mass deposition and body weight. Lean mass reached KO-AL levels within 3 weeks of *ad libitum* feeding, while body weight caught up more gradually (Figure 2.5). However, they maintained stable levels of adiposity through 20 weeks (Figure 2.5). Consistent with reduced adiposity, serum leptin levels were 47.5 and 35.8% lower in KO-PF→AL males at 11-12 weeks and 19-21 weeks, respectively (Supplemental Figure 2.2). While fed and fasting levels of blood glucose were reduced by caloric restriction, GTTs in KO-PF mice at 5 weeks of age were not improved by reduced food intake, consistent with the critical role for hypothalamic LepR signaling in circuits regulating glucose homeostasis (32) (Supplemental Figure 2.3). Reductions in random-fed blood glucose levels of KO-PF^{3wk} males during paired-feeding did not persist after release to *ad libitum* feeding, consistent with the idea that increased caloric intake is a major driver of hyperglycemia in the fed state (Supplemental Figure 2.3). In conclusion, restricted feeding from a young age programmed lasting improvements in BAT morphology and activity, promoting deposition of lean mass at the expense of fat mass during the period of rapid growth that followed release to *ad libitum* feeding.

Reduced caloric intake improves BAT mitochondrial structure regardless of age

Dense packing of cristae within mitochondria is correlated with metabolic output of BAT (33, 34). Conversely, distorted organization of cristae has been proposed to underlie deficits in BAT thermogenesis observed in genetic models of obesity (24, 35, 36). We

performed electron microscopy to examine whether improved mitochondrial organization contributed to enhanced BAT function in KO-PF^{3wk} mice at the end of PF (10 weeks) and after release to *ad libitum* feeding (20 weeks). As expected, lean controls exhibited tightly-packed cristae at 10 and 20 weeks (Figure 2.6A,F), while 26.1% and 17.4% of KO-AL mitochondrial cristae at 10 weeks and 20 weeks, respectively, formed loops, branches or other abnormal configurations (Figure 2.6B,E,G). Paired-feeding from weaning reduced the percent of abnormal cristae by 65.8% (Figure 2.6C,E) and produced marked improvements in mitochondrial organization that persisted even after release to *ad libitum* feeding (Figure 2.6H). In conjunction with improved mitochondrial structure, expression of BAT mitochondrial genes was higher in KO-PF^{3wk} mice than in KO-AL mice at both 10 and 20 weeks (Figure 2.6L,M).

We next considered whether the failure to observe increased energy expenditure in KO mice that were calorically-restricted in adulthood (KO-Adult CR group in Figures 2.1 and 2.2), reflected a failure to impact mitochondrial structure. After 2 weeks of CR, mitochondrial organization was markedly improved, as reflected in increased density of cristae (8.6±.64 KO-AL vs. 12.5±1.8 KO-Adult CR, $p<0.05$) and presence of fewer abnormal cristae (17.5% KO-AL vs. 6.6% KO-Adult CR, $p<0.05$)(Figure 2.6I-K). Despite the dramatic improvement in mitochondrial organization produced by caloric restriction in adult KOs, expression of mitochondrial genes was generally unchanged or reduced (Figure 2.2C, 2.6N), consistent with compensatory decreases in energy expenditure in the weight-reduced state (Figure 2.2B). While restoring densely-packed

cristae in KOs likely increases the capacity of BAT to respond to thermogenic stimuli, it is not sufficient to normalize BAT thermogenic activity.

The peri-weaning period is a critical window for intervention

Studies in diet- and genetically-induced obese models support the idea that the ability to normalize body weight and adiposity declines with age (37-40). As diminished efficacy of interventions can be observed within a few weeks of weaning (38, 39), we assessed metabolic responses of KOs to paired-feeding that was initiated at 5 weeks (KO-PF^{5wk} group in Figure 2.1). We found that REE in roughly half of KO-PF^{5wk} males was higher than KO-ALs at 10 weeks (Figure 2.7A, black bar), similar to the aggregate response observed in KO-PF^{3wk} males (Figure 2.3A). The remainder of the group exhibited decreased energy expenditure (Figure 2.7A, white bar), similar to the response of adults to acute weight loss (Figure 2.2B). Increased REE in a subset of KO-PF^{5wk} mice correlated with a trend toward higher serum fT3 levels as compared to age- and exposure-matched KO-PF^{5wk} mice that decreased REE in response to PF (Figure 2.7B). Moreover, mice that increased REE in response to PF gained significantly less adiposity during the PF period than those that decreased REE (8.3% vs. 26.6%, P=0.01)(Figure 2.7C). This inverse relationship between REE and percent adiposity gained was maintained across the cohort of mice that were PF from 5 weeks (Figure 2.7D). Thus, 5 weeks of age likely represents the outer limit of the critical period for weight loss interventions that do not necessarily involve compensatory reduction in REE in our model. These findings are reminiscent of bimodal responses of children to weight loss, as well the relationship between increased fT3 levels and successful weight loss maintenance (11).

DISCUSSION

We utilized a mouse model of genetically-induced hyperphagia and obesity to study why weight loss interventions in younger obese children produce better outcomes than in older adolescents and adults (41-43). The KO mice exhibited developmental deficits in BAT activity and resting energy expenditure, creating a vicious cycle that further exacerbates obesity. Caloric restriction at any age improved BAT structure and capacity (Figure 2.6), consistent with reports in other genetic models of obesity (44-46). The key difference between early vs. late intervention was that weight loss before 5 weeks was also accompanied by *increased* fT3, BAT activity, and energy expenditure (Figures 2.3 and 2.4), while intervention afterward was associated with *decreases* in these endpoints (Figure 2.2). The extent to which decreases in adiposity were stably maintained in males after 10 weeks of *ad libitum* feeding (19%, Figure 2.5), is similar to the 20-23% reduction achieved by bariatric surgery in adult mice (47, 48).

Our observations are reminiscent of reports that weight loss in some children is not necessarily followed by reduced fT3 (11), while reduced fT3 is nearly always observed in weight-reduced teens (49) and adults (9). As failure to exhibit reduced fT3 in the weight-reduced state was associated with better weight loss maintenance (11), it supports the idea that our mouse model of early-onset obesity can provide novel mechanistic insights into temporal and molecular determinants of efficacious weight-loss strategies in children.

Early-onset hyperphagia and obesity lead to developmental deficits in mitochondrial structure and BAT activity

Decreased energy expenditure in genetically obese rodents precedes the onset of hyperphagia and contributes to increased adiposity (50-54). Cristae malformations that impair mitochondrial function in these models (34, 55) are closely correlated with decreased energy expenditure (24, 35, 36). Thus, it has been proposed that impaired BAT mitochondrial structure reduces the capacity to respond to cold or sympathetic signals, leading to decreased rates of thermogenesis (24, 36, 56-59). Sympathetic signals that activate BAT are also lower in genetically obese mice, and thus could further reduce BAT output (60-63).

While endpoints related to energy expenditure are rarely examined in human adolescents, several studies reported that BAT activity (64-66) and REE (10) are higher than in adults. Failure to develop robust BAT activity in adolescents is associated with increased BMI and adiposity (65, 67), similar to what is found in rodent models (current study and (50, 68, 69)). These observations are consistent with the idea that early impairments in BAT structure and function underlie observations that childhood obesity is often established within the first few years of life (70, 71).

Increasing BAT capacity and activity reduces adiposity in obese mouse models

We observed that KO mice at 10 weeks have more abnormal cristae per mitochondrion as compared to lean control littermates, which is largely reversed by paired feeding (Figure 2.6). While paired feeding in *ob/ob* mice also enhances BAT mitochondrial structure and

capacity, leptin-deficient mice exhibit increased adiposity - the opposite of what is observed in KO-PFs. Combining paired feeding with administration of an exogenous BAT activator, such as T3, leads to reduced adiposity in *ob/ob* mice (72). These observations support the idea that there is thermogenic activator that is disrupted in global leptin knockouts, but is preserved in KO-PFs.

In theory, reductions in BAT-activating signals in *ob/ob* mice could be caused directly by deficits in leptin signaling and/or secondary effects of hyperphagia and increased circulating levels of glucose that accompany the transition to a carbohydrate-based diet at weaning. As we do not observe reductions in adiposity in pair-fed KOs until 6-7 weeks of age, despite the fact that mice have been consuming less food since weaning at 3 weeks, it is likely that factors independent of diet are the primary drivers of increased energy expenditure. The idea that BAT thermogenesis directly contributes to the metabolic improvements in KO-PFs is supported by the fact that reduced adiposity is first detected at 6-7 weeks of age, the same time that this strain develops the capability to mount a thermogenic response to cold (13, 73). It is not likely that "browning" or white adipose depots significantly contributes to metabolic benefits of paired feeding, as we did not detect *Ucp1* expression in gonadal or inguinal depots of KO-PFs (data not shown – please refer to Appendix I). Thus, we hypothesize that the ability of paired feeding to reduce adiposity in the conditional KOs stems from increased endogenous activation of BAT thermogenesis via LepR-mediated signals that are not impacted by *Nkx2.1-Cre*-mediated recombination ((13, 15), as discussed in (73)). The failure to detect an increase in tyrosine hydroxylase protein content in BAT, a surrogate for sympathetic tone (74)

(Supplemental Figure 2.5), raises the possibility that the factors responsible for increased thermogenesis in KO-PFs are not sympathetically driven. Determining whether any of the growing list of adrenergic-independent brown fat activators (75) are involved is an important area for future study.

Hypothalamic leptin signals influence sympathetic outflow to BAT (76, 77) and function of the thyroid axis (13). Therefore, it is possible some features of the mechanism driving increased energy expenditure in KO-PFs may be uniquely activated in this model, or may also apply to other situations involving congenital deficits in thermoregulatory and/or thyroid function. Reports that leptin's ability to reduce adiposity independent of food intake is dependent on BAT thermogenesis (78), is consistent with the possibility that some of the underlying signaling pathways will be shared. Ascertaining the generalizability of these findings is an important area for future research, but is hampered by the lack of mouse models with intact leptin signaling pathways that exhibit pronounced obesity before the end of the critical period at 5 weeks. Even if the pathways responsible for increased REE in KO-PFs are unique to this model, evidence that patterns of BAT innervation and activity are programmed during the peri-weaning period (27, 79) supports the idea that the time window for efficacious interventions in obesity is before puberty.

Working model (Figure 2.8)

In adolescent children (65, 67) and mouse models (current study and (50, 57, 68, 69)), the failure to develop robust BAT thermogenic activity leads to increased adiposity. We

hypothesize that the paradoxical increase in fT3 and REE in young weight-reduced mice or humans stems from improved mitochondrial structure and enhanced capacity to respond to stimuli that are circulating at high levels during adolescence. Patterns of increased BAT activity and rates of REE resulting from early intervention are permanently programmed (27, 79), as they persist even after KO-PFs resume overeating. In contrast, any improvements in BAT capacity after adolescence (KO-CR) would be negated by compensatory decreases in sympathetic tone (9, 80-82), the primary driver of BAT activity in the adult rodent (83). If our model is correct, impacts of interventions that enhance BAT capacity in time to respond to factors driving the peak of BAT activity during adolescence could explain observations that intervention in pre-pubertal children has higher success rates (41-43).

Acknowledgements

We thank the Columbia Diabetes and Endocrinology Research Center Animal Phenotyping Core for help with metabolic cages and BAT histology (P30 DK063608); S. Anderson (Weill Cornell Medical College) for *Nkx2.1-Cre* mice; S. Chua (Albert Einstein College of Medicine) for *Lepr* floxed mice; Marya Shanabrough (Yale University School of Medicine) for embedding samples and performing electron microscopy; and Tony Bianco (RUSH University Medical Center) for deiodinase assays and hormones measurements. This work was supported by R01 DK 089038 (LMZ), National Center for Advancing Translational Sciences, NIH, through Grant Number UL1 TR000040, the HHMI-funded "Med into Grad" program (JSL), T32 GM008464 (LER) and the Russ Berrie Foundation (R.H.).

FIGURES

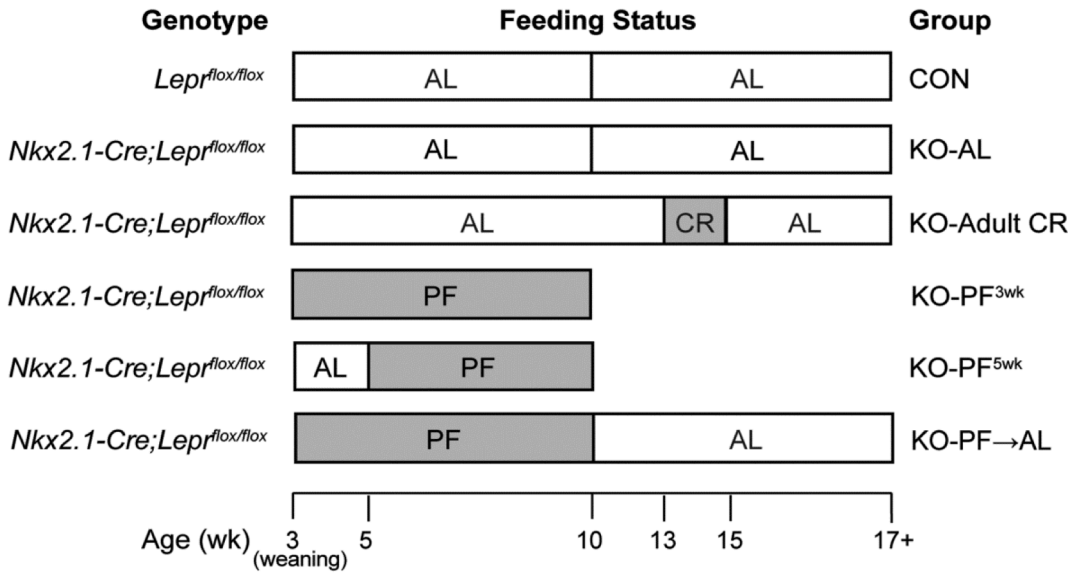

Figure 2.1. Experimental groups. Control and KO-AL groups were fed *ad libitum* throughout the study. Adult CR mice were fed *ad libitum* from 3-13 weeks, then calorically restricted from 13 to 15 weeks of age. KO-PF^{3wk} mice were pair-fed from 3-10 weeks of age, while paired feeding was started at 5 weeks of age in KO-PF5^{wk} mice. KO-PF→AL mice were pair-fed from 3-10 weeks of age and then released to ad libitum feeding for at least 8 weeks.

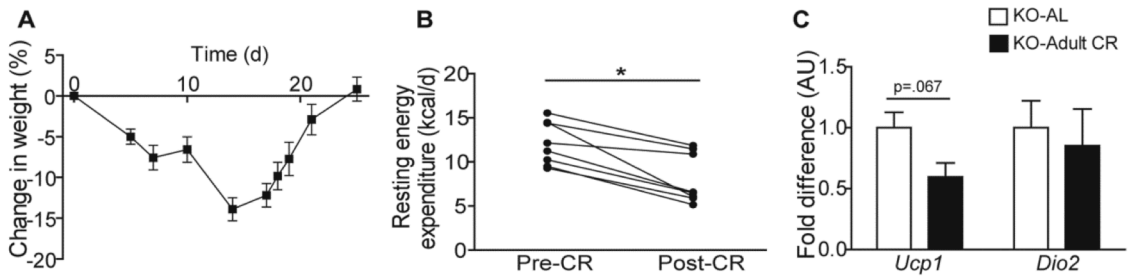

Figure 2.2. Decreased energy expenditure in adult Lep^{HYP}KOs (KO) following weight loss. A) Percent weight change during caloric restriction (CR) and after release to *ad libitum* feeding. B) Resting energy expenditure before CR (Pre-CR) and at the end of the 2-week period of CR (Post-CR). C) Relative expression levels of *Ucp1* and *Dio2* in BAT from *ad libitum*-fed KOs (white bars) vs. KOs after 2wk CR (black bars). Error bars represent SEM. * represents $p<.05$, paired t-test. For gene expression, data were tested for equality of variance, and *p*-values were determined by Student's t-test. Data were generated from n=8 per group from 2 independent cohorts for energy expenditure and n=4-6 per group from 1-2 cohorts for gene expression.

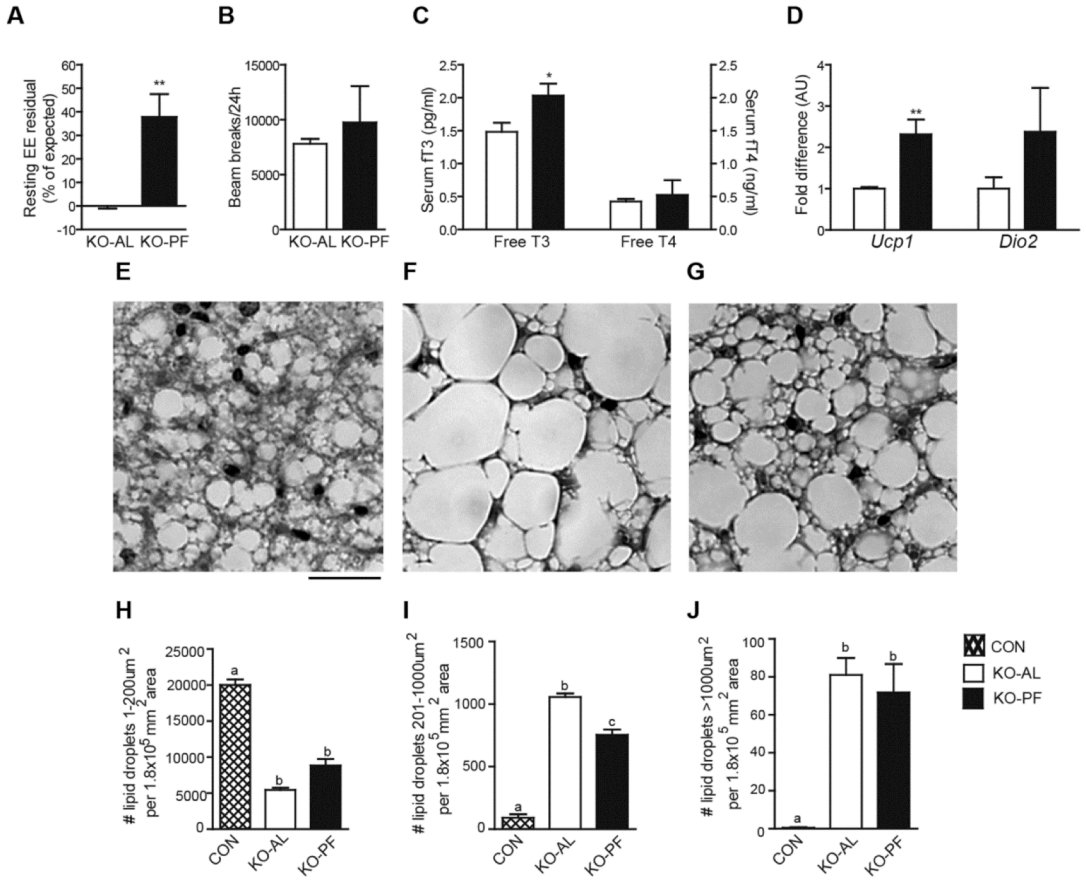

Figure 2.3. Paired-feeding results in increased energy expenditure due to improved BAT function. (A-D) Energy expenditure-related phenotypes at 10 weeks of age, the end of the PF period, in *ad libitum*-fed KOs (white bars) vs. pair-fed KOs (black bars). (A) Resting energy expenditure. (B) Locomotor activity. (C) Serum levels of free T3 and free T4. (D) Relative expression levels of *Ucp1* and *Dio2* in BAT. (E-G) BAT morphology revealed by H&E staining in *ad libitum*-fed controls (E), *ad libitum*-fed KOs (F) and pair-fed KOs (G) taken at 20x magnification, scale bar represents 100μm. (H-J) Quantification of small (<200μm^2)(H), medium (201-1000μm^2)(I), and large (>1001μm^2)(J) lipid droplets in BAT from controls (hatched bars), *ad libitum*-fed KOs (white bars) and pair-fed KOs (black bars). Error bars represent SEM. * represents

$p<.05$, ** represents $p<.01$. (A-D) Data were tested for equality of variance, and *p*-values were determined by either Student's or Welch's t-test accordingly. (H-J) *P*-values were determined by ANOVA and post-hoc Fisher's LSD. Letters (a,b,c) represent differences between groups. Data were generated from: n=5-10 per group from 1-2 independent cohorts for REE; 3-4 per group from 1 cohort for locomotor activity; 3-9 per group from 1-2 independent cohorts for fT3; 3-4 mice from 1 cohort for fT4; n=3-11 per group from 2 independent cohorts for gene expression. Lipid droplet quantification was performed on n=3-5 per group from 1 cohort.

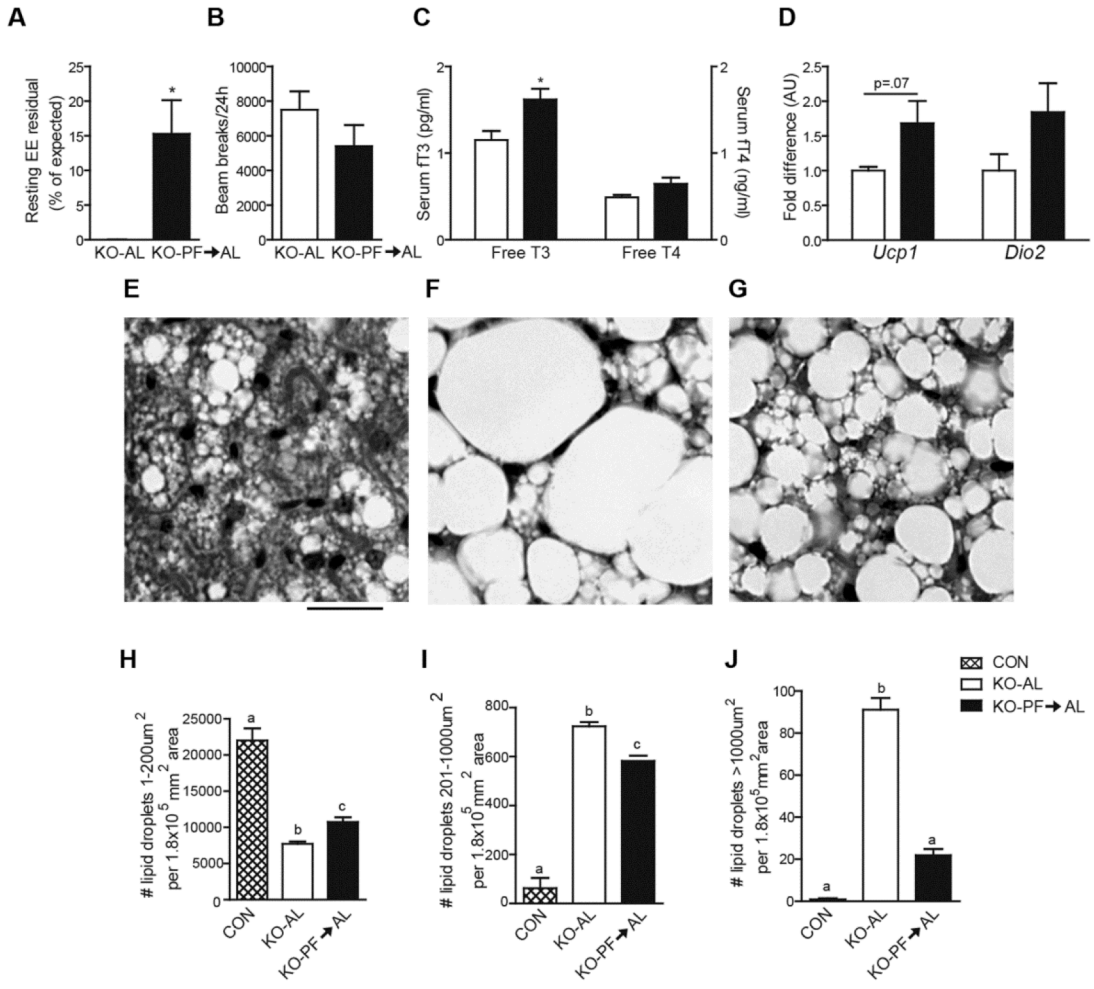

Figure 2.4. Improvements in energy expenditure and BAT morphology persist into adulthood. (A-D) Energy expenditure-related phenotypes at 17-20 weeks of age, after several weeks on *ad libitum* feeding, in KOs that were always fed *ad libitum* (white bars) vs. KOs that were previously pair-fed (black bars). (A) Resting energy expenditure. (B) Locomotor activity. (C) Serum levels of free T3 and free T4. (D) Relative expression levels of *Ucp1* and *Dio2* in BAT. (E-G) BAT morphology revealed by H&E staining in *ad libitum*-fed controls (E), *ad libitum*-fed KOs (F) and previously pair-fed KOs (G) taken at 20x magnification, scale bar represents 100μm. (H-J) Quantification of small (<200μm^2)(H), medium (201-1000μm^2)(I), and large (>1001μm^2)(J) lipid droplets in

BAT from *ad libitum*-fed controls (hatched bars), *ad libitum*-fed KOs (white bars) and previously pair-fed KOs (black bars). Error bars represent SEM. * represents $p<.05$, ** represents $p<.01$. (A-D) Data were tested for equality of variance, and *p*-values were determined by either Student's or Welch's t-test accordingly. (H-J) *P*-values determined by ANOVA and post-hoc Fisher's LSD. Letters (a,b,c) represent differences between groups. Data were generated from: n=6-7 per group from 2-3 independent cohorts for REE; n=3-6 per group from 1 cohort for locomotor activity; n=6-11 per group from 3 independent cohorts for fT3; n=3-9 per group from 1-2 independent cohorts for fT4; n=6-11 per group from 3-4 cohorts for gene expression. Results from lipid droplet analysis are based on analyses of n=4-6 per group from 1-2 independent cohorts.

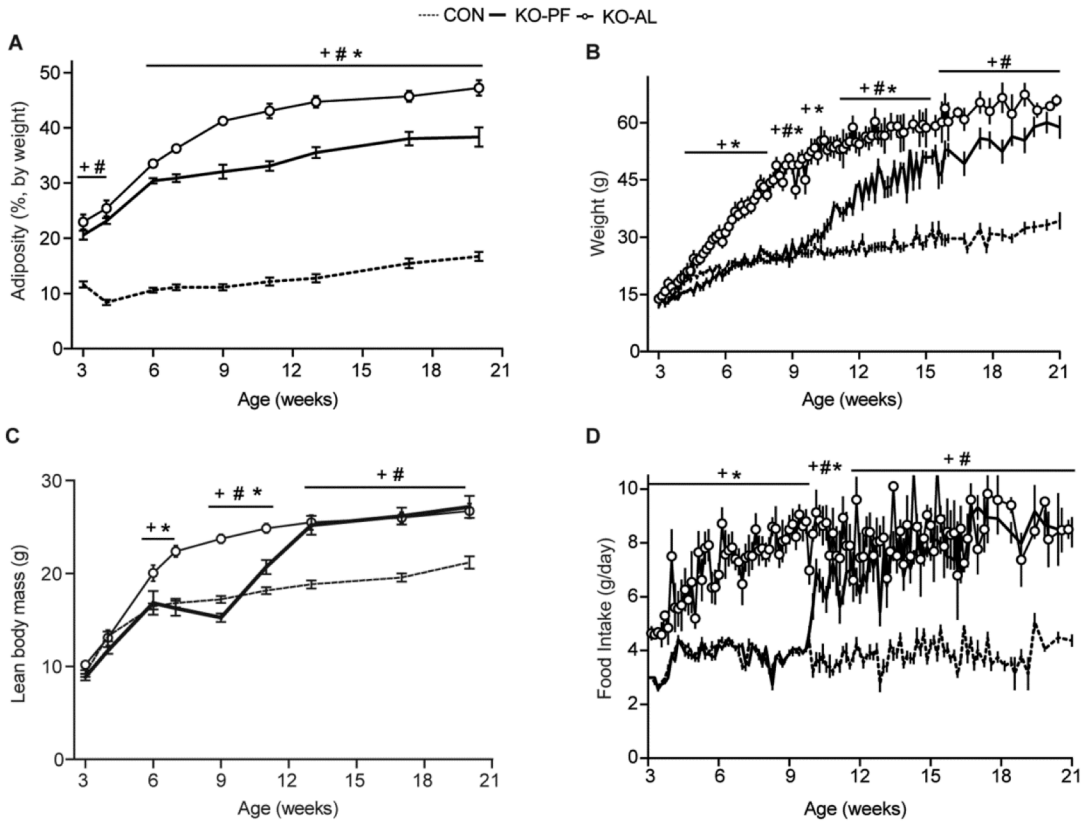

Figure 2.5. Paired-feeding of KO mice at an early age results in persistent changes in body weight and adiposity. Percent body fat (A), body weight (B), naso-anal length (NAL) (C), and food intake (D) in *ad libitum*-fed controls (dashed line) vs. *ad libitum*-fed KOs (medium-thickness line with white circles) vs. KOs that were pair-fed from 3-10 weeks of age (thick line). *P* values were determined by ANOVA and post-hoc Fisher's LSD. * represents $p<.05$ between AL and PF group, # represents $p<.05$ between PF and CON groups, and + represents $p<.05$ between AL and CON groups. Data were generated from n=4-20 per group from 4-5 independent cohorts.

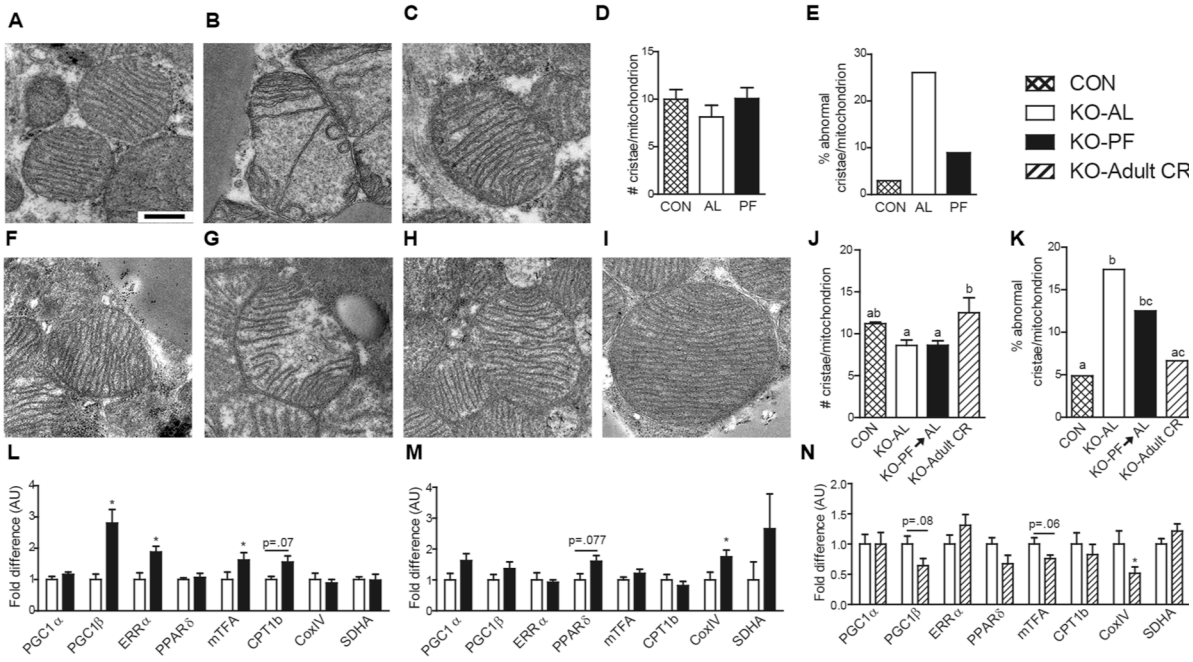

Figure 2.6. Caloric restriction at any age improves BAT mitochondrial structure. Electron micrographs of BAT at 10 weeks of age (A-C) and in adults (F-I). Scale bar represents 500nm. Images were used to calculate average number of cristae per mitochondrion (D, J) and the percent of abnormal cristae (E, K) in *ad libitum*-fed controls (A, F, hatched bars), *ad libitum*-fed KOs (B, G, white bars), KOs pair-fed from 3-10 weeks of age (C, H, black bars) and KOs that were exposed to CR in adulthood (I, diagonal stripes). (L-N) Relative expression levels mitochondrial genes in BAT at 10 weeks (KO-AL vs. KO-PF) (L), 20 weeks (KO-AL vs. KO-PF) (M), and following CR in adulthood (KO-AL vs. KO-Adult CR) (N). *P*-values for mitochondrial analyses were determined by ANOVA and post-hoc Fisher's LSD. *P*-values for % abnormal cristae were determine by performing arcsine transformation prior to an ANOVA and post-hoc test. *P*-values for gene expression were determined by first performing an equality of variance test, then performing Student's or Welch's t-test accordingly. Data were

generated from: n=3-4 per group at 10 weeks from 1 cohort; n=3-6 adults per group at 20 weeks from 1-2 independent cohorts; n=5 KO-adult CR per group from 2 independent cohorts.

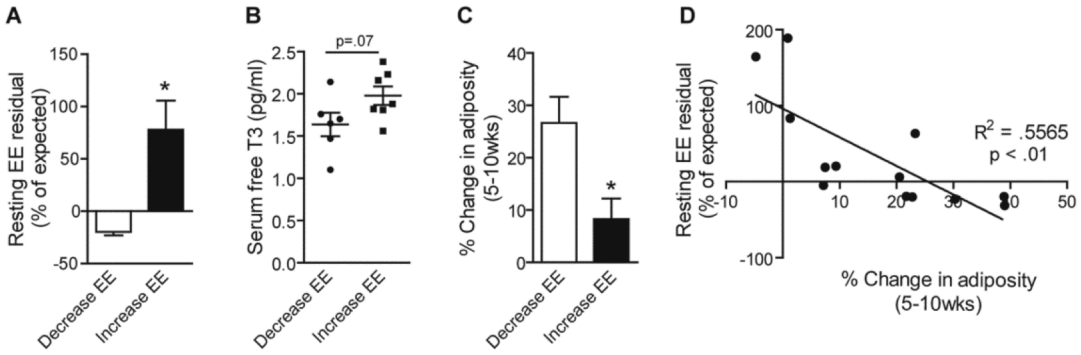

Figure 2.7. There is a critical time period in which to intervene. Physiological phenotypes of KO mice that decreased energy expenditure following PF from 5 weeks of age (white bars) vs. mice that increased energy expenditure (black bars). (A) Resting energy expenditure. (B) Serum free T3. (C) Percent change in body fat from 3-10 weeks. (D) Regression of resting energy expenditure vs. percent change in adiposity. Each symbol in B corresponds to an individual mouse. *P*-values were determined by performing an equality of variance test, then performing Student's or Welch's t-test accordingly. Data were generated from n=13 per group from 3 independent cohorts.

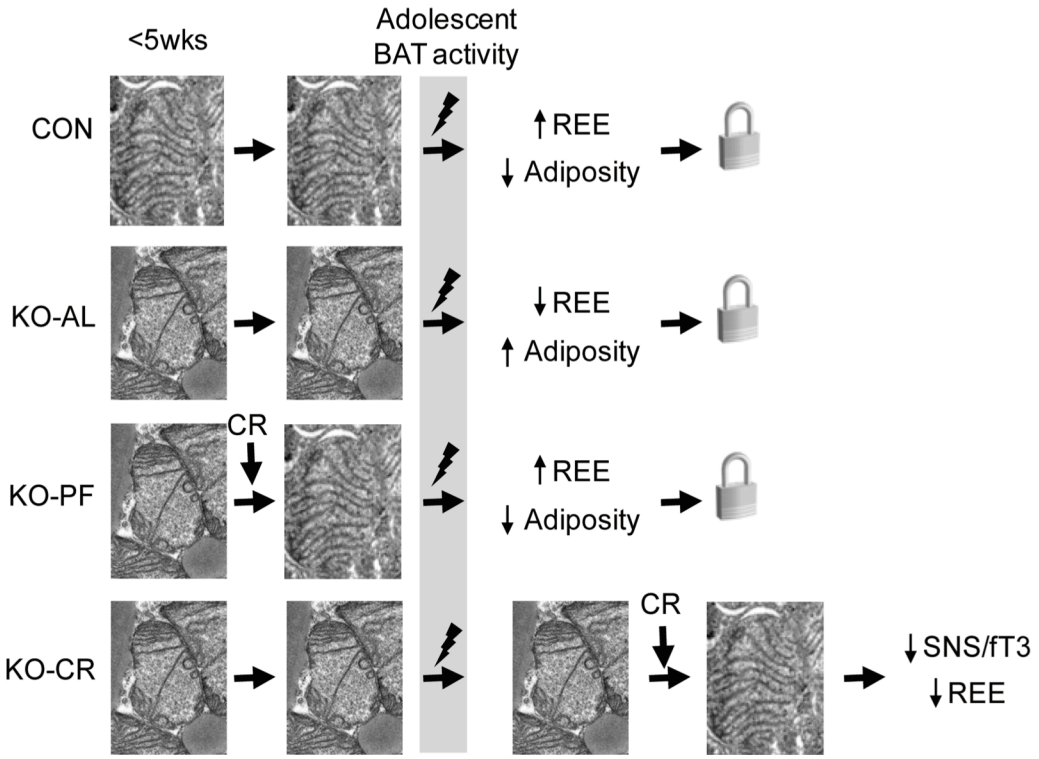

Figure 2.8. Working hypothesis to explain temporal differences in the metabolic response of obese KO mice to weight loss. Caloric restriction improves BAT mitochondrial structure in young (KO-PF) and adult (KO-CR) KOs. When interventions are initiated before 5 weeks of age, enhanced BAT responsiveness to factors that promote activity in adolescence (indicated by a lightning bolt) drive increases in energy expenditure that are stably maintained. After the peak of BAT activity in adolescence, weight loss-induced improvements in BAT capacity are opposed by compensatory decreases in sympathetic tone.

SUPPLEMENTAL FIGURES

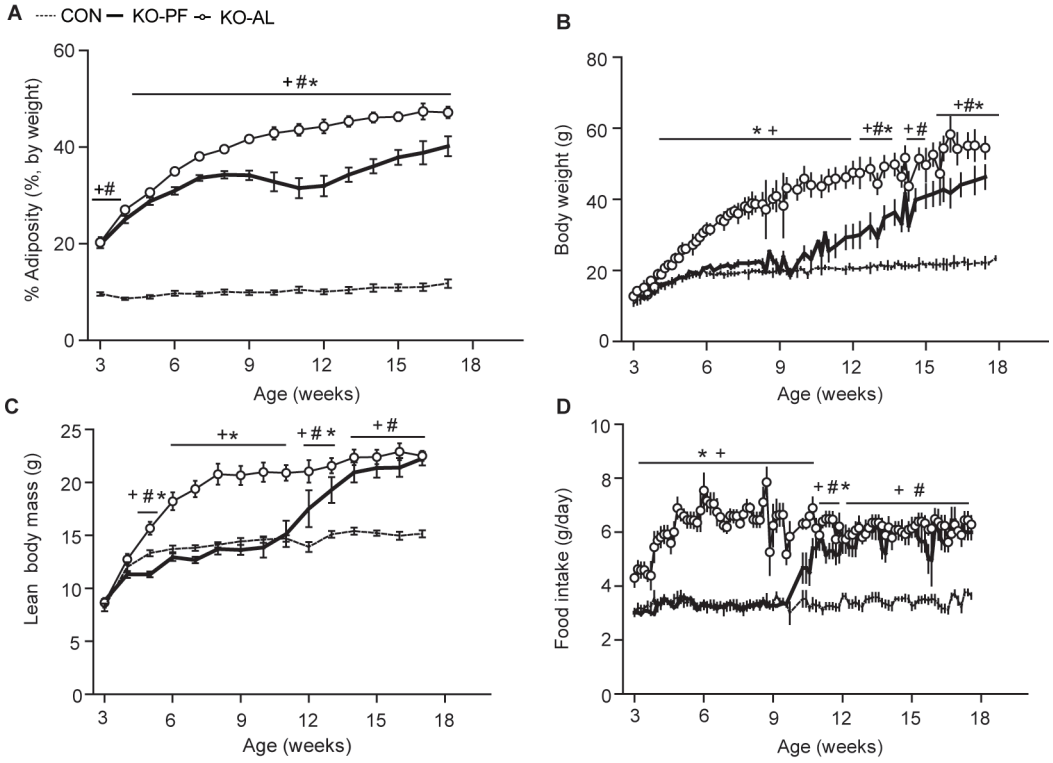

Supplemental Figure 2.1: Paired-feeding of female KO mice at an early age results in persistent changes in body weight and adiposity. Percent body fat (A), body weight (B), naso-anal length (NAL) (C), and food intake (D) in *ad libitum*-fed controls (thin line) vs. *ad libitum*-fed KOs (medium-thickness line with white circles) vs. KOs that were pair-fed from 3-10 weeks of age (thick line). *P*-values were determined by ANOVA and post-hoc Fisher's LSD. * represents $p<.05$ between AL and PF group, # represents $p<.05$ between PF and CON groups, and + represents $p<.05$ between AL and CON groups. Data were generated from n=7-10 per group from 3 independent cohorts.

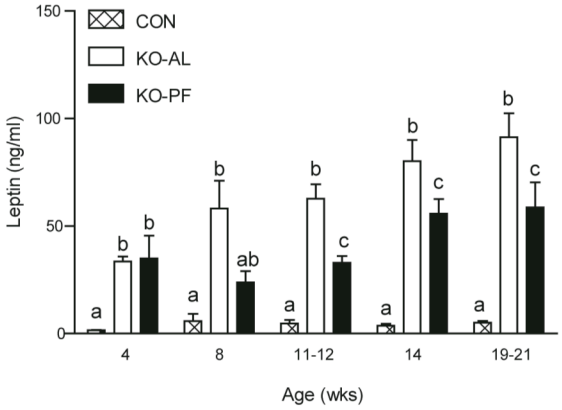

Supplemental Figure 2.2: Lasting impact of paired-feeding on serum leptin levels. Serum leptin levels at 4, 8, 11-12, 14, and 19-21 wks in *ad libitum*-fed controls (hatched bars), *ad libitum*-fed KOs (white bars) and KOs pair-fed from 3-10wks (black bars). Statistical difference calculated by ANOVA and post-hoc Fisher's LSD. Letters (a,b,c) represent differences between groups. Data were generated from n=3-10.

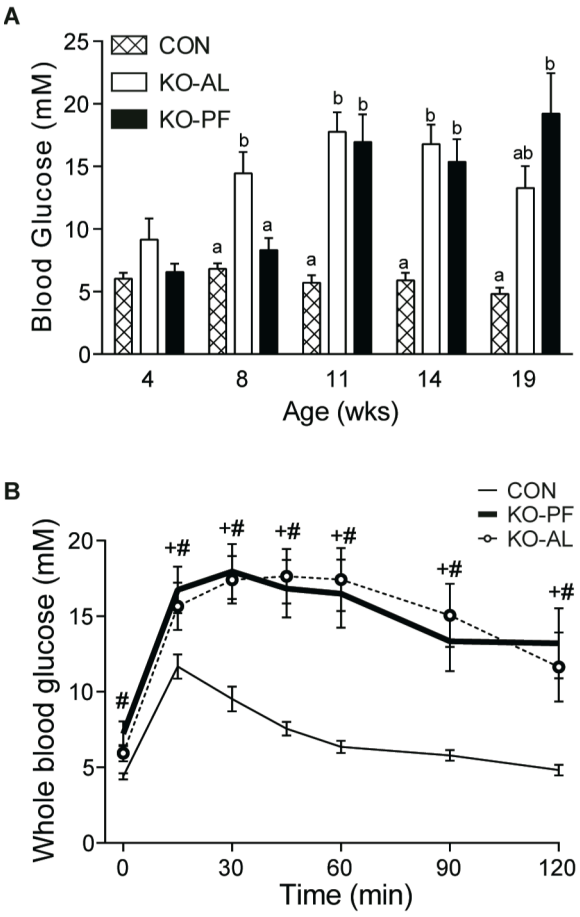

Supplemental Figure 2.3: Improvements in glucose homeostasis during paired-feeding are not maintained. Blood glucose levels in *ad libitum*-fed control (hatched bars, thin line), *ad libitum*-fed KOs (white bars, medium lines with white circles) and KOs pair-fed from 3-10wks (black bars, thick line). (A) Random-fed (am) blood glucose levels at 4, 8, 11, 14, 19wks. (B) Glucose tolerance test in fasted mice at 5wks. Statistical differences were calculated by ANOVA and post-hoc Fisher's LSD. Letters (a,b,c) represent differences between groups. # represents $p<.05$ between PF and CON groups, and + represents $p<.05$ between AL and CON groups. Data were generated from n=3-9 per group from 1-2 independent cohorts for fed glucose; n=6-8 per group from 2 independent cohorts for GTT.

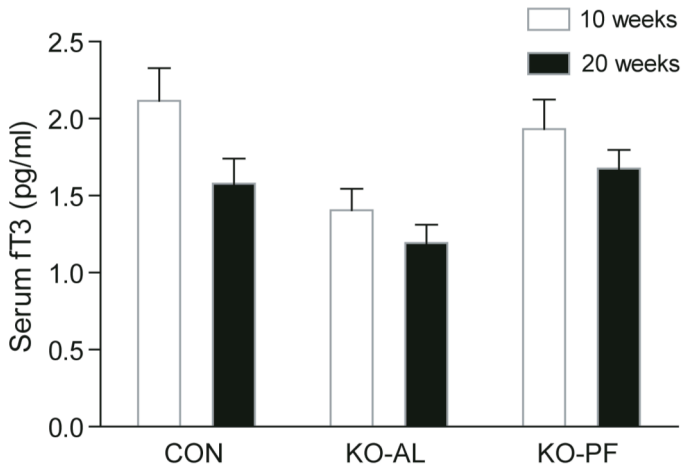

Supplemental Figure 2.4: Serum fT3 levels decrease with age. Serum fT3 levels in 10 week (white bars) vs. 20 week (black bars) in control, KO-AL, and KO-PF mice. Data generated from n = 5-11 mice from independent 2-3 cohorts.

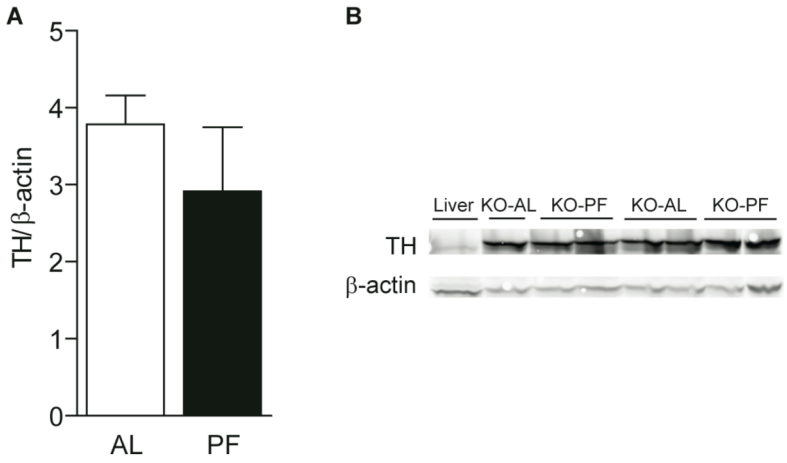

Supplemental Figure 2.5: No change in sympathetic marker tyrosine hydroxylase during paired-feeding. Relative protein expression of tyrosine hydroxylase in brown adipose tissue of *ad libitum*-fed KOs (white bars) and pair-fed KOs (black bar) at 13 weeks of age. Liver was used as a negative control. (A) Average ratio of TH/β-actin protein expression. (B) Representative gel from which data was generated. No statistical differences were calculated using a two-tailed student's t-test. Data generated from n = 3-6 from 1 cohort.

SUPPLEMENTAL TABLE

Primer	Forward (5' to 3')	Reverse (3' to 5')	Data Accession
Beta actin	CGCCACCAGTTCGCCAT	CTTTGCACATGCCGGAGC	NM_007393.3
Ucp1	GTGAAGGTCAGAATGCAAGC	AGGGCCCCCTTCATGAGGTC	NM_009463.3
Dio2	GATGCTCCCAATTCCAGTTG	AGTGAAAGGTGGTCAGGT	Boelen, A. *et al.* (2006). *J. Endocrinology.*
PGC1α	GCGAACCTTAAGTGTGGAAC	CACCACGGTCTTGCAAGAGG	NM_008904.2
PGC1β	GGACGAGCTTTCACTGCTAC	CGTCCTTCAGAGCGTCAGAG	NM_133249.2
ERRα	GAAGACAGCCCCAGTGAACG	GCATGGCGTACAGCTTCTCA	NM_007953.2
PPAR$^{\delta}$	GGACAATCCGCATGAAGCTC	CCAAAGCGGATAGCGTTGTG	NM_011145.3
mTFA	CCCGGCAGAGACGGTTAAA	AGCTTCAATTTTCCCTGAGCC	NM_009360.4
CPT1β	ATCATGTATCGCCGCAAACT	CCATCTGGTAGGAGCACATGG	NM_009948.2
CoxIV	GCAGAGAAGGTGGCCTTGTA	TTCGTTGGAGCGATGGTTCA	NM_053091.2
SDHA	AACTACAAGGGACAGGTGCTG	CTCCCCACAGGCATACAGAC	NM_023281.1

Supplemental Table 2.1. qPCR primers.

Part II: Concluding remarks:

Based on our results, we determined that BAT is the thermogenic organ driving the metabolic phenotype of increased energy expenditure in our model of early intervention. This conclusion was made not only on data presented in the manuscript, but on exclusion of other metabolically relevant tissue, such as liver, inguinal adipose tissue, gonadal adipose tissue, brain. Please refer to Appendix I for additional information.

REFERENCES

1. Ogden CL, Carroll MD, Kit BK, Flegal KM. Prevalence of obesity and trends in body mass index among US children and adolescents, 1999-2010. JAMA. 2012;307(5):483-90.

2. Janssen I, Katzmarzyk PT, Srinivasan SR, Chen W, Malina RM, Bouchard C, et al. Utility of childhood BMI in the prediction of adulthood disease: comparison of national and international references. Obes Res. 2005;13(6):1106-15.

3. Franz MJ, Boucher J. Winning at weight loss. Small losses, big gains. Shedding even a little excess weight improves your health. Support is key to success. Diabetes forecast. 2006;59(4):41-2, 4.

4. Delahanty LM, Pan Q, Jablonski KA, Aroda VR, Watson KE, Bray GA, et al. Effects of weight loss, weight cycling, and weight loss maintenance on diabetes incidence and change in cardiometabolic traits in the Diabetes Prevention Program. Diabetes Care. 2014;37(10):2738-45.

5. Wang Y, Wu Y, Wilson RF, Bleich S, Cheskin L, Weston C, et al. Childhood Obesity Prevention Programs: Comparative Effectiveness Review and Meta-Analysis. 2013/07/19 ed. Rockville (MD): Agency for Healthcare Research and Quality (US); 2013.

6. Guerra PH, Nobre MR, da Silveira JA, Taddei JA. School-based physical activity and nutritional education interventions on body mass index: A meta-analysis of randomised community trials - Project PANE. Prev Med. 2014.

7. Ravussin E, Lillioja S, Knowler WC, Christin L, Freymond D, Abbott WG, et al. Reduced rate of energy expenditure as a risk factor for body-weight gain. N Engl J Med. 1988;318(8):467-72.

8. Leibel RL, Rosenbaum M, Hirsch J. Changes in energy expenditure resulting from altered body weight. N Engl J Med. 1995;332(10):621-8.

9. Rosenbaum M, Hirsch J, Murphy E, Leibel RL. Effects of changes in body weight on carbohydrate metabolism, catecholamine excretion, and thyroid function. Am J Clin Nutr. 2000;71(6):1421-32.

10. Wang Z, Heymsfield SB, Ying Z, Pierson RN, Jr., Gallagher D, Gidwani S. A cellular level approach to predicting resting energy expenditure: Evaluation of applicability in adolescents. Am J Hum Biol. 2010;22(4):476-83.

11. Wolters B, Lass N, Reinehr T. TSH and free triiodothyronine concentrations are associated with weight loss in a lifestyle intervention and weight regain afterwards in obese children. Eur J Endocrinol. 2013;168(3):323-9.

12. Ojeda SR, Urbanski HF, Ahmed CE. The onset of female puberty: studies in the rat. Recent Prog Horm Res. 1986;42:385-442.

13. Ring LE, Zeltser LM. Disruption of hypothalamic leptin signaling in mice leads to early-onset obesity, but physiological adaptations in mature animals stabilize adiposity levels. J Clin Invest. 2010;120(8):2931-41.

14. McMinn JE, Liu SM, Dragatsis I, Dietrich P, Ludwig T, Eiden S, et al. An allelic series for the leptin receptor gene generated by CRE and FLP recombinase. Mamm Genome. 2004;15(9):677-85.

15. Xu Q, Tam M, Anderson SA. Fate mapping Nkx2.1-lineage cells in the mouse telencephalon. J Comp Neurol. 2008;506(1):16-29.

16. Rothwell NJ, Stock MJ. Effect of chronic food restriction on energy balance, thermogenic capacity, and brown-adipose-tissue activity in the rat. Bioscience reports. 1982;2(8):543-9.

17. Enerback S, Jacobsson A, Simpson EM, Guerra C, Yamashita H, Harper ME, et al. Mice lacking mitochondrial uncoupling protein are cold-sensitive but not obese. Nature. 1997;387(6628):90-4.

18. Matthias A, Ohlson KB, Fredriksson JM, Jacobsson A, Nedergaard J, Cannon B. Thermogenic responses in brown fat cells are fully UCP1-dependent. UCP2 or UCP3 do not substitute for UCP1 in adrenergically or fatty scid-induced thermogenesis. J Biol Chem. 2000;275(33):25073-81.

19. Bianco AC, Sheng XY, Silva JE. Triiodothyronine amplifies norepinephrine stimulation of uncoupling protein gene transcription by a mechanism not requiring protein synthesis. J Biol Chem. 1988;263(34):18168-75.

20. Butler AA, Kozak LP. A recurring problem with the analysis of energy expenditure in genetic models expressing lean and obese phenotypes. Diabetes. 2010;59(2):323-9.

21. Kaiyala KJ, Morton GJ, Leroux BG, Ogimoto K, Wisse B, Schwartz MW. Identification of body fat mass as a major determinant of metabolic rate in mice. Diabetes. 2010;59(7):1657-66.

22. Tschop MH, Speakman JR, Arch JR, Auwerx J, Bruning JC, Chan L, et al. A guide to analysis of mouse energy metabolism. Nat Methods. 2012;9(1):57-63.

23. Freake HC, Oppenheimer JH. Thermogenesis and thyroid function. Annu Rev Nutr. 1995;15:263-91.

24. Levin BE, Finnegan MB, Marquet E, Sullivan AC. Defective brown adipose oxygen consumption in obese Zucker rats. Am J Physiol. 1984;247(1 Pt 1):E94-100.

25. Cinti S, Frederich RC, Zingaretti MC, De Matteis R, Flier JS, Lowell BB. Immunohistochemical localization of leptin and uncoupling protein in white and brown adipose tissue. Endocrinology. 1997;138(2):797-804.

26. Doi K, Kuroshima A. Lasting effect of infantile cold experience on cold tolerance in adult rats. The Japanese journal of physiology. 1979;29(2):139-50.

27. Morrison SF, Ramamurthy S, Young JB. Reduced rearing temperature augments responses in sympathetic outflow to brown adipose tissue. J Neurosci. 2000;20(24):9264-71.

28. Sbarbati A, Morroni M, Zancanaro C, Cinti S. Rat interscapular brown adipose tissue at different ages: a morphometric study. International journal of obesity. 1991;15(9):581-7.

29. Bouyer K, Simerly RB. Neonatal leptin exposure specifies innervation of presympathetic hypothalamic neurons and improves the metabolic status of leptin-deficient mice. J Neurosci. 2013;33(2):840-51.

30. Cox JE, Powley TL. Development of obesity in diabetic mice pair-fed with lean siblings. J Comp Physiol Psychol. 1977;91(2):347-58.

31. Cleary MP, Vasselli JR, Greenwood MR. Development of obesity in Zucker obese (fafa) rat in absence of hyperphagia. Am J Physiol. 1980;238(3):E284-92.

32. Berglund ED, Vianna CR, Donato J, Jr., Kim MH, Chuang JC, Lee CE, et al. Direct leptin action on POMC neurons regulates glucose homeostasis and hepatic insulin sensitivity in mice. J Clin Invest. 2012;122(3):1000-9.

33. Skala J, Barnard T, Lindberg O. Changes in interscapular brown adipose tissue of the rat during perinatal and early postnatal development and after cold acclimation. II. Mitochondrial changes. Comparative biochemistry and physiology. 1970;33(3):509-28.

34. Ghadially FN. Ultrastructural pathology of the cell and matrix. 3rd ed. London: Butterworth-Heinemann; 1988.

35. Hogan S, Himms-Hagen J. Abnormal brown adipose tissue in obese (ob/ob) mice: response to acclimation to cold. Am J Physiol. 1980;239(4):E301-E9.

36. Hull D, Vinter J. The development of cold-induced thermogenesis and the structure of brown adipocyte mitochondria in genetically-obese (ob/ob) mice. Br J Nutr. 1984;52(1):33-9.

37. Schroeder M, Moran TH, Weller A. Attenuation of obesity by early-life food restriction in genetically hyperphagic male OLETF rats: peripheral mechanisms. Horm Behav. 2010;57(4-5):455-62.

38. Schroeder M, Gelber V, Moran TH, Weller A. Long-term obesity levels in female OLETF rats following time-specific post-weaning food restriction. Horm Behav. 2010;58(5):844-53.

39. Bumaschny VF, Yamashita M, Casas-Cordero R, Otero-Corchon V, de Souza FS, Rubinstein M, et al. Obesity-programmed mice are rescued by early genetic intervention. J Clin Invest. 2012;122(11):4203-12.

40. Kirchner H, Hofmann SM, Fischer-Rosinsky A, Hembree J, Abplanalp W, Ottaway N, et al. Caloric restriction chronically impairs metabolic programming in mice. Diabetes. 2012;61(11):2734-42.

41. Reinehr T, Kleber M, Lass N, Toschke AM. Body mass index patterns over 5 y in obese children motivated to participate in a 1-y lifestyle intervention: age as a predictor of long-term success. Am J Clin Nutr. 2010;91(5):1165-71.

42. Danielsson P, Kowalski J, Ekblom O, Marcus C. Response of severely obese children and adolescents to behavioral treatment. Arch Pediatr Adolesc Med. 2012;166(12):1103-8.

43. Danielsson P, Svensson V, Kowalski J, Nyberg G, Ekblom O, Marcus C. Importance of age for 3-year continuous behavioral obesity treatment success and dropout rate. Obes Facts. 2012;5(1):34-44.

44. Batt RA, Hambi M. Development of the hypothermia in obese mice (genotype ob/ob). International journal of obesity. 1982;6(4):391-7.

45. Batt RA, Tyler DD, Sutton CM. Influence of restricted food intake on brown adipose tissue function in genetically obese mice (genotype, ob/ob). Biochim Biophys Acta. 1985;838(2):229-35.

46. Himms-Hagen J. Food restriction increases torpor and improves brown adipose tissue thermogenesis in ob/ob mice. Am J Physiol. 1985;248(5 Pt 1):E531-9.

47. Clarke M, Cai G, Saleh S, Buller KM, Spencer SJ. Being Suckled in a Large Litter Mitigates the Effects of Early-Life Stress on Hypothalamic-Pituitary-Adrenal Axis Function in the Male Rat. Journal of Neuroendocrinology. 2013;25(9):792-802.

48. Fisher MO, Nager RG, Monaghan P. Compensatory growth impairs adult cognitive performance. PLoS Biol. 2006;4(8):e251.

49. Lazzer S, Boirie Y, Montaurier C, Vernet J, Meyer M, Vermorel M. A weight reduction program preserves fat-free mass but not metabolic rate in obese adolescents. Obes Res. 2004;12(2):233-40.

50. Trayhurn P, Thurlby PL, James WP. Thermogenic defect in pre-obese ob/ob mice. Nature. 1977;266(5597):60-2.

51. Moore BJ, Horwitz BA, Stern JS. Brown fat thermogenesis and its role in the development of obesity. Brain Res Bull. 1985;14(6):577-83.

52. Kaul R, Schmidt I, Carlisle H. Maturation of thermoregulation in Zucker rats. International journal of obesity. 1985;9(6):401-9.

53. Berce PJ, Moore BJ, Horwitz BA, Stern JS. Metabolism at thermoneutrality and in the cold is reduced in the neonatal preobese Zucker fatty (fa/fa) rat. J Nutr. 1986;116(12):2478-85.

54. Kortner G, Petrova O, Vogt S, Schmidt I. Sympathetically and nonsympathetically mediated onset of excess fat deposition in Zucker rats. Am J Physiol. 1994;267(6 Pt 1):E947-53.

55. Muller TD, Lee SJ, Jastroch M, Kabra D, Stemmer K, Aichler M, et al. p62 links beta-adrenergic input to mitochondrial function and thermogenesis. J Clin Invest. 2013;123(1):469-78.

56. Hogan S, Himms-Hagen J. Abnormal brown adipose tissue in genetically obese mice (ob/ob): effect of thyroxine. Am J Physiol. 1981;241(6):E436-43.

57. Goodbody AE, Trayhurn P. Studies on the activity of brown adipose tissue in suckling, pre-obese, ob/ob mice. Biochim Biophys Acta. 1982;680(2):119-26.

58. Ashwell M, Holt S, Jennings G, Stirling DM, Trayhurn P, York DA. Measurement by radioimmunoassay of the mitochondrial uncoupling protein from brown adipose tissue of obese (ob/ob) mice and Zucker (fa/fa) rats at different ages. FEBS Lett. 1985;179(2):233-7.

59. Masaki T, Yoshimatsu H, Chiba S, Sakata T. Impaired response of UCP family to cold exposure in diabetic (db/db) mice. Am J Physiol Regul Integr Comp Physiol. 2000;279(4):R1305-9.

60. Seydoux J, Assimacopoulos-Jeannet F, Jeanrenaud B, Girardier L. Alterations of brown adipose tissue in genetically obese (ob/ob) mice. I. Demonstration of loss of metabolic response to nerve stimulation and catecholamines and its partial recovery after fasting or cold adaptation. Endocrinology. 1982;110(2):432-8.

61. Knehans AW, Romsos DR. Norepinephrine turnover in obese (ob/ob) mice: effects of age, fasting, and acute cold. Am J Physiol. 1983;244(6):E567-74.

62. Young JB, Landsberg L. Diminished sympathetic nervous system activity in genetically obese (ob/ob) mouse. Am J Physiol. 1983;245(2):E148-54.

63. Ashwell M, Dunnett SB. Fluorescent histochemical demonstration of catecholamines in brown adipose tissue from obese (ob/ob) and lean mice acclimated at different temperatures. J Auton Nerv Syst. 1985;14(4):377-86.

64. Gelfand MJ, O'Hara S M, Curtwright LA, Maclean JR. Pre-medication to block [(18)F]FDG uptake in the brown adipose tissue of pediatric and adolescent patients. Pediatr Radiol. 2005;35(10):984-90.

65. Drubach LA, Palmer EL, 3rd, Connolly LP, Baker A, Zurakowski D, Cypess AM. Pediatric brown adipose tissue: detection, epidemiology, and differences from adults. J Pediatr. 2011;159(6):939-44.

66. Gilsanz V, Smith ML, Goodarzian F, Kim M, Wren TA, Hu HH. Changes in brown adipose tissue in boys and girls during childhood and puberty. J Pediatr. 2012;160(4):604-9 e1.

67. Chalfant JS, Smith ML, Hu HH, Dorey FJ, Goodarzian F, Fu CH, et al. Inverse association between brown adipose tissue activation and white adipose tissue accumulation in successfully treated pediatric malignancy. Am J Clin Nutr. 2012;95(5):1144-9.

68. Himms-Hagen J, Desautels M. A mitochondrial defect in brown adipose tissue of the obese (ob/ob) mouse: reduced binding of purine nucleotides and a failure to respond to cold by an increase in binding. Biochem Biophys Res Commun. 1978;83(2):628-34.

69. Thurlby PL, Trayhurn P. The role of thermoregulatory thermogenesis in the development of obesity in genetically-obese (ob/ob) mice pair-fed with lean siblings. Br J Nutr. 1979;42(3):377-85.

70. Gardner DS, Hosking J, Metcalf BS, Jeffery AN, Voss LD, Wilkin TJ. Contribution of early weight gain to childhood overweight and metabolic health: a longitudinal study (EarlyBird 36). Pediatrics. 2009;123(1):e67-73.

71. Cunningham SA, Kramer MR, Narayan KM. Incidence of childhood obesity in the United States. N Engl J Med. 2014;370(5):403-11.

72. Oh SS, Kaplan ML. Early treatment of obese (ob/ob) mice with triiodothyronine increases oxygen consumption and temperature and decreases body fat content. Proc Soc Exp Biol Med. 1994;207(3):260-7.

73. Chong AC, Greendyk RA, Zeltser LM. Distinct networks of leptin- and insulin-sensing neurons regulate thermogenic responses to nutritional and cold challenges. Diabetes. 2015;64(1):137-46.

74. De Matteis R, Ricquier D, Cinti S. TH-, NPY-, SP-, and CGRP-immunoreactive nerves in interscapular brown adipose tissue of adult rats acclimated at different temperatures: an immunohistochemical study. J Neurocytol. 1998;27(12):877-86.

75. Villarroya F, Vidal-Puig A. Beyond the sympathetic tone: the new brown fat activators. Cell Metab. 2013;17(5):638-43.

76. Zhang Y, Kerman IA, Laque A, Nguyen P, Faouzi M, Louis GW, et al. Leptin-receptor-expressing neurons in the dorsomedial hypothalamus and median preoptic area regulate sympathetic brown adipose tissue circuits. J Neurosci. 2011;31(5):1873-84.

77. Rezai-Zadeh K, Munzberg H. Integration of sensory information via central thermoregulatory leptin targets. Physiol Behav. 2013;121:49-55.

78. Commins SP, Watson PM, Frampton IC, Gettys TW. Leptin selectively reduces white adipose tissue in mice via a UCP1-dependent mechanism in brown adipose tissue. Am J Physiol Endocrinol Metab. 2001;280(2):E372-7.

79. Young JB, Weiss J, Boufath N. Effects of rearing temperature on sympathoadrenal activity in young adult rats. Am J Physiol Regul Integr Comp Physiol. 2002;283(5):R1198-209.

80. Landsberg L, Young JB. Fasting, feeding and regulation of the sympathetic nervous system. N Engl J Med. 1978;298(23):1295-301.

81. Levin BE, Dunn-Meynell AA. Defense of body weight against chronic caloric restriction in obesity-prone and -resistant rats. Am J Physiol Regul Integr Comp Physiol. 2000;278(1):R231-7.

82. Leibel RL, Berry EM, Hirsch J. Metabolic and hemodynamic responses to endogenous and exogenous catecholamines in formerly obese subjects. Am J Physiol. 1991;260(4 Pt 2):R785-91.

83. Cannon B, Nedergaard J. Brown adipose tissue: function and physiological significance. Physiol Rev. 2004;84(1):277-359.

CHAPTER 3: Influences of BAT Development Start in the Peri-weaning Period

This work was completed with the help of Rim Hassouna, who helped generate data for female mice and serum IGF-1 assays and helped collect organs across all time points of the study.

Note: The experiments within this chapter are still a work in progress.

Part I: Current Data

INTRODUCTION

With the childhood obesity rate at nearly 17% within the United States (1), it is important to develop more efficacious strategies in combating this epidemic. In Chapter 2 we reported that the age at which obesity intervention is implemented could determine success versus failure in a mouse model of early-onset hyperphagia and obesity. We found that initiating caloric restriction at weaning produced sustained reductions in adiposity due to increased energy expenditure (EE), while interventions after 5 weeks of age were associated with compensatory decreases in EE (2). Increased EE resulted from improvements in brown adipose tissue (BAT) capacity to respond to endogenous stimuli, but not in increased sympathetic tone (2). Together with reports suggesting that deficits in BAT activity in children are linked to subsequent increases in adiposity (3-5), our findings raise the possibility that improving BAT capacity may be a therapeutic target for childhood obesity intervention.

Rodent development is highly compressed, as pubertal maturation is largely completed within a 4 week period after weaning. Thus, the human correlate of the immediate post-weaning period in mice, which was identified in our study as a critical time for intervention, likely spans infancy through early adolescence. It is widely accepted that BAT plays an important role in maintaining thermogenesis in human infants (as discussed in (6, 7)). BAT is first detected in the developing fetus at approximately 5 months of gestation (8). The distribution of brown adipocytes is maximal in infancy, detected mostly in the interscapular region (9), and begins to decline during childhood (9-12). BAT activity is critical during the early postnatal period to regulate body temperature at birth, as newborns do not shiver (9). In childhood and early adolescents, the perirenal region is the most abundant classical BAT depot, which can also be present in lesser quantities in adults (11, 13, 14). BAT thermogenic capacity, as defined by uncoupling protein 1 (UCP1) levels, declines between 6-9 months of age (9) leading to the longstanding assumption that BAT did not contribute to energy balance in adulthood. Later studies highlighted the relevancy of BAT in adults, and identified beige adipocytes in the supraclavicular region (13).

The publication of 3 simultaneous studies in 2009, sparked the growing appreciation that brown adipocytes (or inducible beige adipocytes) can be activated in adults (6, 15, 16). These papers validated the use of 18^{F}-fluorodeoxyglucose (FDG) positron emission tomography (PET) and computed tomography (CT) to quantify BAT activity. Due to the involvement of radiolabeled tracers, there are few analyses of BAT activity in children.

Two groups performed retrospective analyses of BAT activity in children that received PET scans in the course of treatment for cancer. Data from both studies are consistent with the idea that there is an expansion of BAT in the supraclavicular depot during childhood, with a peak activity occurring during puberty (3, 4). Increased BAT mass in adolescents (as compared to patients under 10 years of age) is independent of environmental temperature and BAT activation status (4, 17). In males, BAT activity peaks between 13-15 years of age and is 4-fold higher than levels in adults (3). The peak of BAT activity is slightly later in females, 15-17 years of age, and is marked by a 3-fold increase over adult levels (3). Similar to what is seen in adults, BAT activity can still be recruited upon cold stimulation after the decline of basal activity levels (6, 16, 18-20).

Using the *Nkx2.1-Cre;Lepr*$^{fl/fl}$ model of early-onset hyperphagia and obesity (hereby referred to as KO), we found that 5 weeks of age marks the end of the period when weight loss can be achieved without a compensatory decrease in EE (Chapter 2) (2). Most studies of BAT development in rodents focused on gestation and the neonatal period, when mitochondrial cristae are tightly packed and BAT capacity is maximal (21, 22). The equivalent phase of BAT recruitment and activation in the interscapular depot in humans is likely achieved within the first few months of life (9). There is evidence that there is an expansion of BAT depots during childhood, which is followed by a peak of BAT activity in teens (3, 4).

The primary goal of this study was to fill a critical gap in our knowledge of BAT development during the peri-weaning period in rodents, the likely equivalent of

childhood and early adolescence in humans. To this end, we characterized the size of BAT depot in conjunction with markers of BAT capacity and activity from 2-13 weeks of age. We found that an expansion in the size of the BAT depot between 2-3 weeks of age was accompanied by a dramatic decrease in BAT capacity and activity. BAT activity increased across the first two post-weaning weeks, peaking at 5 weeks of age. Since sympathetic tone does not correlate with energy expenditure during this period in rodents (23), we sought to identify neuroendocrine factors that might enhance BAT activity during this period. Our initial efforts focused on insulin-like growth factor 1 (IGF-1), because the peak in BAT activity occurs at a similar time as the peak in serum IGF-1 levels (3, 24). Moreover, reports that IGF-1 promotes the differentiation, proliferation, and thermogenic activation of brown adipocytes *in vitro* (25-27), raise the possibility that IGF-1 also enhances BAT maturation during the post-weaning period in mice. Finally, we explored whether the beneficial effects of paired-feeding on EE in the KO model are due to effects on maturation processes in the post-weaning period.

METHODS

Mouse husbandry. Mouse husbandry was kept the same as in Chapter 2 (page 57).

Generation of Lepr^{HYP}KO mice. To disrupt LepRb signaling in the hypothalamus, mice homozygous for the floxed allele of *Lepr* (FVB.BKS(D)-*Lepr^{db}* provided by S. Chua, Albert Einstein College of Medicine) (28) were crossed with the *Nkx2.1-Cre* driver line (C57BL/6J-Tg(Nkx2.1-Cre)2Sand/J provided by S. Anderson, Weill Cornell Medical College) (29). F1 heterozygotes (*Nkx2.1-Cre;Lepr$^{fl/+}$*) were intercrossed to create an F2 generation of *Lepr$^{Nkx2.1}$*KO mice and Lepr$^{fl/fl}$ control mice. Genotyping performed was the same as described in Chapter 2 (page 57).

Paired-feeding paradigm. Paired-feeding was carried out as per the methods section in Chapter 2 (page 57). Mice were sacrificed in the fed state at either 5 weeks or 13 weeks of age.

Preservation of organs. On the day before sacrifice, mice were brought to the laboratory overnight. Mice were allowed *ad libitum* access to food unless otherwise specified. On the morning of sacrifice, mice were anesthetized using 2.5% Avertin (0.02mL/g i.p.) before undergoing a terminal bleed (serum) and cervical dislocation. Brown adipose tissue was collected and half the depot was preserved in All Protect (Qiagen) for RNA quantification while the other half was flash frozen in liquid nitrogen for protein extraction. 3 week BAT samples were also collected in 4% paraformaldehyde, 0.08% gluteraldehyde for 4 hours and then overnight in 4% paraformaldehyde (for electron microscopy (EM)). Samples in All Protect were stored in the -20°C freezer, flash frozen samples were stored in the -80°C freezer. Bone marrow was extracted from

the femur using cold PBS. Bone marrow was centrifuged at 1500g for 5 minutes and the supernatant was discarded. The pellet was re-suspended using Trizol and samples were stored in the -80°C freezer until later use. Pituitary, hypothalamus, white adipose tissue depots and liver were stored in All Protect (Qiagen) and stored in the -20°C freezer.

Electron microscopy analysis of brown adipose tissue. Electron microscopy was performed by Tamas Horvath at Yale University using the same procedure as mentioned in Chapter 2 (page 59).

Gene expression. We isolated total RNA using the RNeasy Universal Mini kit (Qiagen) and synthesized cDNA using Transcriptor First Strand cDNA Synthesis kit (Roche). We used a LightCycler 480 SYBR Green I Master System (Roche) in quantitative PCR experiments. We normalized the expression of target genes against *b-actin*.

Measurement of free T3 and IGF-1. All blood samples were collected at sacrifice and blood was allowed to clot for 1h and then centrifuged at 4500g for 10min. Serum was decanted and stored at -20˚C until used in IGF-1 (Enzo) or fT3/fT4 analysis (Leinco Technology, Inc) ELISAs, per the manufacturer's protocol.

Protein analysis: Proteins were extracted and quantified as describe Brown adipose tissue proteins were extracted in RIPA buffer (ThermoFisher Scientific) with the addition of protease and phosphatase inhibitors (ThermoFisher Scientific). Protein quantification was performed via the Pierce BCA protein assay kit (ThermoFisher Scientific). Western blotting was performed using 30µg of protein from each sample in AL-KO vs. control analysis, and polyacrylamide gel electrophoresis was performed using a 10% Tris-glycine gel. AL-KO vs. AL-PF was performed using 15µg of protein from each sample. UCP1

was detected using anti-UCP1 (Abcam) (1:4000 dilution) normalized to b-actin (Abcam) (1:20000 dilution), both primary antibodies were incubated at 4˚C overnight. Fluorescent secondary antibodies were used (Rockland, LI-COR) for fluorescent imaging. Fluorescence was measured via Odyssey v3.0 imaging program.

Statistical Analysis: Data are presented as group mean ± SEM. We performed statistical comparisons between 2 groups using an equality of variance test, and then performing Student's or Welch's t-test accordingly. We performed statistical comparisons between multiple groups using a one-way ANOVA, followed Fisher's PLSD post-hoc analysis. Data using percentages were transformed using arcsine transformation, before performing a one-way ANOVA and post-hoc test. We considered a p-value of 0.05 or less to be statistically significant. Statistical significance was determined using Excel and GraphPad software.

RESULTS IN PROGRESS

BAT capacity in lean mice decreases between 2-3 weeks of age

First, we examined whether the high oxidative capacity and activity of neonatal BAT (21, 26, 30) are maintained through lactation. To this end, we compared the expression of several genes related to BAT capacity and function between 2 to 3 weeks of age in lean mice. We found that the expression of markers of BAT activity, such as *Ucp1* and deiodinase 2 (*Dio2*), was reduced by 82.3% ($p<.05$) and 79.4% ($p=.01$), respectively (Figure 3.1A). Additionally, expression of the gene encoding cytochrome c oxidase IV (*CoxIV*), the final step in the electron transport chain (31, 32), was reduced by 68.7% ($p=.07$) (Figure 3.1A). Taken together, we found that 2 to 3 weeks of age is a time of impaired BAT oxidative capacity.

It was previously reported that mitochondrial cristae formation and mitochondrial respiration are maximal in the first postnatal week (21). Therefore, we next asked whether the decreased expression of markers of BAT activity was correlated with changes in mitochondrial structure. Reductions in thermogenic gene expression in the BAT were accompanied by distorted mitochondrial structure (Figure 3.1B,C). The BAT mitochondria at 3 weeks of age contained the same total number of cristae/mitochondrion as at 10 weeks of age (Figure 3.1D), but had more abnormal cristae/mitochondrion (22.4% abnormal at 3 weeks compared to 10 weeks 2.94%) (Figure 3.1E,F).

The size of the BAT depot expands between 2-3 weeks of age

As the initial period of BAT "unmasking" (33) and activation in human neonates is followed by a period of expansion in the size of the depot during childhood (4), we next asked whether a similar process occurs in rodents. We found that BAT weight almost doubled in size from 2-3 weeks of age (0.043g ±.009, n=4 at 2 weeks vs. 0.08g ±.011, n=5 at 3 weeks)(p<.05) (Figure 3.2A). After this initial expansion, BAT weight remained constant from 3 weeks of age into adulthood (Figure 3.2B). In contrast, liver (Figure 3.2C), inguinal adipose tissue (iFat) (Figure 3.2D), and gonadal adipose tissue (gFat) (Figure 3.2E) increased in weight from 3 to 5 weeks of age in parallel to total body weight.

Evidence for a peak of BAT activity in lean mice at 5 weeks of age

Since BAT capacity (as reflected in mitochondrial structure) was impaired at 3 weeks of age relative to 10 weeks of age (Figure 3.1B,C), we next determined when BAT activity is restored. We found that BAT *Ucp1* transcript levels increased by 92% from 3 to 4 weeks of age (p<.01) (Figure 3.3A), but then decreased by 39% (p<.05) from 4 to 5 weeks of age (Figure 3.3A). Adult-like levels of *Ucp1* were achieved by 6-7 weeks, after which they were stably maintained. In contrast to our findings at the transcript level, we found no change in BAT UCP1 protein levels from 3 to 4 weeks of age in control mice. We observed a 123% increase in BAT UCP1 at 5 weeks of age compared to 3 weeks of age (p<.01) (Figure 3.3B), which was followed by 45.5% decrease from 5 to 6 weeks (p=.06). Stable levels of UCP1 protein were then maintained through 13 weeks (Figure 3.3B).

We next determined whether the peak of BAT UCP1 protein expression at 5 weeks is associated with changes in the expression of panel of genes linked to mitochondrial capacity and biogenesis (*Mfn2*, *Mics1*, *Opa1*, *Tfam*, *Prohibitin*) and oxidative phosphorylation/thermogenic activity (*Ucp1, Dio2, Errα, Pgc1β, CoxIV, Cytochrome* c). Most gene expression profiles did not track with the pattern of UCP1 (Supplemental Figure 3.1), but those that did were associated with mitochondrial structure. We found *mitofusin2* (*Mfn2*) (34) was increased by 103% at 4 weeks of age compared to 3 weeks of age (p=.088) and increased by 113% from 3 to 5 weeks of age (p<.05) (Figure 3.3C). *Mics1* (35) expression increased from 4 to 5 weeks of age (52%, p<.05), achieving adult-like levels by 7 weeks of age (38% increase from 5 to 7 weeks of age, p=.05) (Figure 3.3D). Although there was no significant change in carnitine palmitoyltransferase 1b (*Cpt1b*) from 3 to 5 weeks of age (21.2%, NS) (Supplemental Figure 3.1D), there was a significant (65%) increase in *Cpt1b* from 4 to 7 weeks of age (p=.01) (Supplemental Figure 3.1D). Additionally, *CoxIV* gradually increased from 3 to 6 weeks of age (32.3%, p=.02) (Supplemental Figure 3.1E).

Efforts to identify circulating BAT activators in the post-weaning period

In effort to determine what is responsible for increased UCP1 protein at 5 weeks of age, we measured levels of several BAT-activating factors in the serum across the post-weaning period.

1) Thyroid hormone

We found that serum levels of free triiodothyronine (fT3) were similar in control mice at 5 weeks of age compared to older ages (Supplemental Figure 3.2A). Additionally, BAT *Dio2* (responsible for the conversion of thyroxine (T4) to T3) was expressed in inverse pattern as UCP1 protein, with lower levels at 4-5 weeks than at other ages (Supplemental Figure 3.2B).

2) IGF-1

While serum IGF-1 is elevated at the same time of the peak in BAT activity in humans (3, 24), we did not observe a peak in serum IGF-1 in males (Figure 3.4B) or females (Supplemental Figure 3.3A). Serum IGF-1 levels were not associated with growth, as body weight and length were stable from 5 weeks of age (Figure 3.4C,D). We found that liver *Igf-1* mRNA expression, the primary source of serum IGF-1 (36, 37), was not increased at 5 weeks compared to later ages (Figure 3.4A). Bone marrow *Igf-1*, another source of serum IGF-1, and BAT *Igf-1* receptor (*Igf1-R*) were also not changed across the post-weaning period (Figure 3.4E,F).

Autocrine IGF-1 signaling plays an important role in BAT development during gestation (38). Therefore, we examined whether BAT-derived IGF-1 might also influence developmental processes in the post-weaning period. We found that *Igf-1* levels were slightly increased from 2 to 3 weeks of age, during the period of BAT expansion (Figure 3.5). BAT *Igf-1* levels were further increased between 3-5 weeks of age (when BAT

weight is relatively stable), directly preceding the age of peak BAT UCP1 (Figure 3.3, 3.5). After 5 weeks of age, there was a dramatic decline in *Igf-1* levels (43.7% reduction in *Igf-1* from 4 to 6 weeks of age, (p=.018)) (Figure 3.5).

A developmental delay of BAT capacity in the KO-AL mice

The development of thermogenic circuits is delayed in KO mice fed an *ad libitum* diet (KO-AL), as they are cold intolerant until 6 weeks of age (39). We next examined whether processes regulating the increase in mitochondrial capacity and function in the post-weaning period, hereafter referred to as "mitochondrial consolidation", are impaired in KO-AL mice. The sharp increase in UCP1 protein from 3 to 5 weeks of age was not seen in KO-AL mice (Figure 3.6A) (ANOVA NS).

We also compared the expression profiles of several BAT mitochondrial genes in KO-AL vs. lean controls at 5 week of age. *Ucp1* expression was decreased in KO-ALs by 52% (p<.05) (Figure 3.6B), while UCP1 protein was decreased by 41% (NS) (Figure 3.6A). KO-AL mice also exhibited reduced BAT *Pgc1β* (41.3%, p=.07), *Errα* (50.2%, p<.01), *Mics1* (55%, p<.01), *Tfam* (35.5%, NS), *Mfn2* (34.2%, NS) and *Opa1* (42.2%, p=.05) expression at 5 weeks of age compared to controls (Figure 3.6C).

Expression of *Igf-1* in BAT was reduced by 61.4% of KO-AL mice vs. controls at 5 weeks (NS) (Figure 3.6D). This difference was diminished by 9 weeks of age (Figure 3.6E), and by 13 weeks, there was a trend toward increased BAT *Igf-1* in KO-ALs compared to control mice (NS) (Figure 3.6F).

Evidence that paired-feeding restores developmental processes regulating BAT function

We previously reported that paired-feeding of KOs from 3-10 weeks (KO-PF) leads to increased BAT capacity and activity at 10 weeks (2). We next asked whether we could detect this change as early as 5 weeks, during the peak of UCP1 expression seen in lean controls. Similar to what has been shown previously, there was a discrepancy between expression and protein levels of UCP1. We found that UCP1 protein was expressed at higher levels in KO-PFs vs. KO-ALs at 5 weeks of age, but this was not reflected in *Ucp1* transcript levels (Figure 3.7A,C,). As we reported previously (2), KO-PF mice exhibited increased *Ucp1* gene and protein expression levels at 13 weeks of age compared to KO-ALs (Figure 3.7B,C).

We also evaluated *Igf-1* expression in BAT and IGF-1 protein in the serum. *Igf-1* expression was not increased in KO-PFs at 5 or 13 weeks of age compared to KO-ALs (Figure 3.7D,E). Serum IGF-1 in KO-AL mice followed a similar pattern as in controls, but was blunted in the KO-PFs (Supplemental Figure 3.3B), consistent with their pattern of reduced growth rate at this time (Figure 2.5C)(2).

DISCUSSION

Our previous research implicated 3-5 weeks of age as a period when caloric restriction could lead to lasting increases in BAT activity and reduced adiposity. In this study, we characterized changes in markers of BAT capacity and activity across the peri-weaning period. We next explored whether influences on these processes might underlie the metabolic improvements associated with early intervention. We found that 2 to 3 weeks of age was a time of BAT expansion, coinciding with reduced thermogenic capacity in control mice. We identified an increase in BAT *Igf1* from 3 to 4 weeks of age, after which levels declined. This increase was followed by a peak in thermogenic gene expression at 5 weeks of age in control mice, supporting a role for *Igf1* in BAT mitochondrial "consolidation" at this time. The peak of thermogenic gene expression was blunted at 5 weeks of age in KO-AL compared to controls, and subsequently rescued by paired-feeding.

BAT undergoes rapid expansion within the first weak after weaning

Within a week after birth in rodents, mitochondrial cristae are tightly packed and BAT capacity is maximal (26, 27). Therefore, most studies of BAT development do not extend past 2 weeks of age. We found that cristae in lean mice lose this tight organization at 3 weeks of age (Figure 3.1B-F), making their mitochondrial structure comparable to that of KO mice at 3 weeks (Supplemental Figure 3.4). Cristae disorganization was accompanied by reduced expression of BAT *Ucp1, Dio2* and *CoxIV* from 2 to 3 weeks of age (Figure 3.1A). These findings are consistent with reports that respiratory activity and

volume of the inner mitochondrial membrane is reduced in the period preceding weaning in rats (21, 22).

We found that the period of reduced thermogenic gene expression in BAT coincided with a doubling of BAT weight (Figure 3.2A), raising the possibility that they are mechanistically linked. The process underlying the increase in BAT weight has not yet been elucidated. In theory, BAT expansion might reflect proliferation; if so, newly-born immature cells would not be expected to have tightly packed cristae. Alternatively, increased BAT weight could also be explained by increased cell size due to the accumulation of larger lipid droplets, which could also interfere with mitochondrial capacity. Further work is needed to elucidate this process.

The role of IGF-1 signaling in BAT development and function

We found an increase in the expression of thermogenic genes from 3 to 5 weeks of age (Figure 3.3). These changes were preceded by increased BAT *Igf-1* expression from 2 to 4 weeks of age (Figure 3.5), consistent with the idea that *Igf-1* plays a role in the maturation of BAT at this time. IGF-1 has thermogenic effects on brown adipocytes (27), and promotes differentiation of brown adipocytes during fetal development (25, 26). Therefore, several groups have used Cre/lox approaches to study the role of IGF-1 signaling in adipose tissue development and function. Mice lacking either IGF-1R or IGF-1 in adipose tissue (using the *Ap2*-Cre driver) exhibit normal BAT weights (40, 41), suggesting that either IGF-1 or IGF-1R is not necessary for BAT development. Mice lacking adipose tissue derived IGF-1R exhibit increased body weight by 10 weeks of age

(41), supporting the role of BAT IGF-1 signaling in energy homeostasis. Recently, IGF-1R has been knocked out specifically in the BAT, using the *Ucp1*-Cre driver (42). This mouse model does not differ in body weight, yet has reduced cold tolerance (42). It is possible that compensatory increases in the expression of insulin receptor (IR) (38, 43) is responsible for diminished body weight phenotypes in IGF-1R KOs. In support of this idea, eliminating the redundancy in the system (IR/IGF-1R double knock out in adipose tissue) leads to 80% reductions in BAT weight and cold intolerance (38). In summary, while IGF-1 signaling likely plays an important role in BAT development, it is difficult to study because of compensation in the system.

Evidence for a peak of BAT activity at 5 weeks of age

The increase in mitochondrial gene expression at 4-5 weeks of age supports the idea that there might be a peak of BAT thermogenic function in the peri-pubertal period, similar to what is found in humans (3). We found that the increase in UCP1 protein content at 5 weeks was not reflected in *Ucp1* mRNA expression (Figure 3.3A,B). This phenomenon is well documented in the literature (44, 45). For example, while Xue *et al.* (2007) reported that BAT *Ucp1* mRNA expression is maximal at P1, the peak of UCP1 protein is not observed until P10 (44). These inconsistencies may stem from differences in the stability of UCP1 mRNA and protein under different environmental conditions. The half-life ($t_{1/2}$) of *Ucp1* transcript is 8-10 hours (46, 47). Not only is the UCP1 protein more stable than the transcript at baseline ($t_{1/2}$ 20 hours), but this stability is further enhanced in the stimulated state ($t_{1/2}$ 70 hours) (48). We hypothesize that increased BAT

UCP1 from at 5 weeks of age reflects a time window when BAT capacity and activity are restored, following the transient decrease between 2-3 weeks.

Expression of genes related to mitochondrial structure in the post-weaning period

Of the 13 genes analyzed in BAT, we found that the gene that best correlated with the changes in UCP1 protein in the peri-weaning period was *Mfn2*. MFN2 is a mitochondrial fusion protein, and its induction in BAT and skeletal muscle correlates with increased EE (34). Conversely, its expression is reduced in obese animals (49). First, we found *Mfn2* to be slightly decreased at 2 weeks compared to 3 weeks of age (Supplemental Figure 3.5) (NS), coinciding with the disruption we found in mitochondrial structure at this time (Figure 3.1B). An important issue to be addressed in the future is the structure of mitochondria at 2 weeks of age, to confirm that cristae disorganization is occurring at 3 weeks of age, as opposed to a delay in the maturation of cristae in mice relative to rats.

We found that *Mfn2* was increased between 4-5 weeks of age compared to 3 weeks of age (Figure 3.3C), supporting the idea that it plays a role in the activation of BAT during this time period. In *vitro*, *Mfn2* is regulated by estrogen related receptor α (*Errα*) (34); however, we do not see any changes in *Errα* expression across the post-weaning period (Supplemental Figure 3.1). Although *Errα* is necessary for the thermogenic response of BAT to cold (50), it is not yet clear whether *Errα* is necessary for the maturation of BAT. *Errα* KO mice exhibit normal EE (51) and cold-stimulated upregulation of thermogenic gene expression in BAT, although some *Errα* KO mice display cold intolerance in response to a 3 day cold challenge (34, 50). This could be an artifact of reduced

mitochondrial abundance, as the mitochondrial cristae organization pattern was unchanged (50). *Mfn2* has been shown to be regulated by peroxisome proliferator-activated receptor gamma coactivator 1 alpha (*Pgc1α*) (34), and therefore it would be interesting to look at *Pgc1α* gene expression during this time period.

The upregulation seen in *Mics1* is important, as *Mics1* has a known regulatory role in mitochondrial cristae organization (35), and knock-down of *Mics1* leads to disruption of cristae formation (35). Furthermore, although both genes regulate cristae organization, *Mics1* and *Opa1* are distinct and do not seem to influence one another (35). Therefore, our data support a role for *Mics1*, not *Opa1*, as the mediator of cristae formation during this time period.

Thermogenic circuitry in KO mice is developmentally delayed

We hypothesized that the peak of BAT UCP1 in the peri-weaning period would be disrupted in the obese KO-AL model. Consistent with our hypothesis, KO-AL mice do not exhibit an increase in BAT *Ucp1* mRNA or protein levels, nor *Igf-1* levels across time points (Figure 3.6). In fact, BAT *Igf-1* and *Ucp1* levels were reduced at 5 weeks in KO-AL mice compared to controls (Figure 3.6A,B,D). At 7 and 9 weeks of age, after the end of the peak in control mice, KO-AL and control mice have similar gene expression levels (Figure 3.6A,B,E), supporting the idea that KO-AL mice never developed a peak in BAT expression levels. Similarly, mitochondrial genes that were increased between 3-5 weeks of age in control mice (*Ucp1, Mfn2, Mics1, Igf1*) were reduced in KO-AL mice at 5 weeks of age (Figure 3.6B,C). The reduction of *Mics1* in KO-AL vs. control mice is

consistent with the observation that KO mice have disorganized cristae (as seen at 10 weeks of age) (Figure 2.6B)(2). These data support the hypothesis that the reduced BAT activity in KO-AL mice stems from a failure to "reconsolidate" BAT mitochondrial structure after weaning.

Impact of paired-feeding on BAT maturation in the post-weaning period

We previously showed that KO-PF mice have increased EE compared to KO-AL mice (Figure 2.3A, 2.4A) (2). Therefore, we hypothesized that paired-feeding might rescue the processes driving the "reconsolidation" of BAT mitochondrial cristae and the increase in BAT capacity and activity in the peri-weaning period. In support of this idea, we found that paired-feeding resulted in increased UCP1 protein levels at 5 weeks of age (Figure 3.7C). An important caveat is that we only had n=2 mice for the KO-AL in this cohort to compare with KO-PF mice, and therefore this experiment must be repeated. Furthermore, KO-AL mice are developmentally delayed, so it is important to carry out studies to map the maximal time point (if any) at which UCP1 might be elevated in BAT to fully determine whether the peak is delayed or entirely absent.

In previous studies, we reported that KO-PF mice exhibited increased *Ucp1* expression levels at 10 weeks of age (Figure 2.3D) (2). Although we did not find *Ucp1* mRNA to be increased at 5 weeks of age in the KO-PF mice, we found increased UCP1 protein levels when compared to KO-AL (Figure 3.7A,C). It is possible that the failure to observe increased *Ucp1* expression at 5 weeks in KO-PFs stems from differences in the prandial state when the mice were euthanized. The published data were generated from mice in

the fasted state, while the new data were generated from mice in the fed state. In our experience, increases in BAT *Ucp1* expression in older KO-PFs vs. KO-ALs are not as significant in the fed state (13 weeks of age, Figure 3.7B), as compared to the fasted state (10 and 20 weeks of age, Figure 2.3D, 2.4D) (2). These observations are consistent with the idea that the response to fasting is blunted in KO-PF mice relative to AL-KO mice. This issue will be discussed further in Chapter 4.

Part II: Outstanding Issues

The main weakness of this study is that UCP1 is the sole readout of BAT activity. We first explored whether we could use longitudinal measurements of EE in the Columbus Instruments Comprehensive Lab Animal Monitoring System (CLAMS) Oxymax metabolic cages to detect increased BAT activity in the post-weaning period. We initially tried to derive a multiple regression metabolic equation suitable for each age (in weekly increments). Because absolute and relative amounts of lean and fat mass were changing on a daily basis during this period, we were not able to develop a method to make meaningful statements about EE. In theory, comparisons of energy consumed versus energy expended, as well as total VO2 could be used to determine how fuel utilization changes over time within an individual animal. Going forward, functional BAT activity assays, such as glucose uptake studies, could be used to determine whether the increased BAT UCP1 correlates to metabolic activity of the BAT.

Please refer to Chapter 4 for the future directions of this project.

Part III: Future Outlook

In this study, we discovered that BAT capacity and activity are very dynamic in the peri-weaning period; a marked decline in these parameters between 2-3 weeks of age is followed by improvements in the post-weaning period. The decrease in BAT capacity occurs during a time when the mass of the BAT depot doubles. Due to the compression of rodent development, it is difficult to translate the events under investigation here into humans. There are two ages when BAT expansion has been reported in humans: infancy and puberty (4, 9, 12). If expansion is also followed by reductions in BAT capacity (i.e., due to the presence of immature mitochondria in newly-born cells), it is possible that the subsequent "consolidation" of mitochondrial structure could contribute to high levels of BAT activity reported in infants and teens (4, 9, 12). As this process is impaired by obesity and rescued by weight loss, we hypothesize that the process of "consolidation" might represent a novel target for interventions in obese children. The identification of biomarkers for this process is critical to test this idea in humans.

ACKNOWLEDGEMENTS

We thank the Columbia Diabetes and Endocrinology Research Center Animal Phenotyping Core for help with metabolic cages (P30 DK063608); S. Anderson (Weill Cornell Medical College) for *Nkx2.1-Cre* mice; S. Chua (Albert Einstein College of Medicine) for *Lepr* floxed mice; This work was supported by R01 DK 089038 (LMZ), National Center for Advancing Translational Sciences, NIH, through Grant Number UL1 TR000040, the HHMI-funded "Med into Grad" program (JSL), and the Russ Berrie Foundation (RH).

FIGURES

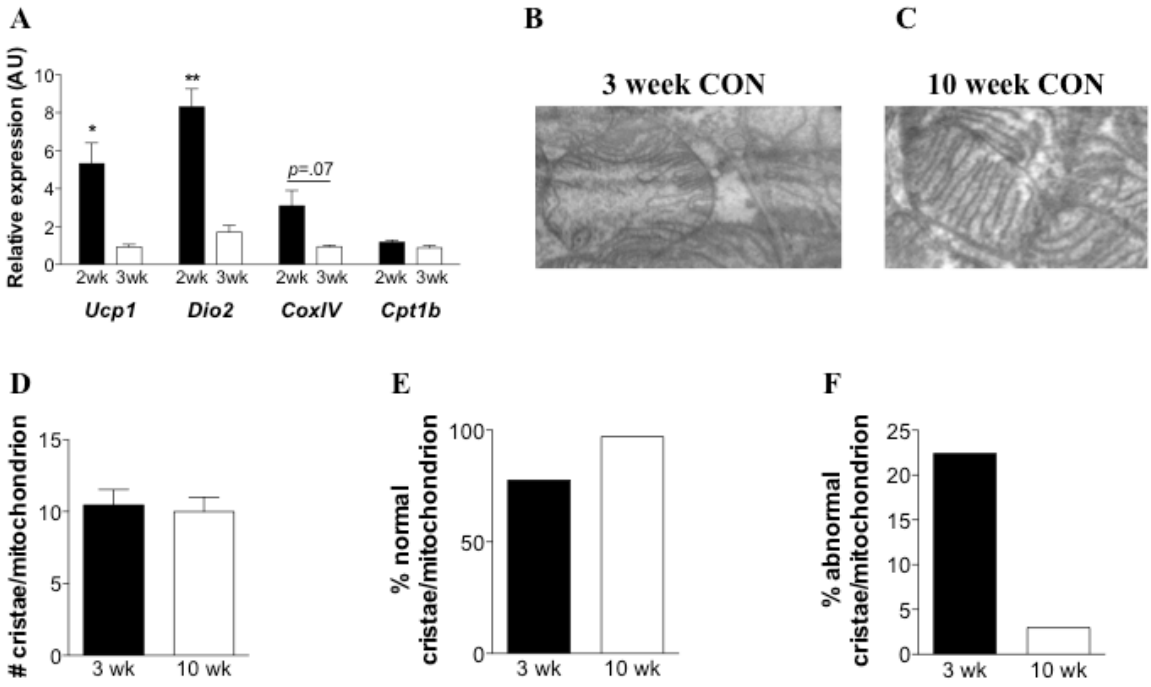

Figure 3.1. 2 to 3 weeks is a time of reduced BAT capacity in control mice. (A) Gene expression levels from 2 vs. 3 weeks of age. (B) 3 week BAT mitochondria. (C) 10 week BAT mitochondria. (D) Total number of cristae per mitochondrion, (E) percent normal cristae per mitochondrion, and (F) percent abnormal cristae/mitochondrion in 3 vs. 10 weeks of age. Error bars represent standard error of mean. Significance was determined between groups by Student's or Welch's t-test accordingly. For (E) and (F), data underwent arcsin transformation prior to statistical analysis. Data for gene expression was generated from 2wk; n=4, 4wk; n=5. Mitochondrial analysis was generated from 3wk; n=2, 10wk; n=4.

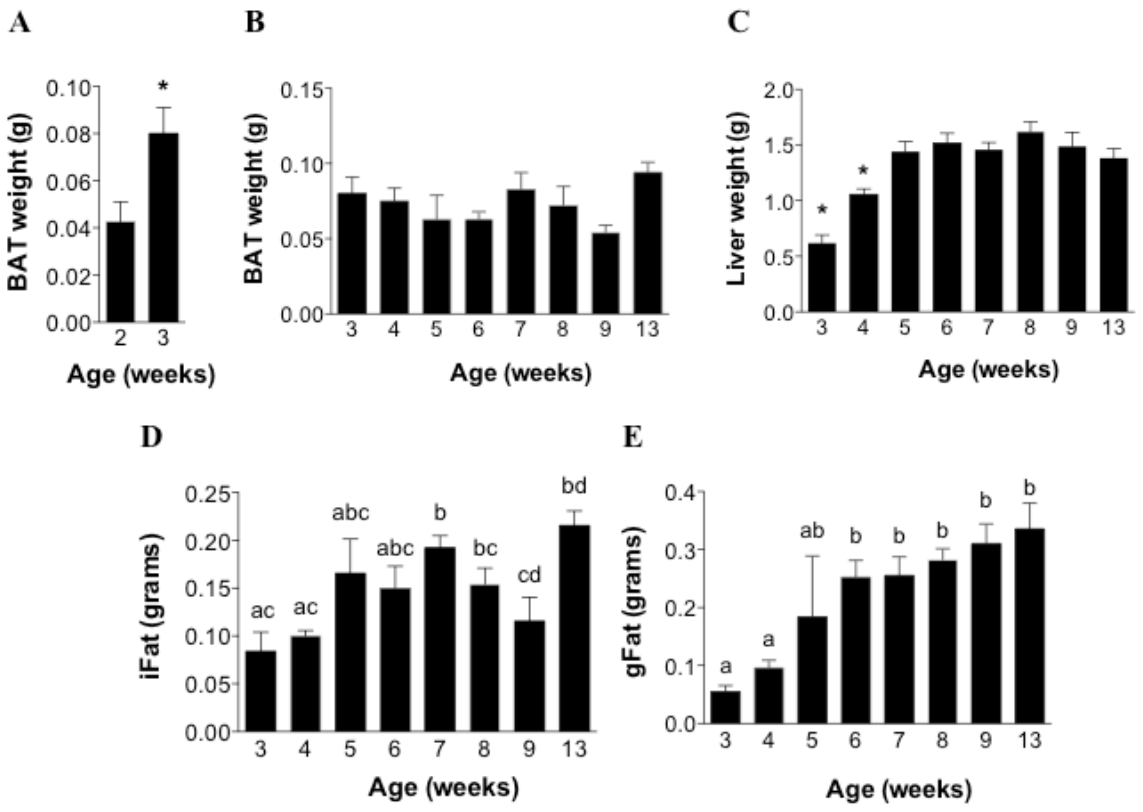

Figure 3.2. BAT expansion occurs from 2 to 3 weeks of age in control mice. (A) BAT weight from 2 to 3 weeks of age. (B) BAT, (C) liver, (D) iFat, and (E) gFat weights over time. Significance in (A) was determined between groups by Student's or Welch's t-test accordingly. Significance in (B-E) was determined between groups using one-way ANOVA and Student's or Welch's t-test accordingly. (A) * represents <.05. (B) * represents statistical difference (<.05) from all other groups. (C-E) Different letters (a,b,c) represent statistical significance. Data generated from (A) n=4-5 in each group, (B-E) n=2-7 within each group.

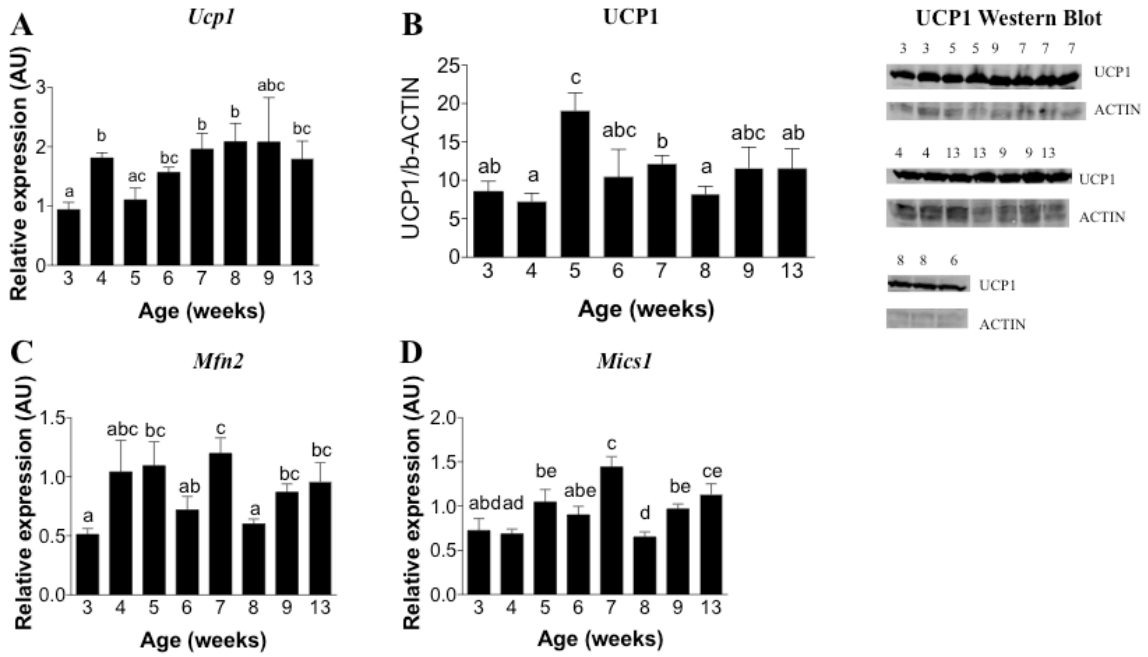

Figure 3.3. Peak in BAT thermogenic and mitochondrial genes at 5 weeks of age in control mice. (A) BAT *Ucp1* gene expression and (B) UCP1 protein over time. (C) *Mfn2* and (D) *Mics1* gene expression in BAT over time. Significance was determined between groups using one-way ANOVA and Student's or Welch's t-test accordingly. Different letters (a,b,c) represent statistical significance. Data generated from n=4-7 within each group.

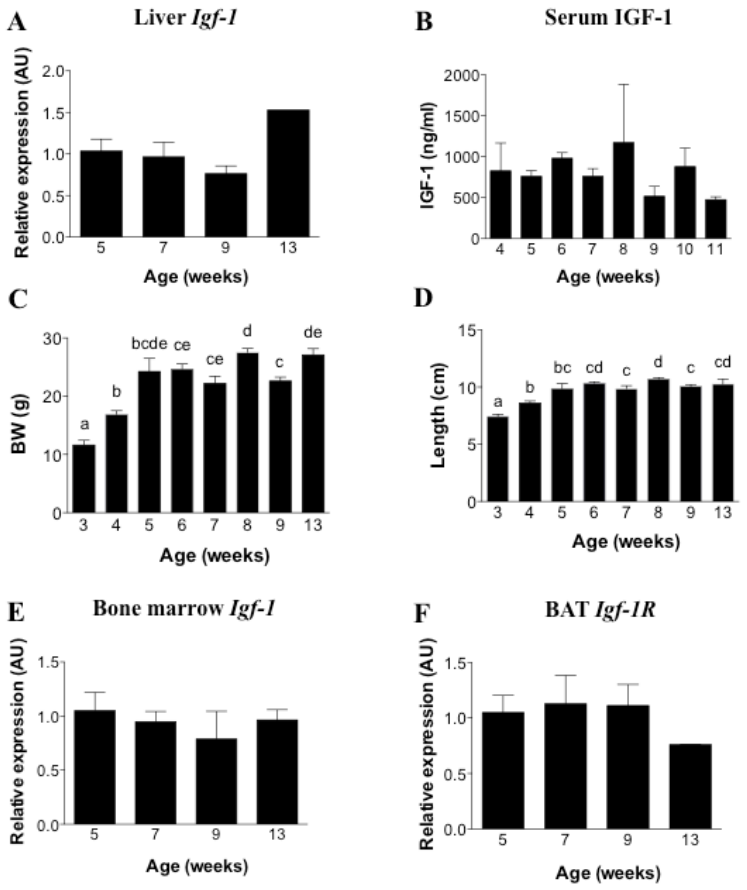

Figure 3.4. Serum IGF-1 does not track with growth rate. (A) Liver *Igf-1* and (B) serum IGF-1 levels. (C) Body weight gain. (D) Naso-anal length across ages. (E) Bone marrow *Igf-1*. (F) BAT *Igf-1R* expression levels. Significance was determined between groups using one-way ANOVA and Student's or Welch's t-test accordingly. Different letters (a,b,c) represent statistical significance. Data generated from n=2-9 within each group. Liver expression data (A) generated from n=1-5.

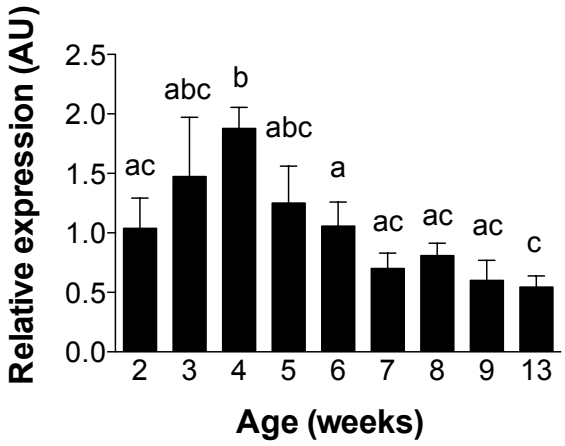

Figure 3.5. BAT *Igf-1* is upregulated between 2-5 weeks of age in control mice. Significance was determined between groups using one-way ANOVA and Student's or Welch's t-test accordingly. Different letters (a,b,c) represent statistical significance. Data generated from n=3-7 in each age group.

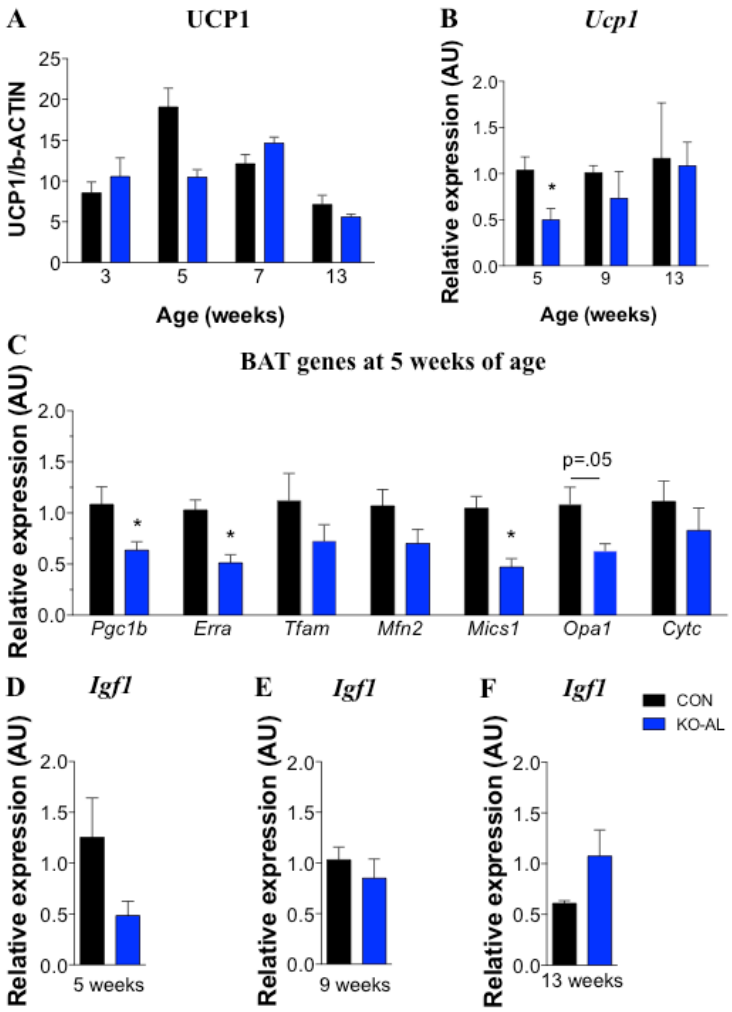

Figure 3.6. KO-AL mice do not exhibit a peak in BAT thermogenic function.

(A) BAT UCP1 protein levels at 3, 5, 7, and 13 weeks of age in control vs. KO mice. (B) BAT *Ucp1* gene expression levels at 5, 9 and 13 weeks of age between control vs. KO mice. (C) Mitochondrial gene expression analysis in control vs. KO mice. *Igf-1* gene expression in control vs. KO mice at (D) 5, (E) 9, and (F) 13 weeks of age. Black bars represent control mice, blue bars represent KO mice. Error bars represent standard error of the mean. Significance was determined between groups by Student's or Welch's t-test accordingly. * represents $p<.05$. Data generated from controls; n=2-7, KO-AL; n=2-5.

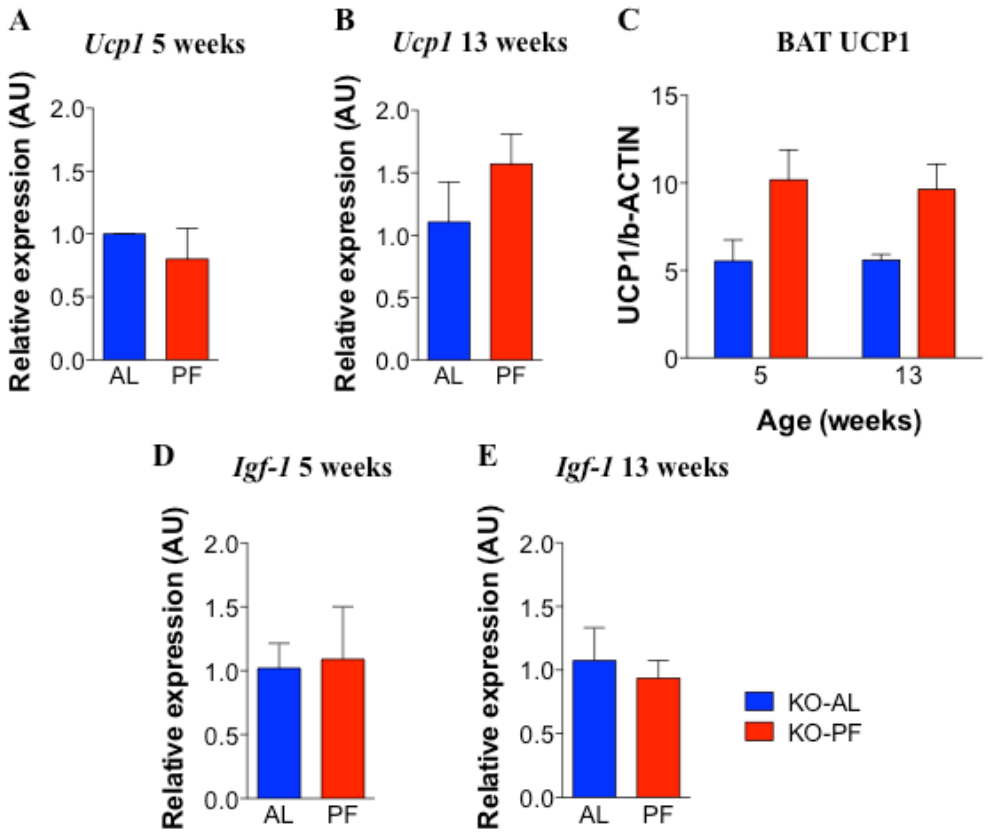

Figure 3.7. Paired-feeding rescues thermogenic activation in BAT at 5 weeks of age. (A) BAT *Ucp1* gene expression at 5 weeks of age. (B) BAT UCP1 protein levels at 5 and 13 weeks of age. BAT *Igf-1* gene expression at (C) 5 weeks and (D) 13 weeks of age in KO-AL vs. KO-PF mice. Blue bars represent KO-AL mice, red bars represent KO-PF mice. Error bars represent standard error of mean. There was no significance between groups, as determined by Student's or Welch's t-test. Data generated from AL; n=2-3, PF; n=3-6.

SUPPLEMENTAL FIGURES

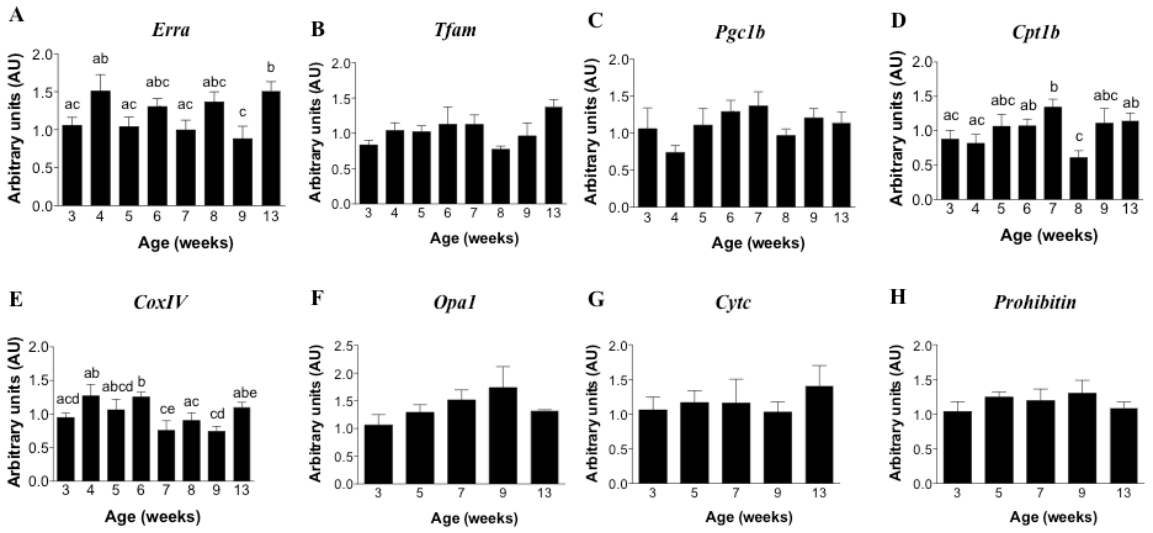

Supplemental Figure 3.1. Unchanged mitochondrial related genes across different ages in control mice. BAT (A) *Errα*, (B) *Tfam*, (C) *Pgc1β*, (D) *Cpt1b,* (E) *CoxIV,* (F) *Opa1*, (G) *Cytc*, (H) prohibitin across the peri-weaning period. Error bars represent standard error of mean. Significance was determined between groups using one-way ANOVA and Student's or Welch's t-test accordingly. Arbitrary units represent relative expression compared to *b-actin*. Different letters (a,b,c) represent statistical significance. Data generated from n=2-7 mice in each group.

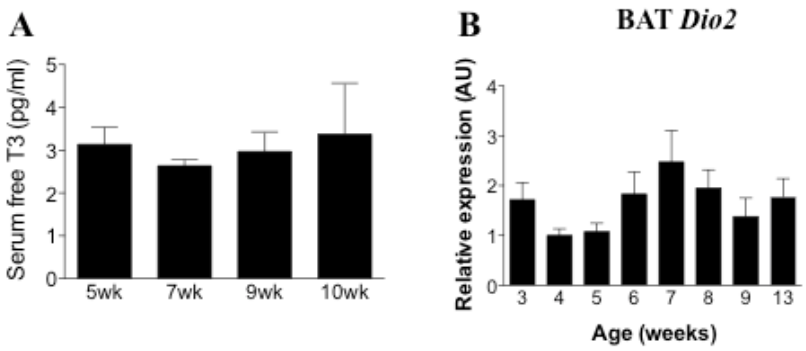

Supplemental Figure 3.2. Serum T3 and BAT *deiodinase 2* expression levels are unchanged during the early peri-weaning period. (A) Serum T3 and (B) BAT *Dio2* expression levels through the peri-weaning period. Error bars represent standard error of the mean. There was no significance between groups, as determined by Student's or Welch's t-test accordingly. Data generated from n=3-8 in each group.

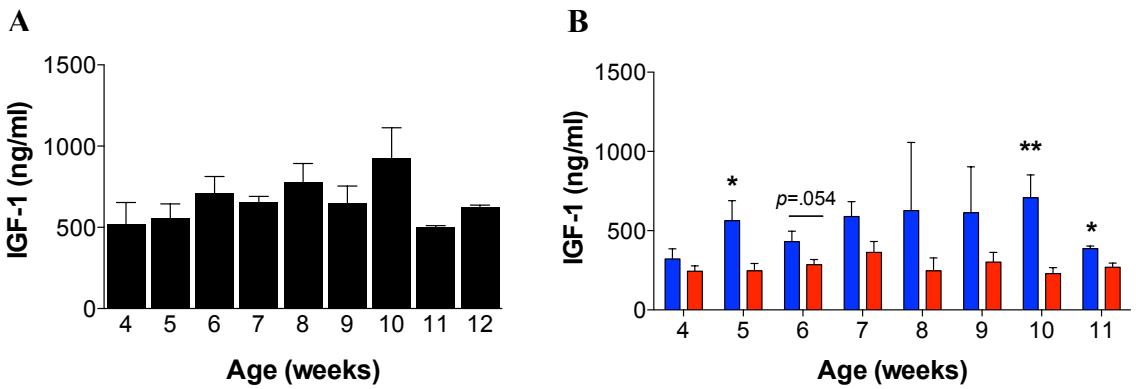

Supplemental Figure 3.3. Serum IGF-1 follows a similar pattern in female wild type and male AL-KO mice, but is blunted in KO-PF during the peri-weaning period. (A) Female serum IGF-1 levels. (B) Male KO-AL and KO-PF serum IGF-1 levels. Significance was determined between groups using one-way ANOVA and Student's or Welch's t-test accordingly. Different letters represent statistical significance. * represents $p<.05$ between KO-AL and KO-PF. (A) Data generated from n=2-8 in each group. (B) Data generated from n=3-9 mice.

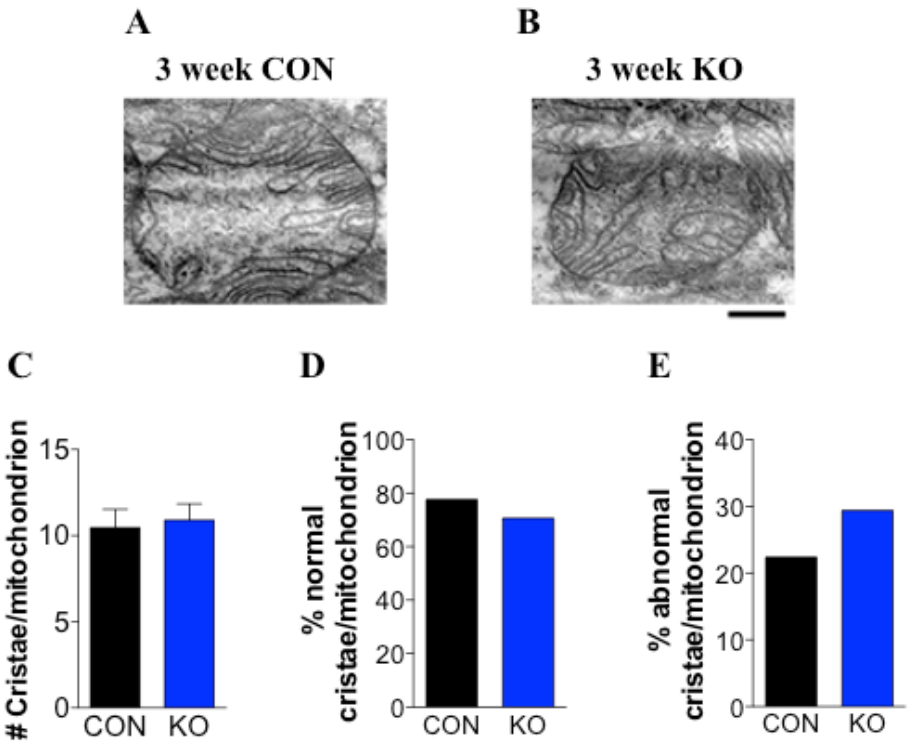

Supplemental Figure 3.4. 3 week control and KO mice have similar mitochondrial structure. Electron micrograph of (A) control and (B) KO mice at 3 weeks of age. (C) Total number of cristae per mitochondrion. (D) Percent normal cristae per mitochondrion. (E) Percent abnormal cristae per mitochondrion. Scale bar represents 500nm. Error bars represent standard error of mean. No significance difference was found for (C) using Student's t-test. For (D) and (E), data underwent arcsin transformation prior to statistical analysis, no statistical significance was found. Data generated from control; n=2, KO; n=4.

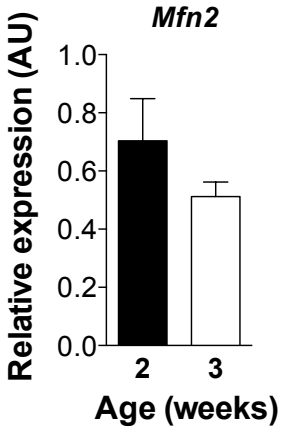

Supplemental Figure 3.5. Reduced BAT *Mfn2* expression from 2 to 3 weeks of age. Black bar represents 2 weeks of age, white bar represents 3 weeks of age. Error bars represent standard error of mean. No statistical significance was found using Student's t-test. Data generated from 2 weeks; n=4, 3 weeks; n=5.

REFERENCES

1. Ogden CL, Carroll MD, Kit BK, Flegal KM. Prevalence of childhood and adult obesity in the United States, 2011-2012. JAMA. 2014;311(8):806-14.

2. Lerea JS, Ring LE, Hassouna R, Chong AC, Szigeti-Buck K, Horvath TL, et al. Reducing Adiposity in a Critical Developmental Window Has Lasting Benefits in Mice. Endocrinology. 2016;157(2):666-78.

3. Drubach LA, Palmer EL, Connolly LP, Baker A, Zurakowski D, Cypess AM. Pediatric brown adipose tissue: detection, epidemiology, and differences from adults. J Pediatr. 2011;159(6):939-44.

4. Gilsanz V, Smith ML, Goodarzian F, Kim M, Wren TA, Hu HH. Changes in brown adipose tissue in boys and girls during childhood and puberty. J Pediatr. 2012;160(4):604-9.

5. Chalfant JS, Smith ML, Hu HH, Dorey FJ, Goodarzian F, Fu CH, et al. Inverse association between brown adipose tissue activation and white adipose tissue accumulation in successfully treated pediatric malignancy. Am J Clin Nutr. 2012;95(5):1144-9.

6. Virtanen KA, Lidell ME, Orava J, Heglind M, Westergren R, Niemi T, et al. Functional brown adipose tissue in healthy adults. New England Journal of Medicine. 2009;360(15):1518-25.

7. Yeung HW, Grewal RK, Gonen M, Schöder H, Larson SM. Patterns of (18)F-FDG uptake in adipose tissue and muscle: a potential source of false-positives for PET. J Nucl Med. 2003;44(11):1789-96.

8. Merklin RJ. Growth and distribution of human fetal brown fat. Anat Rec. 1974;178(3):637-45.

9. Lean ME, James WP, Jennings G, Trayhurn P. Brown adipose tissue uncoupling protein content in human infants, children and adults. Clin Sci (Lond). 1986;71(3):291-7.

10. Heaton JM. The distribution of brown adipose tissue in the human. J Anat. 1972;112(Pt 1):35-9.

11. Tanuma Y, Tamamoto M, Ito T, Yokochi C. The occurrence of brown adipose tissue in perirenal fat in Japanese. Arch Histol Jpn. 1975;38(1):43-70.

12. Ponrartana S, Aggabao PC, Chavez TA, Dharmavaram NL, Gilsanz V. Changes in Brown Adipose Tissue and Muscle Development during Infancy. J Pediatr. 2016 March 30;[epub ahead of print].

13. Sharp LZ, Shinoda K, Ohno H, Scheel DW, Tomoda E, Ruiz L, et al. Human BAT possesses molecular signatures that resemble beige/brite cells. PLoS One [Internet]. 2012; 7(11):[e49452 p.].

14. Svensson PA, Lindberg K, Hoffmann JM, Taube M, Pereira MJ, Mohsen-Kanson T, et al. Characterization of brown adipose tissue in the human perirenal depot. Obesity (Silver Spring). 2014;22(8):1830-7.

15. Cypess AM, Lehman S, Williams G, Tal I, Rodman D, Goldfine AB, et al. Identification and importance of brown adipose tissue in adult humans. New England Journal of Medicine. 2009;360(15):1509-17.

16. van Marken Lichtenbelt WD, Vanhommerig JW, Smulders NM, Drossaerts JM, Kemerink GJ, Bouvy ND, et al. Cold-activated brown adipose tissue in healthy men. New England Journal of Medicine. 2009;360(15):1500-8.

17. Gelfand MJ, O'hara SM, Curtwright LA, Maclean JR. Pre-medication to block [(18)F]FDG uptake in the brown adipose tissue of pediatric and adolescent patients. Pediatr Radiol. 2005;35(10):984-90.

18. Yoneshiro T, Aita S, Matsushita M, Kameya T, Nakada K, Kawai Y, et al. Brown adipose tissue, whole-body energy expenditure, and thermogenesis in healthy adult men. Obesity (Silver Spring). 2011;19(1):13-6.

19. Saito M, Okamatsu-Ogura Y, Matsushita M, Watanabe K, Yoneshiro T, Nio-Kobayashi J, et al. High incidence of metabolically active brown adipose tissue in healthy adult humans: effects of cold exposure and adiposity. Diabetes. 2009;58(7):1526-31.

20. Hanssen MJ, van der Lans AA, Brans B, Hoeks J, Jardon KM, Schaart G, et al. Short-term cold acclimation recruits brown adipose tissue in obese humans. Diabetes. 2015;[Epub ahead of print].

21. Skála J, Barnard T, Lindberg O. Changes in interscapular brown adipose tissue of the rat during perinatal and early postnatal development and after cold acclimation. II. Mitochondrial changes. Comp Biochem Physiol. 1970;33(3):509-28.

22. Lindgren G, Barnard T. Changes in interscapular brown adipose tissue of rat during perinatal and early postnatal development and after cold acclimation. IV. Morphometric investigation of mitochondrial membrane alterations. Exp Cell Res. 1972;70(1):81-90.

23. Iossa S, Lionetti L, Mollica MP, Barletta A, Liverini G. Energy intake and utilization vary during development in rats. J Nutr. 1999;129(8):1593-6.

24. LeRoith D. Insulin-Like Growth Factors. The New England Journal of Medicine. 1997;336:633-40.

25. Lorenzo M, Valverde AM, Teruel T, Benito M. IGF-I is a mitogen involved in differentiation-related gene expression in fetal rat brown adipocytes. J Cell Biol. 1993;123(6 pt 1):1567-75.

26. Teruel T, Valverde AM, Alvarez A, Benito M, Lorenzo M. Differentiation of rat brown adipocytes during late foetal development: role of insulin-like growth factor I. Biochem J. 1995;310(pt 3):771-6.

27. Guerra C, Benito M, Fernández M. IGF-I induces the uncoupling protein gene expression in fetal rat brown adipocyte primary cultures: role of C/EBP transcription factors. Biochem Biophys Res Commun. 1994;201(2):813-9.

28. McMinn JE, Liu SM, Dragatsis I, Dietrich P, Ludwig T, Eiden S, et al. An allelic series for the leptin receptor gene generated by CRE and FLP recombinase. Mamm Genome. 2004;15(9):677-85.

29. Xu Q, Tam M, Anderson SA. Fate mapping Nkx2.1-lineage cells in the mouse telencephalon. J Comp Neurol. 2008;506(1):16-29.

30. Obregón MJ, Ruiz de Oña C, Hernandez A, Calvo R, Escobar del Rey F, Morreale de Escobar G. Thyroid hormones and 5'-deiodinase in rat brown adipose tissue during fetal life. Am J Physiol. 1989;257(5 pt 1):E625-E31.

31. Li Y, Park JS, Deng JH, Bai Y. Cytochrome c oxidase subunit IV is essential for assembly and respiratory function of the enzyme complex. J Bioenerg Biomembr. 2006;38(5-6):283-91.

32. Kadenbach B, Hüttemann M, Arnold S, Lee I, Bender E. Mitochondrial energy metabolism is regulated via nuclear-coded subunits of cytochrome c oxidase. Free Radic Biol Med. 2000;29(3-4):211-21.

33. Cannon B, Nedergaard J. Brown Adipose Tissue: Function and Physiological Significance. Physiol Rev. 2004;84:277-359.

34. Soriano FX, Liesa M, Bach D, Chan DC, Palacín M, Zorzano A. Evidence for a mitochondrial regulatory pathway defined by peroxisome proliferator-activated receptor-gamma coactivator-1 alpha, estrogen-related receptor-alpha, and mitofusin 2. Diabetes. 2006;55(6):1783-91.

35. Oka T, Sayano T, Tamai S, Yokota S, Kato H, Fujii G, et al. Identification of a novel protein MICS1 that is involved in maintenance of mitochondrial morphology and apoptotic release of cytochrome c. Mol Biol Cell. 2008;19(6):2597-608.

36. Butler AA, LeRoith D. Minireview: tissue-specific versus generalized gene targeting of the igf1 and igf1r genes and their roles in insulin-like growth factor physiology. Endocrinology. 2000;142(5):1685-8.

37. Yakar S, Liu JL, Stannard B, Butler A, Accili D, Sauer B, et al. Normal growth and development in the absence of hepatic insulin-like growth factor I. Proc Natl Acad Sci USA. 1999;96(13):7324-9.

38. Boucher J, Mori MA, Lee KY, Smyth G, Liew CW, Macotela Y, et al. Impaired thermogenesis and adipose tissue development in mice with fat-specific disruption of insulin and IGF-1 signalling. Nat Commun. 2012;3:902.

39. Ring LE, Zeltser LM. Disruption of hypothalamic leptin signaling in mice leads to early-onset obesity, but physiological adaptations in mature animals stabilize adiposity levels. J Clin Invest. 2010;120(8):2931-41.

40. Chang HR, Kim HJ, Xu X, Ferrante AW, Jr. Macrophage and adipocyte IGF1 maintain adipose tissue homeostasis during metabolic stresses. Obesity (Silver Spring). 2016;24(1):172-83.

41. Klöting N, Koch L, Wunderlich T, Kern M, Ruschke K, Krone W, et al. Autocrine IGF-1 action in adipocytes controls systemic IGF-1 concentrations and growth. Diabetes. 2008;57(8):2074-82.

42. Viana-Huete V, Guillén C, García-Aguilar A, García G, Fernández S, Kahn CR, et al. Essential role of IGFIR in the onset of male brown fat thermogenic function: Regulation of glucose homeostasis by differential organ-specific insulin sensitivity. Endocrinology. 2016;en20151623.

43. Nakae J, Kido Y, Accili D. Distinct and overlapping functions of insulin and IGF-I receptors. Endocr Rev. 2001;22(6):818-35.

44. Xue B, Rim JS, Hogan JC, Coulter AA, Koza RA, Kozak LP. Genetic variability affects the development of brown adipocytes in white fat but not in interscapular brown fat. J Lipid Res. 2007;48(1):41-51.

45. Yamashita H, Yamamoto M, Ookawara T, Sato Y, Ueno N, Ohno H. Discordance between thermogenic activity and expression of uncoupling protein in brown adipose tissue of old rats. 49. 1994;2(B54-B59).

46. Rehnmark S, Bianco AC, Kieffer JD, Silva JE. Transcriptional and posttranscriptional mechanisms in uncoupling protein mRNA response to cold. Am J Physiol. 1992;262(1 pt 1):E58-E67.

47. Bianco AC, Sheng XY, Silva JE. Triiodothyronine amplifies norepinephrine stimulation of uncoupling protein gene transcription by a mechanism not requiring protein synthesis. J Biol Chem. 1988;263(34):18168-75.

48. Puigserver P, Herron D, Gianotti M, Palou A, Cannon B, Nedergaard J. Induction and degradation of the uncoupling protein thermogenin in brown adipocytes in vitro and in vivo. Evidence for a rapidly degradable pool. Biochem J. 1992;284(pt 2):393-8.

49. Bach D, Pich S, Soriano FX, Vega N, Baumgartner B, Oriola J, et al. Mitofusin-2 determines mitochondrial network architecture and mitochondrial metabolism. A novel regulatory mechanism altered in obesity. Journal of Biological Chemistry. 2003;278(19).

50. Villena JA, Hock MB, Chang WY, Barcas JE, Giguère V, Kralli A. Orphan nuclear receptor estrogen-related receptor alpha is essential for adaptive thermogenesis. Proc Natl Acad Sci USA. 2007;104(4):1418-23.

51. Luo J, Sladek R, Carrier J, Bader JA, Richard D, Giguère V. Reduced fat mass in mice lacking orphan nuclear receptor estrogen-related receptor alpha. Mol Cell Biol. 2003;23(22):7947-56.

Chapter 4: Concluding Remarks and Future Directions

Part I: Generalizability of lessons learned from rodent models of early intervention

While there are many established mouse models of diet- and genetic-induced obesity, increased adiposity is rarely seen early enough to be useful in studies of early intervention (see Chapter 1 for full review). *Db/db* and *ob/ob* mice exhibit early-onset hyperphagia and obesity, but they do not respond normally to caloric restriction (CR), because they preferentially maintain fat mass vs. lean mass (1-5). As described in Chapter 2, we used the *Nkx2.1-Cre;Lepr*$^{flox/flox}$ mice (KO) to study whether early intervention could produce lasting improvements in obesity-related outcomes. We found that paired-feeding KO mice from 3-10 weeks of age (KO-PF) results in persistent reductions in adiposity, likely due to enhanced capacity and activity in brown adipose tissue (BAT) (Chapter 2)(6). Comparisons between our findings and two other models of early intervention will be discussed below.

Otsuka Long-Evans Tokushima Fatty rats (OLETF) exhibit early-onset hyperphagia and obesity due to a deficit in CCK receptor signaling (7). These studies demonstrated differences between males and females; caloric restriction from 3-6 weeks of age produced lasting reductions in obesity in males only (7, 8). Although the effect on males was attributed to decreased food intake, endpoints related to energy expenditure were not assessed. This is in contrast to our KO model, which has the same response to early paired-feeding regardless of gender (Chapter 2)(6). However, we cannot exclude the

possibility that CR in the OLETF rat model would also produce lasting effects in females if the intervention was extended to 10 weeks, as we had done in our model.

Mice lacking POMC in the arcuate nucleus of the hypothalamus (arc*Pomc*-/-) (with normal expression in the brainstem and pituitary) have been used to study early intervention (9). Restoring *Pomc* expression at any age could correct the hyperphagia, yet the impact of restoring *Pomc* expression on body weight was dependent on the age at which the intervention was initiated. Interventions beginning at postnatal day 25 (P25) could completely rescue the lean phenotype, while those initiated later were less effective, particularly in males (9). These data support our hypothesis that baselines of energy expenditure are established in the peri-weaning period, likely between 4-6 weeks of age. The major difference in the degree of body weight rescue in the arc*Pomc*-/- mice and in our KO model is likely due to large differences in food intake in the two systems.

Part II: Defining the developmental window to establish thermoregulatory circuits

Concluding Remarks

Obesity is associated with reductions in sympathetic tone onto the BAT (10, 11), resulting in abnormal BAT morphology and function (12-14). Rearing in small litter size, a method of early overfeeding resulting in increased body weight later in life, results in mice with impairments in BAT morphology (i.e., larger lipid droplets (15)), activity (as evidenced by reduced BAT temperature (15)), and reduced capacity to respond to a cold challenge (16). These impairments in BAT function are similar to what is seen in

ob/ob mice, which are cold intolerant unless slowly acclimated (13). Taken together, these data support the role of BAT thermoregulation in the maintenance of body temperature, body weight and energy homeostasis, thus leading researchers to investigate how to harness BAT activation as a therapeutic target for the obesity epidemic.

Similar to what is seen in the *ob/ob* mice, mitochondrial structure in KO mice is disorganized compared to control mice throughout all ages after weaning (as seen by increased number of abnormal cristae/mitochondrion) (Figure 2.6B,G)(6). We found that the KO and control mice have similar mitochondrial structure at 3 weeks of age (Supplemental Figure 3.4), implicating the functional development of BAT after 3 weeks of age as an important indicator of later thermogenic capacity. Importantly, the control mice can survive cold at 3 weeks of age regardless of the initial mitochondrial structure, while the KO mice cannot (17). These observations support the idea that deficits in thermoregulatory circuits, rather than mitochondrial disorganization *per se*, is responsible for cold intolerance of KOs at 3 weeks. At least some components of the thermoregulatory circuits eventually develop in KOs, as they can defend against a cold challenge at 6 weeks of age (17).

Control mice exhibit a peak in the thermogenic protein (UCP1) at 5 weeks of age (Figure 3.3B), whereas the KO mice do not (Figure 3.6A). This phenomenon seems to be restored in the KO-PF mice (Figure 3.7C), leading to the hypothesis that paired-feeding increases BAT capacity to respond to endogenous signals driving thermogenic activity at 5 weeks of age; this enhanced capacity persists even after release to *ad libitum* feeding.

How paired-feeding rescues the BAT thermoregulatory system remains unclear. While the increase in *Igf-1* expression in the peri-weaning period occurs at the right time to play a role in this process, the failure to see an upregulation in *Igf-1* in KO-PF compared to KO-AL (Figure 3.7D,E) argues against the idea that this is the mechanism by which paired-feeding is working. This is an important question of future research.

Future Directions

(i) Cold tolerance: To examine whether paired-feeding corrects the developmental delay in the thermogenic circuits of the KO mice, we must look at markers of thermoregulatory system at this time. Previously, the Zeltser lab showed that the KO mice are able to defend body temperature in response to cold by 6 weeks of age. It is important to note that it has been reported that 75 minutes (which was the duration of cold exposure at this time) is not long enough to mount a thermogenic response of BAT (18), therefore the ability to maintain body temperature at this time might rely on other mechanisms, such as shivering from skeletal muscle. The *s/s* mouse model, which exhibits early-onset obesity as a result of impaired leptin-mediated signaling through the Stat3 pathway, (19), can tolerate 75 minutes of cold exposure better than the *db/db* mice, which has been attributed to their increased lean mass deposition (18). If true, the response of our KO mouse to cold at 6 weeks is to be expected, as lean mass deposition is increased at this time (Figure 2.5C). To test BAT functionality, cold exposure should be prolonged (i.e. 4-12 hours). The hypothesis that the KO-PF mice will develop the ability to tolerate cold more rapidly is supported by the studies in *ob/ob* mice. Caloric restriction improves cold tolerance in obese mice at any age (20-22), which is likely attributed to improved BAT

thermogenic capacity in response to food restriction (6, 21, 22). It will be interesting to determine whether KO-AL mice have impaired response to a longer cold challenge in adulthood, and whether paired-feeding corrects this deficit in adulthood, even after *ad libitum* feeding resumes. This will parse out the effects of early paired-feeding on the later thermoregulatory system. Additionally, it is well established that BAT deiodinase 2 (Dio2) is necessary for maintenance of body temperature in response to cold (23), and KO-PF mice exhibit increased BAT *Dio2* compared to KO-AL mice at 10 and 20 weeks of age (Figure 2.3D, 2.4D), further supporting the hypothesis that they should have improved response to cold throughout adulthood.

(ii) Fasting-induced torpor: When food is unavailable, mice are known to go into a state of torpor, leading to dramatic reductions in core body temperature and metabolism (24). Our lab previously showed that the KO mice are more sensitive to fasting when singly housed, and are more likely to enter the torpor state initiated by an overnight fast compared to control mice (25), similar to what is seen in *ob/ob* mice (22). We hypothesize that this phenomenon might be rescued in the KO-PF mice. To test this, we can measure body temperature after an overnight fast in KO-PF versus KO-AL mice, to elucidate whether paired-feeding rescues these mice from dramatic reductions in body temperature in response to fasting. This phenomenon is also seen in triiodothyronine (T3) levels, which are reduced in the fasting state in KO-AL compared to controls, yet the difference disappears in the fed state (Figure 4.1). In the fed vs. fasted state, control mice exhibited a 38% reduction in serum free T3 levels (fT3) (p=.08), while KO-AL mice exhibited a 61.5% reduction in serum fT3 levels from the fed to fasted state ($p<.05$)

(Figure 4.1). Additionally, KO-AL mice had 22% higher serum fT3 levels compared to control mice in the fed state, while they exhibited 25% lower serum fT3 in the fasted state when compared to controls. This is further reminiscent of previous work done in *ob/ob* mice, which showed that reductions in fT3 in response to fasting are much greater in *ob/ob* compared to controls, even though the fed baseline levels of fT3 were the same between the two groups (22). Therefore, KO mice seem to be more sensitive to nutritional perturbations in the system, and further work is needed to determine whether paired-feeding rescues this sensitivity.

Part III: The role of IGF-1 in BAT development

Concluding Remarks

Insulin-like growth factor 1 (IGF-1) is important for BAT development, and adipose specific IGF1R/insulin receptor (IR) double knockout results in a smaller BAT depot (26). Additionally, knocking out IGF-1R specifically in adipose tissue results in increased body weight gain at 10 weeks of age (27), consistent with an important role in BAT formation and/or function. In our current study, we found that upregulation of BAT *Igf-1* (Figure 3.5) preceded the increased UCP1 content at 5 weeks of age in control mice (Figure 3.3B). Taken together, we hypothesize that *Igf-1* plays a role in "consolidation" and restructuring of the BAT depot after tissue expansion, and this "consolidation" is necessary for increased thermogenic capacity of the BAT in the wild type system. In support of this idea, there is evidence that *Igf-1* plays a crucial role in mitochondrial stabilization in cardiomyocytes (28), although this has not been examined in BAT.

Future Directions

(i) Mitochondrial structure: Originally, it was thought that BAT differentiation and thermogenic initiation was completed prior to weaning (29, 30). We discovered that BAT expansion in the last week of weaning is associated with a precipitous decline in BAT capacity and thermogenic activity. We do not yet know what is driving the expansion of the depot at this time, and we do not know whether this expansion is mechanistically linked to disorganized mitochondrial structure at 3 weeks. First, it is important to confirm that cristae are tightly packed at 2 weeks in mice, because studies of mitochondrial structure in the neonatal period were performed in rats (31, 32). Then, we must determine what is driving increased BAT mass between 2-3 weeks of age – proliferation and/or increased adipocyte size due to increased lipid accumulation.

(ii) Mitochondrial consolidation and activation initiated by paired-feeding: We do not yet know the time point at which tight packing of mitochondrial cristae is restored cristae, only that it happens before 10 weeks of age in control (and pair-fed) mice (Figure 2.6A,C). In this dissertation I reported that BAT *Igf-1* expression is blunted in KO-AL mice compared to controls at 5 weeks of age (Figure 3.6D), consistent with the hypothesis that deficits in *Igf-1*-mediated BAT mitochondrial "consolidation" contribute to obesity in this model. Paired-feeding does not enhance BAT *Igf-1* at 5 weeks of age compared to KO-AL mice (Figure 3.7D). These data suggest that paired-feeding does not correct for the blunted *Igf-1* levels seen at 5 weeks of age in the KO mice. Therefore, paired-feeding (which is known to correct for mitochondrial capacity (21)), might be acting on mitochondrial "consolidation" independent of the *Igf-1* pathway. Since paired-

feeding results in increased fT3 levels (Figure 2.3C, 2.4C)(6), it is possible that fT3 is driving mitochondrial consolidation in the KO-PF mice. Therefore, chronic treatment with fT3 during the paired-feeding period might result in improvements in mitochondrial packing.

(iii) Mitochondrial structure vs. activation: We hypothesize that the increased environmental stress due to single housing during paired-feeding enhances BAT capacity and activation during the critical time window. To parse out the effects of paired-feeding vs. environmental stimuli on energy expenditure, rearing mice in thermoneutral conditions would mitigate the cold stress of the single-housing environment. The thermoneutral environment negates the need for BAT, and therefore BAT is more unilocular, resembling WAT, and contains reduced UCP1 (33, 34). Moreover, BAT mitochondrial cristae appear more disorganized under thermoneutral conditions (34). Paired-feeding might still result in improved mitochondrial structure at thermoneutrality, as paired-feeding can correct for cristae organization defects in the mitochondria (21), but mice would not be subject to constant activating signals (i.e. cold), thereby resulting in reduced basal metabolic rate (BMR) compared to those pair-fed at room temperature.

Part IV: Concluding Remarks

We and others have shown that caloric restriction and/or paired-feeding results in improvements of mitochondrial capacity (6, 21, 22). Improvements in capacity alone, however, are not enough to elicit improvements in thermogenesis (35). Because our mice are singly housed throughout the experimental paradigm, paired-feeding does not only

improve mitochondrial structure (capacity), but increases activation in response to environmental stress which might upregulate thermogenic genes during a critical time period.

Current efforts in the lab have focused on discerning the relevance of BAT mitochondrial structure in humans. As discussed at length throughout this dissertation, human BAT activity has been identified, and is inversely correlated with age (36-38) and BMI status (39, 40). It has not yet been elucidated whether mitochondrial capacity is disrupted in BAT of obese individuals. We have sought to address this question by acquiring fat samples from pediatric obesity patients (Appendix II). Our current methods to acquire BAT and isolate mitochondria in these patients need to be refined. Our research has the potential to identify mitochondrial disorganization in adolescents as a contributing factor to subsequent obesity status in humans. Ideally, future research will be focused on acquiring BAT samples from individuals early in life, detecting whether mitochondrial structure is impaired, and using that information along with longitudinal analysis on weight status to determine whether mitochondrial structure preceding obesity could be used as a biomarker to determine future obesity risk.

Elucidating the driving mechanism by which paired-feeding is increasing BMR in young obese rodents will be a valuable tool to provide insight into the treatment of pediatric obesity. Even if the right age to intervene is identified, calorie restriction might not be enough to elicit long-term weight loss success. The combination of the improved BAT capacity (upon caloric restriction) and activation (cold, adrenergic stimulation) might be

the key role to permanently enhance BMR. This idea is supported by the studies suggesting that combination therapies (dieting plus physical activity) produce more favorable sustained weight loss outcomes (41).

FIGURES

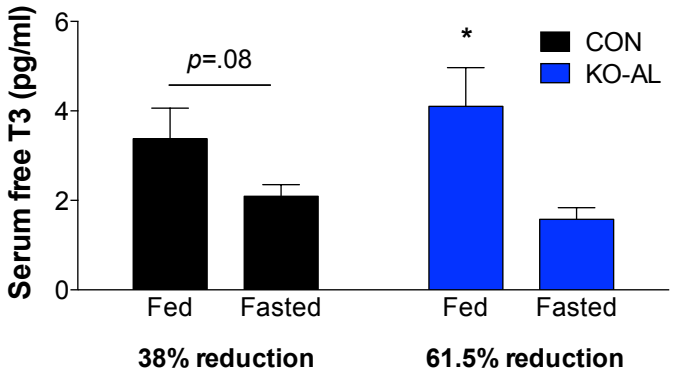

Figure 4.1. Fasting elicits a greater decrease in serum T3 in KO-AL than control mice. Black bars represent controls in the fed and fasted state, blue bars represent KO-AL in the fed and fasted state. Error bars represent standard error of the mean. Statistical significance was determined by Student's t-test. * represents $p<.05$. Data were generated from control; n=3-5, KO-AL; n=4-5.

REFERENCES

1. Alonso LG, Maren TH. Effect of food restriction on body composition of hereditary obese mice. Am J Physiol. 1955;183(2):284-90.

2. Chlouverakis C. Effect of caloric restriction on body weight loss and body fat utilization in obese hyperglycemic mice (Obob). Metabolism. 1972;21(1):10-7.

3. Dubuc PU. Effects of limited food intake on the obese-hyperglycemic syndrome. Am J Physiol. 1976;230(6):1474-9.

4. Dubuc PU, Cahn PJ, Willish P. The effects of exercise and food restriction on obesity and diabetes in young ob/ob mice. Int J Obes. 1984;8(3):271-8.

5. Bates SH, Kulkarni RN, Seifert M, Myers MG, Jr. Roles for leptin receptor/STAT3-dependent and -independent signals in the regulation of glucose homeostasis. Cell Metabolism. 2005;1(3):169-78.

6. Lerea JS, Ring LE, Hassouna R, Chong AC, Szigeti-Buck K, Horvath TL, et al. Reducing Adiposity in a Critical Developmental Window Has Lasting Benefits in Mice. Endocrinology. 2016;157(2):666-78.

7. Schroeder M, Moran TH, Weller A. Attenuation of obesity by early-life food restriction in genetically hyperphagic male OLETF rats: peripheral mechanisms. Hormones and behavior. 2010;57(4-5):455-62.

8. Schroeder M, Gelber V, Moran TH, Weller A. Long-term obesity levels in female OLETF rats following time-specific post-weaning food restriction. Horm Behav. 2010;58(5):844-53.

9. Bumaschny VF, Yamashita M, Casas-Cordero R, Otero-Corchón V, de Souza FS, Rubinstein M, et al. Obesity-programmed mice are rescued by early genetic intervention. J Clin Invest. 2012;122(11):4203-12.

10. Young JB, Landsberg L. Diminished sympathetic nervous system activity in genetically obese (ob/ob) mouse. Am J Physiol. 1983;245(2):E148-E54.

11. Knehans AW, Romsos DR. Norepinephrine turnover in obese (ob/ob) mice: effects of age, fasting, and acute cold. Am J Physiol. 1983;244(6):E567-E74.

12. Trayhurn P, James WP. Thermoregulation and non-shivering thermogenesis in the genetically obese (ob/ob) mouse. Pfluegers Arch. 1978;373:189-93.

13. Hogan S, Himms-Hagen J. Abnormal brown adipose tissue in obese mice (*ob/ob*): response to acclimation to cold. Am J Physiol. 1980;239:E301-E9.

14. Hogan S, Himms-Hagen J. Abnormal brown adipose tissue in genetically obese mice (*ob/ob*): effect of thyroxine. Am J Physiol. 1981;241(6):E436-E43.

15. de Almeida DL, Fabrício GS, Trombini AB, Pavanello A, Tófolo LP, da Silva Ribeiro TA, et al. Early overfeed-induced obesity leads to brown adipose tissue hypoactivity in rats. Cell Physiol Biochem. 2013;32(6):1621-30.

16. Xiao XQ, Williams SM, Grayson BE, Glavas MM, Cowley MA, Smith MS, et al. Excess weight gain during the early postnatal period is associated with permanent reprogramming of brown adipose tissue adaptive thermogenesis. Endocrinology. 2007;148(9):4150-9.

17. Ring LE, Zeltser LM. Disruption of hypothalamic leptin signaling in mice leads to early-onset obesity, but physiological adaptations in mature animals stabilize adiposity levels. J Clin Invest. 2010;120(8):2931-41.

18. Bates SH, Dundon TA, Seifert M, Carlson M, Maratos-Flier E, Myers MG, Jr. LRb-STAT3 signaling is required for the neuroendocrine regulation of energy expenditure by leptin. Diabetes. 2004;53(12):3067-73.

19. Bates SH, Stearns WH, Dundon TA, Schubert M, Tso AW, Wang Y, et al. STAT3 signalling is required for leptin regulation of energy balance but not reproduction. Nature. 2003;421(6925):856-9.

20. Batt RA, Hambi M. Development of the hypothermia in obese mice (genotype ob/ob). Int J Obes. 1982;6(4):391-7.

21. Batt RA, Tyler DD, Sutton CM. Influence of restricted food intake on brown adipose tissue function in genetically obese mice (genotype, ob/ob). Biochim Biophys Acta. 1985;838(229-235).

22. Himms-Hagen J. Food restriction increases torpor and improves brown adipose tissue thermogenesis in ob/ob mice. Am J Physiol. 1985;248(5 pt 1):E531-E9.

23. de Jesus LA, Carvalho SD, Ribeiro MO, Schneider M, Kim SW, Harney JW, et al. The type 2 iodothyronine deiodinase is essential for adaptive thermogenesis in brown adipose tissue. J Clin Invest. 2001;108(9):1379-85.

24. Swoap SJ. The pharmacology and molecular mechanisms underlying temperature regulation and torpor. Biochem Pharmacol. 2008;76(7):817-24.

25. Chong AC, Greendyk RA, Zeltser LM. Distinct networks of leptin- and insulin-sensing neurons regulate thermogenic responses to nutritional and cold challenges. Diabetes. 2015;64(1):137-46.

26. Boucher J, Mori MA, Lee KY, Smyth G, Liew CW, Macotela Y, et al. Impaired thermogenesis and adipose tissue development in mice with fat-specific disruption of insulin and IGF-1 signalling. Nat Commun. 2012;3:902.

27. Klöting N, Koch L, Wunderlich T, Kern M, Ruschke K, Krone W, et al. Autocrine IGF-1 action in adipocytes controls systemic IGF-1 concentrations and growth. Diabetes. 2008;57(8):2074-82.

28. Pi Y, Goldenthal MJ, Marín-García J. Mitochondrial involvement in IGF-1 induced protection of cardiomyocytes against hypoxia/reoxygenation injury. Mol Cell Biochem. 2007;301(1-2):181-9.

29. Teruel T, Valverde AM, Alvarez A, Benito M, Lorenzo M. Differentiation of rat brown adipocytes during late foetal development: role of insulin-like growth factor I. Biochem J. 1995;310(pt 3):771-6.

30. Guerra C, Benito M, Fernández M. IGF-I induces the uncoupling protein gene expression in fetal rat brown adipocyte primary cultures: role of C/EBP transcription factors. Biochem Biophys Res Commun. 1994;201(2):813-9.

31. Skála J, Barnard T, Lindberg O. Changes in interscapular brown adipose tissue of the rat during perinatal and early postnatal development and after cold acclimation. II. Mitochondrial changes. Comp Biochem Physiol. 1970;33(3):509-28.

32. Lindgren G, Barnard T. Changes in interscapular brown adipose tissue of rat during perinatal and early postnatal development and after cold acclimation. IV. Morphometric investigation of mitochondrial membrane alterations. Exp Cell Res. 1972;70(1):81-90.

33. Razzoli M, Frontini A, Gurney A, Mondini E, Cubuk C, Katz LS, et al. Stress-induced activation of brown adipose tissue prevents obesity in conditions of low adaptive thermogenesis. Mol Metab. 2015;5(1):19-33.

34. Arbuthnott E. Brown adipose tissue: structure and function. Proc Nutr Soc. 1989;48(2):177-82.

35. Cannon B, Nedergaard J. Brown Adipose Tissue: Function and Physiological Significance. Physiol Rev. 2004;84:277-359.

36. Yoneshiro T, Aita S, Matsushita M, Kameya T, Nakada K, Kawai Y, et al. Brown adipose tissue, whole-body energy expenditure, and thermogenesis in healthy adult men. Obesity (Silver Spring). 2011;19(1):13-6.

37. Hanssen MJ, van der Lans AA, Brans B, Hoeks J, Jardon KM, Schaart G, et al. Short-term cold acclimation recruits brown adipose tissue in obese humans. Diabetes. 2015;[Epub ahead of print].

38. Bahler L, Verberne HJ, Admiraal W, Stok WJ, Soeters MR, Hoekstra JB, et al. Differences in Sympathetic Nervous Stimulation of Brown Adipose tissue between the young and old and the lean and obese. J Nucl Med. 2015;[epub ahead of print].

39. van Marken Lichtenbelt WD, Vanhommerig JW, Smulders NM, Drossaerts JM, Kemerink GJ, Bouvy ND, et al. Cold-activated brown adipose tissue in healthy men. New England Journal of Medicine. 2009;360(15):1500-8.

40. Cypess AM, Lehman S, Williams G, Tal I, Rodman D, Goldfine AB, et al. Identification and importance of brown adipose tissue in adult humans. New England Journal of Medicine. 2009;360(15):1509-17.

41. McGovern L, Johnson JN, Paulo R, Hettinger A, Singhal V, Kamath C, et al. Clinical review: treatment of pediatric obesity: a systematic review and meta-analysis of randomized trials. J Clin Endocrinol Metab. 2008;93(12):4600-5.

APPENDIX I: Organ Contribution to Increased Energy Expenditure in KO-PF Mice

In effort to determine the mechanism by which energy expenditure is increased in pair-fed (KO-PF) mice, we examined metabolically active tissue known to regulate energy expenditure. We analyzed gene expression in pituitary, hypothalamus (Appendix Figure 1.1, 1.2), white adipose tissue (Appendix Figure 1.3, 1.4, 1.5), skeletal muscle (Appendix Figure 1.6), liver (Appendix Figure 1.7, 1.8), brown adipose tissue (BAT) (Appendix Figure 1.9-1.13) and plasma catecholamine levels (Appendix Figure 1.14). Based on our findings below, we were able to rule out contributions of other organs in modulating energy expenditure in the KO-PF mice at 10 and 20 weeks of age compared to KO-AL mice. Ongoing studies are being carried out to determine the mechanism by which BAT is activated in KO-PF mice at a young age. All mice were fasted overnight before sacrifice.

Pituitary and hypothalamus

One of the most striking phenotypes observed in KO-PF mice compared to the KO-AL mice was the elevated triiodothyronine (T3) level. Because the hypothalamic-pituitary-thyroid axis (HPT) is an important regulator of thyroid levels, we looked at whether the HPT axis was more active in the KO-PF mice. We did not find evidence that any changes in the HPT axis occurred during paired-feeding (Appendix Figure 1.1, 1.2), therefore ruling out HPT regulation of the elevated T3 levels.

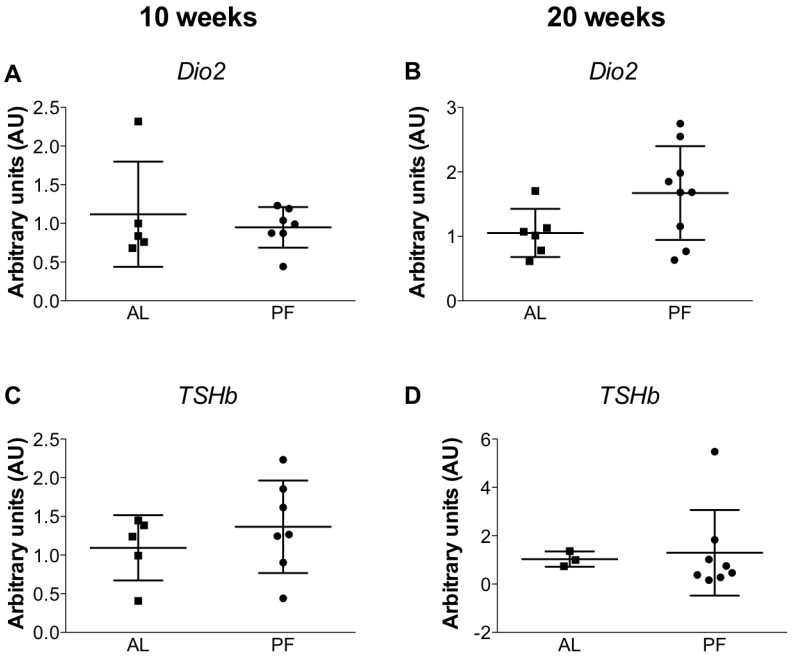

Appendix Figure 1.1. Pituitary *Dio2* and *TSHb* do not differ between PF and AL mice at 10 and 20 weeks of age. (A) Pituitary *Dio2* at 10 weeks (AL; n=5, PF; n=7) and (B) 20 weeks (AL; n=6, PF; n=9). (C) Pituitary *TSHb* at 10 weeks (AL; n=5, PF; n=7) and (D) 20 weeks (AL; n=3, PF; n=8). No statistical significance was found using Student's and Welch's T-test accordingly. Abbreviations: *Dio1*; Deiodinase 1. *TSHb*; Thyroid stimulating hormone *β*. Arbitrary units: relative expression to *β-actin*.

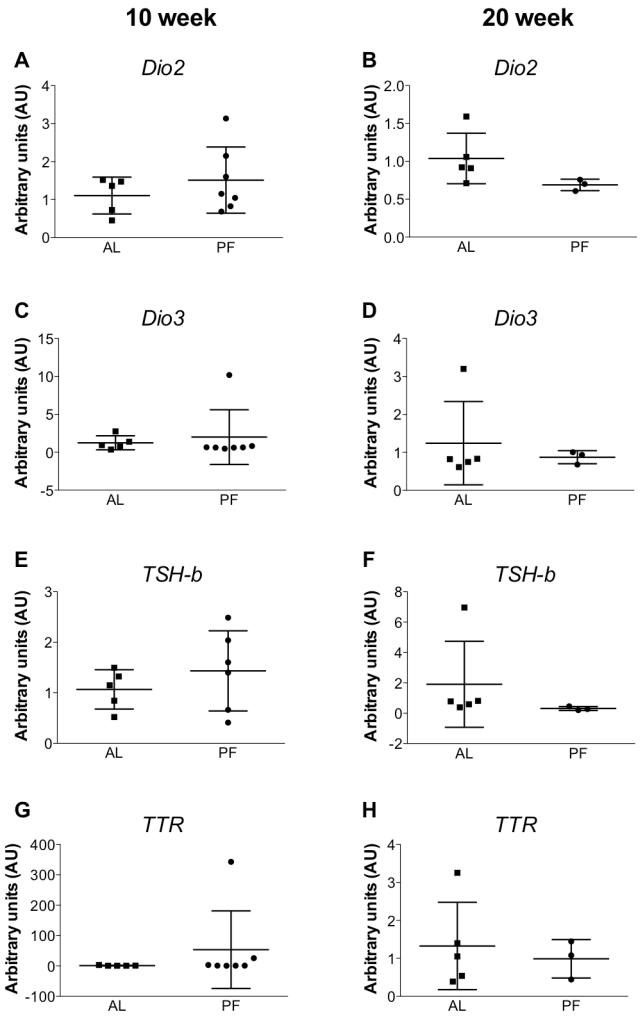

Appendix Figure 1.2. Hypothalamus gene expression at 10 and 20 week of age between paired-feeding and *ad libitum* KO does not differ. (A) *Dio2* at 10 weeks (AL; n=5, PF; n=7) and (B) 20 weeks (AL; n=5, PF; n=3). (C) *Dio3* at 10 weeks (AL; n=5, PF; n=7) and (D) 20 weeks (AL; n=5, PF; n=3). (E) *TSH-b* at 10 weeks (AL; n=5, PF; n=5) and (F) at 20 weeks (AL; n=5, PF; n=3). (G) *TTR* at 10 weeks (AL; n=5, PF; n=7) and (H) 20 weeks (AL; n=5, PF; n=3). Abbreviations: *Dio2*; Deiodinase 2. *Dio3;* Deiodinase 3. *TSHb;* Thyroid stimulating hormone-β. *TTR*; Transthyretin. Arbitrary units: relative expression to *β-actin*.

White adipose tissue

To determine whether browning of inguinal and gonadal brown adipose tissue influenced energy expenditure in the KO-PF mice, we examined white adipose tissue (WAT) depots of uncoupling protein 1 (*Ucp1)* expression. It was necessary to dilute cDNA to a 1/5 dilution in order to detect any *Ucp1,* and there was no detectable difference between the KO-PF and KO-AL at either 10 or 20 weeks of age in inguinal adipose tissue (iFat) (Appendix Figure 1.3 A,B) or gonadal adipose tissue (gFat) (Appendix figure 1.4 A,B). Additionally there was no change in β_3-adrenergic receptor *(β_3-AR*) in iFat (Appendix Figure 1.3 C,D) and gFat (Appendix Figure 1.4 C,D), further supporting the hypothesis that browning of WAT is not driving the metabolic phenotype in these mice. Additionally, we looked at Hormone sensitive lipase (*Hsl*) in WAT, which was not changed (Appendix figure 1.5).

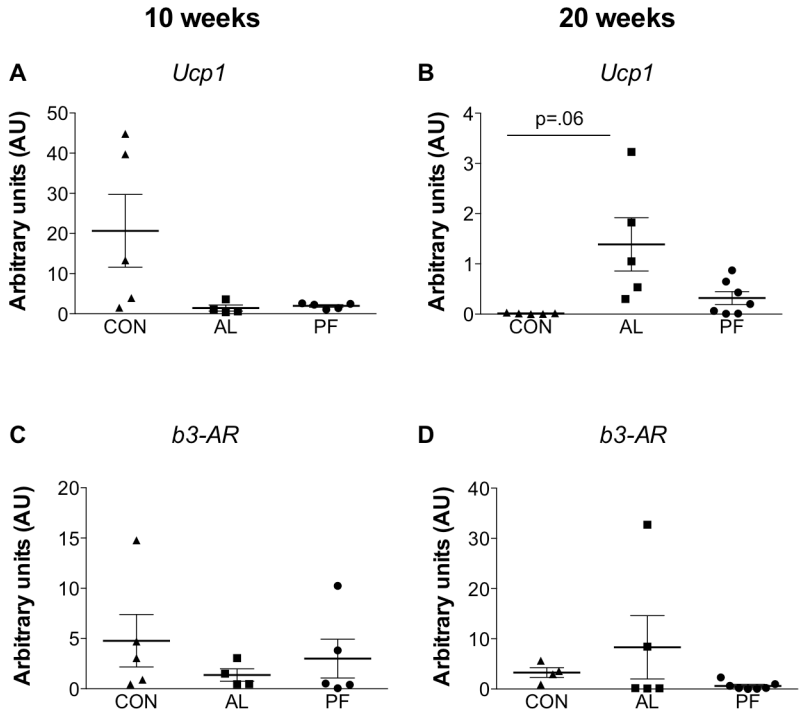

Appendix Figure 1.3. Increased energy expenditure is not due to browning of inguinal fat. (A) *Ucp1* at 10 weeks (CON; n=5, AL; n=4, PF; n=4) and (B) 20 weeks (CON; n=5, AL; n=5, PF; n=7). (C) *β_3AR* at 10 weeks (CON; n=5, AL; n=4, PF; n=5) and (D) 20 weeks (CON; n=4, AL; n=5, PF; n=7). Significance was determined using one way ANOVA followed by post-hoc LSD. Student's or Welch's T-test was performed accordingly. Abbreviations: *Ucp1;* Uncoupling protein 1. β3-AR; β-3 adrenergic receptor. Arbitrary units: relative expression to *β-actin*.

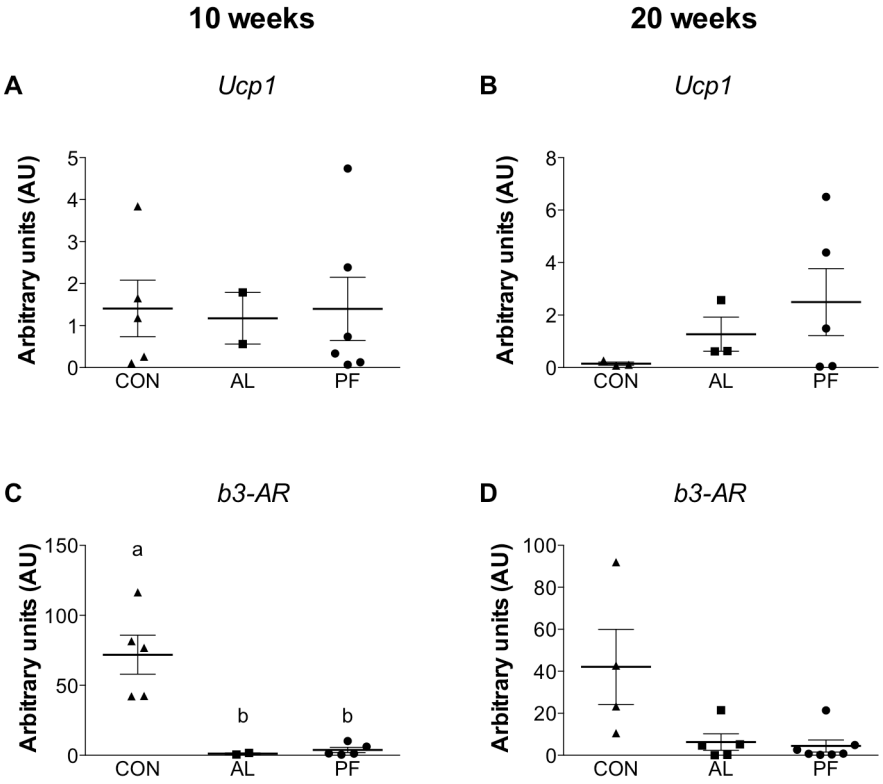

Appendix Figure 1.4. Increased energy expenditure is not due to browning of gonadal fat. (A) *Ucp1* at 10 weeks (CON; n=5, AL; n=2, PF; n=6) and (B) 20 weeks (CON; n=3, AL; n=3, PF; n=5). (C) *b_3AR* at 10 weeks (CON; n=5, AL; n=2, PF; n=5) and (D) 20 weeks (CON; n=4, AL; n=5, PF; n=7). Significance was determined using one way ANOVA followed by post-hoc LSD. Student's or Welch's T-test was performed accordingly. Abbreviations: *Ucp1;* Uncoupling protein 1. β3AR; β-3 adrenergic receptor. Arbitrary units: relative expression to *β-actin*.

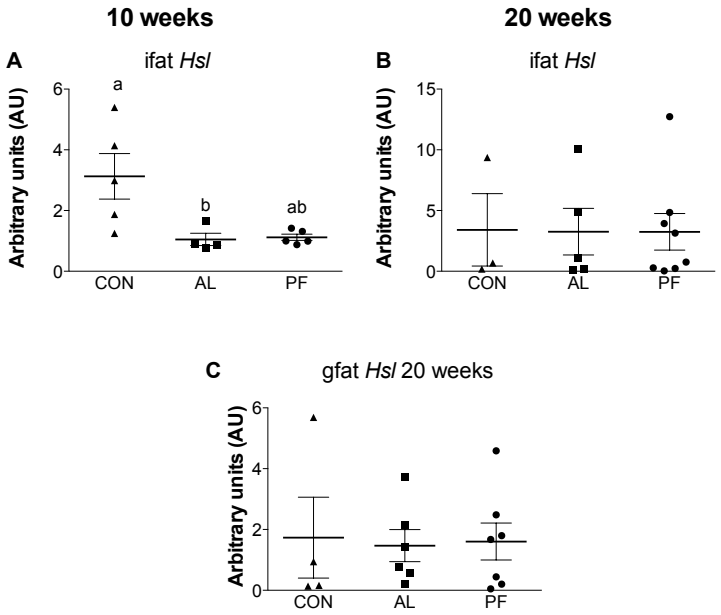

Appendix Figure 1.5. *Hsl* is WAT is not changed by paired-feeding. (A) Ifat *Hsl* at 10 weeks (CON; n=5, AL; n=4, PF; n=5) and (B) 20 weeks (CON; n=3, AL; n=5, PF; n=8). (C) Gfat *Hsl* at 20 weeks (CON; n=4, AL; n=6, PF; n=7). Significance was determined using one way ANOVA followed by post-hoc LSD. Student's or Welch's t-test was performed accordingly. Abbreviations: *Hsl;* hormone sensitive lipase. Arbitrary units: relative expression to *β-actin*.

Skeletal Muscle

To determine the contribution of skeletal muscle uncoupling protein in the energy expenditure phenotype in KO-PF mice at 10 weeks of age, we looked at uncoupling protein 3 (*Ucp3)* gene expression. We did not see increased *Ucp3* in skeletal muscle at 10 weeks of age in the KO-PF mice compared to the KO-AL mice (Appendix Figure 1.6). We found *Ucp3* in the skeletal muscle to be reduced in KO-PF at 10 weeks of age compared to KO-AL (Appendix Figure 1.6). This dramatic decrease might be a compensatory mechanism of the skeletal muscle due to the increased BAT thermogenesis.

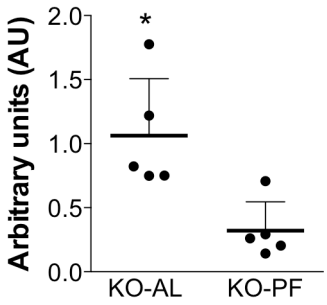

Appendix Figure 1.6. Skeletal muscle *Ucp3* (Uncoupling protein 3) does not contribute to increased energy expenditure in KO-PF mice at 10 weeks of age. (KO-AL; n=5, KO-PF; n=5). Significance was determined using Student's t-test. Arbitrary units: relative expression to *β-actin*.

Liver

To try and determine the mechanism by which energy expenditure is increased, we looked at several genes implicated in transcription of BAT activators as well as the bile acid pathway. Deiodinase 1 (*Dio1)* mRNA levels, the primary deiodinase in the liver to convert thyroxine (T4) to triiodothyronine (T3). *Dio1* was not changed between groups (Appendix Figure 1.7A,B). Fibroblast growth factor-21 (*Fgf21)* was unchanged in liver of KO-PF versus KO-AL mice (Appendix Figure 8C,D). Additionally, insulin-like growth factor binding protein (*Igfbp*) was unchanged (Appendix Figure 1.7E,F). Bile acids are known to influence BAT activity via its receptor (TGR5), and bile acid supplementation has been shown to dampen weight gain on a high fat diet (1). We therefore looked at the bile acid conversion pathway (Cytochrome p450s (CYPs)). The bile acid pathway was unchanged in these mice (Appendix Figure 1.8) with the exception of liver *Cyp7a1,* the rate limiting step in bile acid synthesis. *Cyp7a1* was upregulated in KO-PF mice at 20 weeks only (Appendix Figure 1.8), which could contribute to the sustained energy expenditure phenotype in the KO-PF mice. Overall, liver gene expression was unchanged by paired-feeding (Appendix Figure 1.7,1.8).

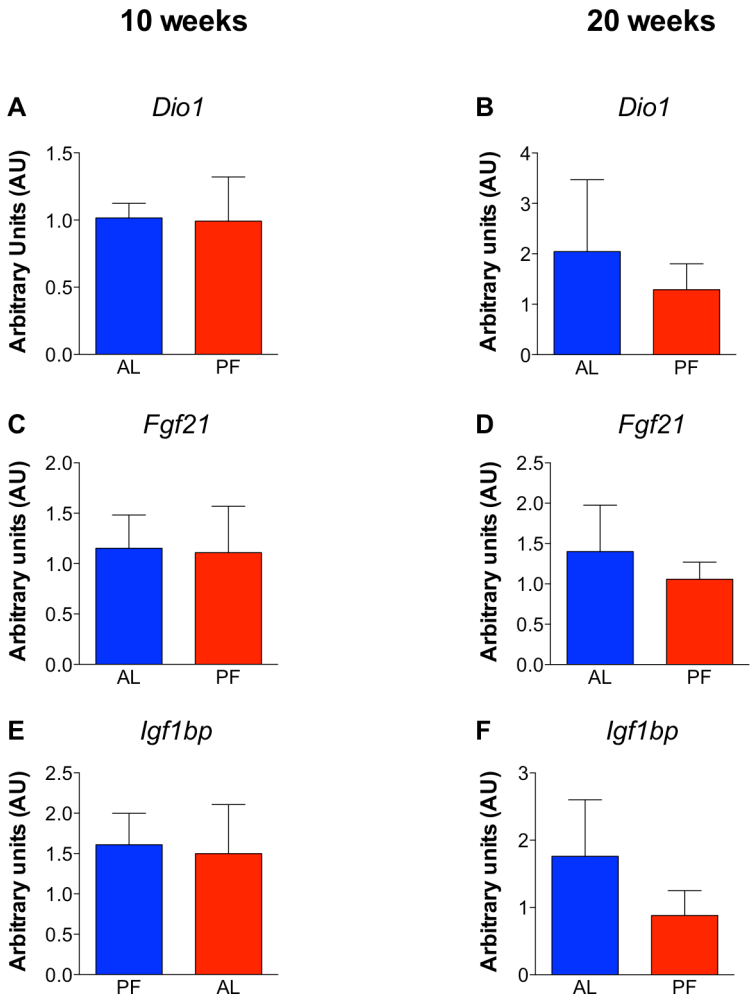

Appendix Figure 1.7. Liver gene expression. (A) Liver *Dio1* at 10 weeks (AL; n=4, PF; n=5) and 20 weeks (B) (AL; n=5, PF; n=9). (C) Liver *Igf1* at 10 weeks (AL; n=4, PF; n=6) and (D) 20 weeks (AL; n=6, PF; n=8). (E) Liver *Igfbp* at 10 weeks (AL; n=4, PF; n=6) and (F) 20 weeks (AL; n=6, PF; n=8). Error bars represent standard error of mean. Blue bars represent KO-AL, red bars represent KO-PF. No significance was found between groups by Student's or Welch's t-test accordingly. Abbreviations: *Dio1*; Deiodinase 1. *Fgf21*; Fibroblast growth factor 21. *Igf1bp*; Insulin-like growth factor 1 binding protein. Arbitrary units: relative expression to *β-actin*.

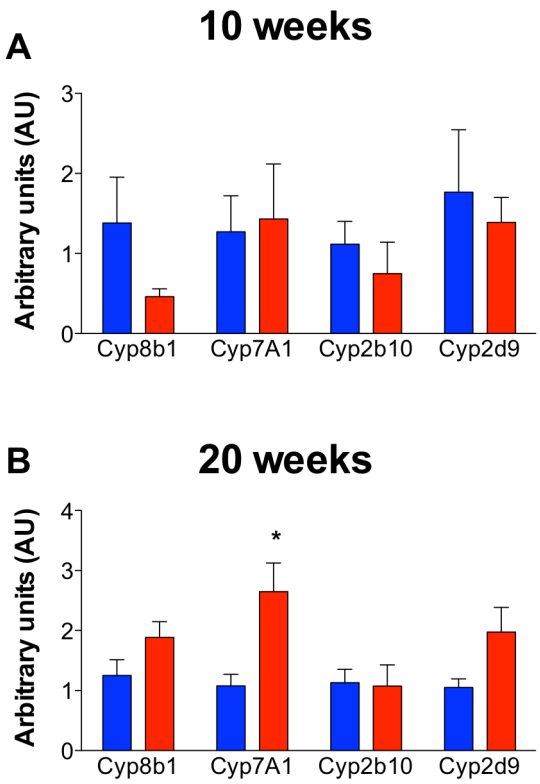

Appendix Figure 1.8. Bile acid conversion pathway. (A) Liver *Cyp8b1, Cyp7A1, Cyp2b10, Cyp2d9* mRNA levels at 10 weeks (AL; n=4, PF; n=6). (B) Liver *Cyp8b1, Cyp7A1, Cyp2b10, Cyp2d9* mRNA levels at 20 weeks (B) (AL; n=6, PF; n=8). Error bars represent standard error of mean. Blue bars represent KO-AL, red bars represent KO-PF. Significance was found between groups by Student's or Welch's t-test accordingly. Abbreviation: CYP: Cytochrome p450. Arbitrary units: relative expression to *β-actin*.

Brown adipose tissue

We looked at BAT FGF-21 signaling to rule out FGF-21 as a potential candidate for increasing energy expenditure in the KO-PF mice. BAT *Fgf21* was not increased in KO-PF mice at 10 or 20 weeks of age (Appendix Figure 1.9A,B). Additionally, FGF21 receptor duplex *(β-klotho* and *FgfR1*) was unchanged in KO-PF mice at 10 or 20 weeks of age (Appendix Figure 1.9A,B).

Because one of the major phenotypes in our model is increased energy expenditure, we looked at the adrenergic receptors in the brown adipose tissue to determine whether there were differences induced by paired-feeding. We found no differences in adrenergic receptor levels in KO-PF versus KO-AL mice at 10 and 20 weeks of age (Figure 1.10). Additionally, we decided to look at other BAT activators, such as the receptor to bone morphogenic protein (BMP) 8b, *Bmp8R*, and Natriuretic peptides *(NP)*. *Bmp8bR* was not upregulated in BAT of KO-PF mice (Appendix Figure 1.11). Furthermore, the natriuretic peptide (NP) receptors were not different (Appendix Figure 1.11) at 10 or 20 weeks of age in KO-PF.

Due to changes in the mitochondrial pathway in BAT of KO-PF mice (Chapter 2), we assayed other markers of lipolysis, oxidative phosphorylation and mitochondrial biogenesis. These genes were unaltered (Appendix Figure 1.12, 1.13).

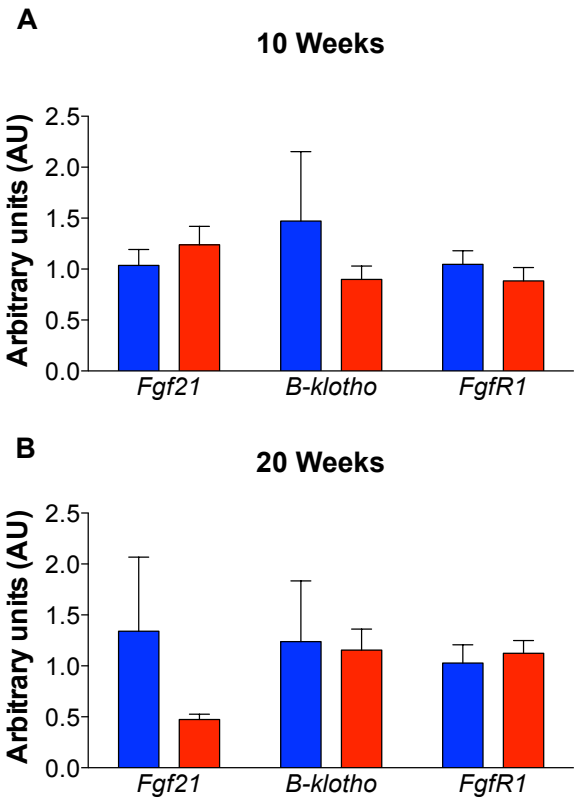

Appendix Figure 1.9. BAT FGF21 signaling is not increased in PF-KO mice. (A) BAT *Fgf21*, *β-klotho,* and *FgfR1* at 10 weeks of age (CON; n=6-9, AL; n=3-4, PF; n=5-7). (B) BAT *Fgf21*, *β-klotho,* and *FgfR1* at 20 weeks of age (CON; n=6, AL; n=3, PF; n=6-7). Error bars represent standard error of mean. Blue bars represent KO-AL, red bars represent KO-PF. No significance was found between groups by Student's or Welch's t-test accordingly. Abbreviations: *Fgf21*; Fibroblast growth factor 21. *FgfR1*; Fibroblast growth factor receptor 1. Arbitrary units: relative expression to *β-actin*.

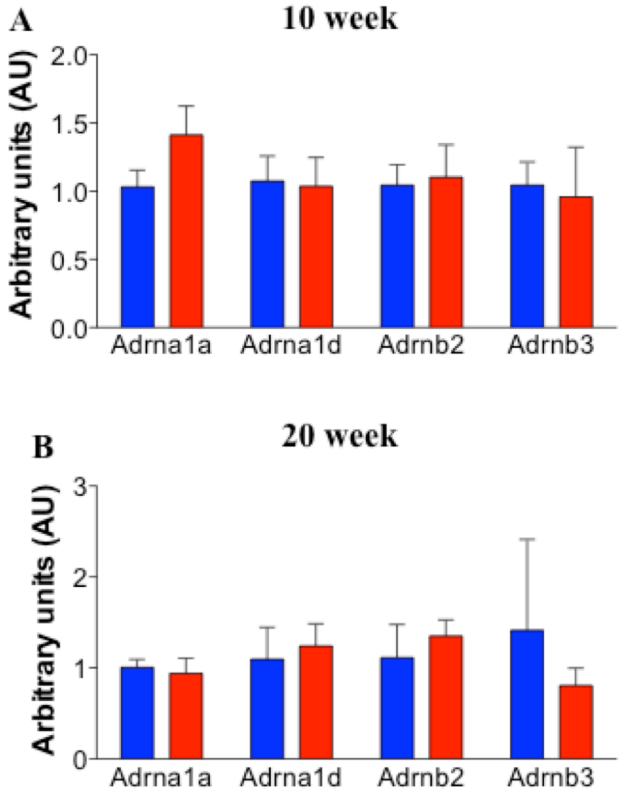

Appendix Figure 1.10. Adrenergic receptors are unchanged in BAT of KO-AL versus KO-PF. Adrenergic receptor1a, 1d, b2, b3 expression at (A) 10 weeks (AL; n=4-5, PF; n=5-7) and (B) 20 weeks (AL; n=2-3, PF; n=6-7). Error bars represent standard error of mean. Blue bars represent KO-AL, red bars represent KO-PF. No significance was found between groups by Student's or Welch's t-test accordingly. Abbreviations: Adrn; Adrenergic receptor. Arbitrary units: relative expression to *β-actin*.

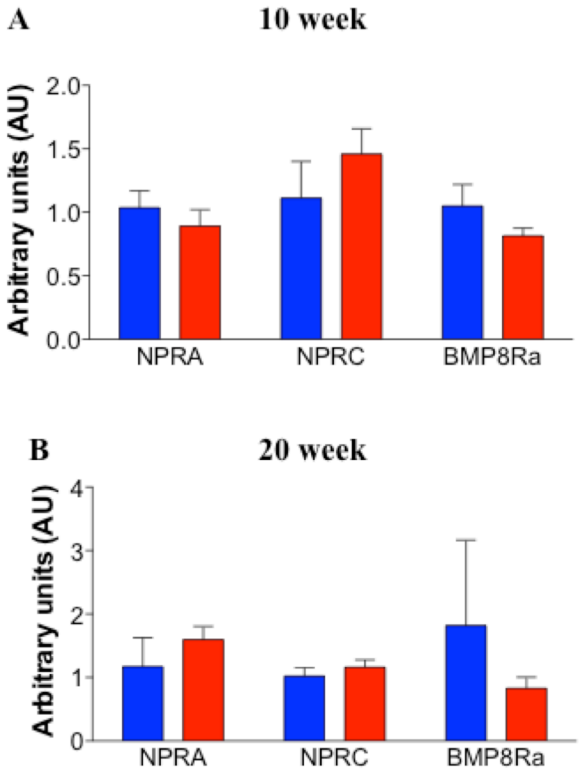

Appendix Figure 1.11. BAT Natriuretic peptide receptors and bone morphogenic protein receptors are unchanged. (A) *NprA, NprC*, and *Bmp8bR* at 10 weeks of age (AL; n=5, PF; n=7) and (B) *NprA, NprC,* and *Bmp8bR* at 20 weeks of age (AL; n=3, PF; n=6-7). Error bars represent standard error of mean. Blue bars represent KO-AL, red bars represent KO-PF. No significance was found between groups by Student's or Welch's t-test accordingly. Abbreviations: *NprA/C*; natriuretic peptide receptor A/C. *Bmp8bR*; Bone morphogenic protein 8b receptor. Arbitrary units: relative expression to *β-actin*.

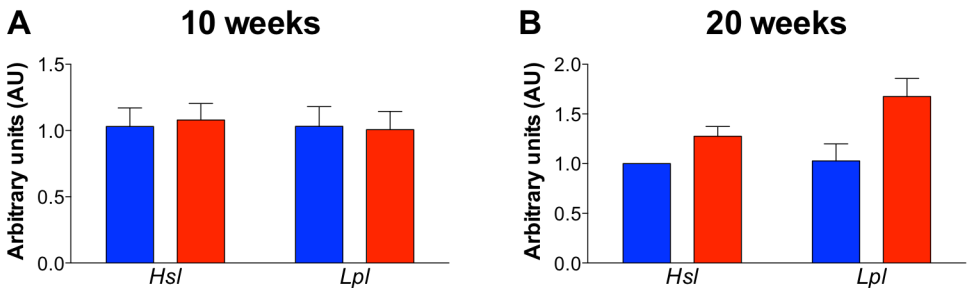

Appendix Figure 1.12. BAT hormone sensitive lipase and lipoprotein lipase are unchanged in KO-AL versus KO-PF. *Hsl* and *Lpl* at (A) 10 weeks of age (AL; n=4, PF; n=5) and (B) 20 weeks of age (AL; n=1-3, PF; n=6-7) in BAT. Error bars represent standard error of mean. Blue bars represent KO-AL, red bars represent KO-PF. No significance was found between groups by Student's or Welch's t-test accordingly. Abbreviations: *Hsl*; Hormone sensitive lipase. *Lpl*; Lipoprotein lipase. Arbitrary units: relative expression to *β-actin*.

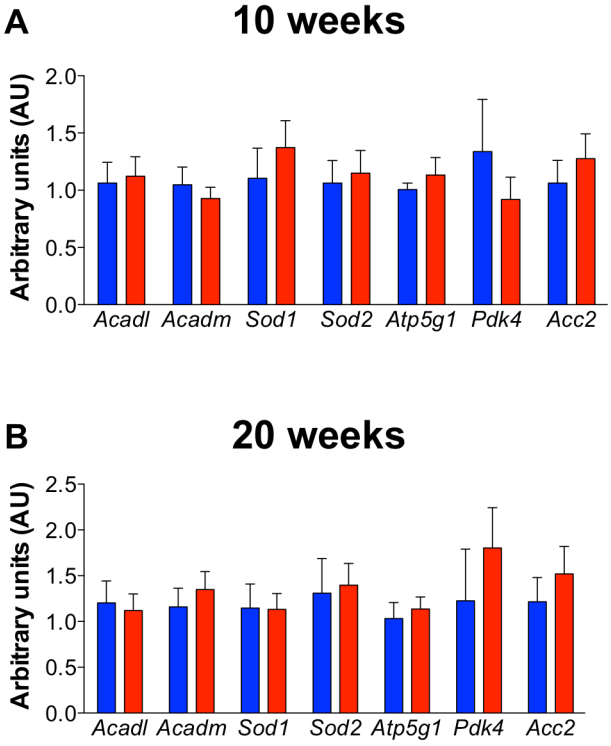

Appendix Figure 1.13. A subset of mitochondrial genes are not upregulated in KO-PF mice compared to KO-AL. (A) *Acadl, Acadm, Sod1, Sod2, Atp5g1, Pdk4,* and *Acc2* at 10 weeks of age (AL; n=5, PF; n=7). (B) *Acadl, Acadm, Sod1, Sod2, Atp5g1, Pdk4,* and *Acc2* at 20 weeks of age (AL; n=3-6, PF; n=7-12). Error bars represent standard error of mean. Blue bars represent KO-AL, red bars represent KO-PF. No significance was found between groups by Student's or Welch's t-test accordingly. Abbreviations: *Acadl*; Acyl-CoA dehydrogenase, long chain. *Acadm*; Acyl-CoA dehydrogenase, medium chain. *Sod1/2*; superoxide dismutase 1/2. *Atp5g1*; ATP synthase, H+ transporting, mitochondrial Fo complex, subunit C1. *Pdk4*; Pyruvate dehydrogenase kinase 4. *Acc2*; Acetyl-CoA carboxylase. Arbitrary units: relative expression to *β-actin*.

Plasma catecholamine levels

As discussed at length in the introduction section, norepinephrine (NE) activates BAT. KO-AL mice exhibited increased circulating NE (Appendix Figure 1.14), indicative of NE-resistance. Paired-feeding normalized serum NE to control levels (Appendix Figure 1.14), supporting the idea that paired-feeding enhances NE sensitivity.

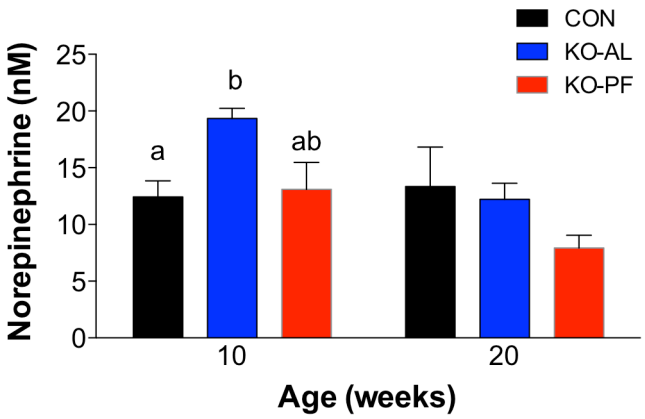

Appendix Figure 1.14. Norepinephrine is normalized at 10 weeks of age in KO-PF mice. CON 10, 20 weeks; n=5; KO-AL 10, 20 weeks; n=3, KO-PF 10, 20weeks; n=3. Error bars represent standard error of the mean. Black bars represent control mice, blue bars represent KO-AL mice, red bars represent KO-PF mice. Statistical significance was determined using One-way ANOVA on each age group, and then performing Student's or Welch's t-test accordingly.

REFERENCES

1. Watanabe M HS, Mataki C, Christoffolete MA, Kim BW, Sato H, Messaddeq N, Harney JW, Ezaki O, Kodama T, Schoonjans K, Bianco AC, Auwerx J. Bile acids induce energy expenditure by promoting intracellular thyroid hormone activation. Nature. 2006;439(7075):484-9.

APPENDIX II: The Epigastric Depot as a Source of Brown Adipose Tissue in Humans

INTRODUCTION

2.1% of the pediatric population is morbidly obesity (body mass index >40kg/m^2) (1), and currently 17% of children 2-19 years of age are obese (2). With the increased pediatric and adolescent obesity rates, bariatric surgery is being implemented at an earlier age to yield dramatic improvements in metabolic health status (3). The current methods of bariatric surgery approved for use in the adolescent population are sleeve gastrectomy, adjustable gastric banding, and gastric bypass (4). As seen with the adult population, bariatric surgery in the adolescent patient population yields drastic metabolic improvements, including improvements in glucose homeostasis post-surgery (5).

Brown adipose tissue (BAT), once thought to be only relevant during infancy (as discussed in (6, 7)), is being investigated as a potential therapeutic target for obesity treatments. It is known that infants contain classical BAT (cBAT) in the interscapular region (8), yet adult BAT is thought to be more of the beige origin (9, 10), with exception to the deep neck and perirenal regions (10-13). Further complicating the field, brown and beige adipose tissue have been found to be co-expressed within white adipose tissue (WAT) depots (9). It has been reported that there are depots of beige/brown adipose tissue within the epigastric region (14), therefore we collaborated with Dr. Jeffery Zitsman at Columbia University (an adolescent bariatric surgeon), to investigate this depot in obese and lean patients undergoing surgery. Dr. Zitsman obtained adipose tissue samples from the epigastric region, a region widely accessible during laparoscopic

surgery, to determine 1) if BAT can be acquired in adolescent bariatric surgery patients in the epigastric region and 2) if BAT acquired from obese patients contain distorted mitochondrial structure and reduced thermogenic gene expression compared to lean individuals.

METHODS

Sample collection: Dr. Zitsman collected epigastric peritoneal adipose tissue, visceral adipose tissue, and falciform samples from obese patients undergoing bariatric surgery as well as lean patients undergoing appendectomy/cholecystectomies (Appendix Table 2.1). Samples were placed in either All Protect (Qiagen) for RNA analysis and stored in the -20°C freezer, Z-Fix overnight and embedded in paraffin for immunohistochemical (IHC) staining, or 4% paraformaldehyde (PFA) + gluteraldehyde for 4 hours, 4% PFA overnight, and transferred to .1M phosphate buffer for electron microscopy by the Horvath Lab at Yale University.

Gene expression analysis: First, we performed gene expression analysis on an array of markers of both white and brown adipose tissue; general BAT/beige markers include (15): *Ucp1, Dio2, Pgc1α, β3-AR and Fgf21*, white adipose tissue markers include: *Leptin,* and *Asc-1*. Other genes used to differentiate brown adipose tissue, white adipose tissue, and beige adipose tissue (cBAT: *Zic1, Prdm16*, *Cidea.* Beige; *Tmem26.* cBAT/beige; *Pat2, P2rx5*. WAT; *Hoxc9)* (15) were not consistently present via qPCR analysis, and therefore could not be used as a readout.

Immunohistochemical Analysis: Paraffin embedded sections were deparrifinized in xylene and rehydrated in ethanol. Antigen retrieval was performed using 10mM sodium

citrate (pH 6). Sections were blocked for endogenous peroxidase by hydrogen peroxide and blocked for non-specific staining using normal horse serum (NHS). Sections were stained with 1:1600 dilution of UCP1 (ab10983) in 5% NHS overnight. Sections were incubated in biotinylated secondary antibody. Samples were incubated in Vectastain ABC Reagent (Vector Laboratory). Samples were stained using 3, 3' Diaminobenzidine (DAB) (Vector Labs), and counterstained with hematoxylin blue.

RESULTS

It has recently been described that many identifiable BAT depots in humans are primarily made up of beige adipocytes (10), and that beige adipocytes are heterogeneous in population (9). We surveyed collected samples for markers of cBAT, beige, WAT, and general markers of BAT (see methods section). We found high variability between samples irrespective of the collected depot, and heterogeneity within the samples themselves in gene expression and protein levels, consistent with documented reports of the BAT found in humans (9).

Visceral adipose tissue

Although it is promising that we acquired markers for brown adipocytes in our epigastric samples, many visceral adipose tissue also displayed signatures of BAT. Of the 4 visceral samples from obese patients shown in Appendix Figure 2.1, 4 out of 4 samples were positive for *Leptin* and 1 sample was positive for BAT as shown by increased *Ucp1*. The gene expression array from the visceral adipose tissue acquired from the lean patient was positive for BAT, as indicated by elevated *Ucp1, Dio2, Ppargc1α, Fgf21,* and

negligible *Leptin* and *Asc-1* levels (Appendix Figure 2.2). In addition, falciform samples, a ligament found around the liver and collected as a negative control, was positive for UCP1 via immunohistochemistry (IHC) and was positive for *Ucp1* gene expression (Appendix Figure 2.3A, Appendix Table 2.2), indicating that the falciform sample was heterogeneous. Although the falciform from lean patient 1 was relatively negative in expression of brown and white adipose tissue by qPCR (Figure 2.3B), the sample stained positive for UCP1 on IHC (Appendix Table 2.3), further supporting the claim that samples are not uniform.

Epigastric adipose tissue

As hypothesized, the epigastric region does contained BAT positive tissue. As exemplified in Appendix Figure 2.4, most epigastric regions contained both *Ucp1* and *Leptin*, further exemplifying the heterogeneity of the depot. Of the samples shown, 2 out of 4 samples were positive for *Ucp1,* while 2 out of 4 samples were negative for *Ucp1* (Appendix Figure 2.4). Interestingly, one sample was negative for *Ucp1,* yet positive for the BAT marker *Ppargc1α* (Appendix Figure 2.4C). Additionally, 1 out of 4 of the epigastric samples was completely negative for BAT, and was positive for WAT. Occasionally, samples were collected from the same depot within an individual with a different approach to acquire the sample (anterior versus posterior approach). These samples were generally similar in gene analysis (Appendix Figure 2.5).

Infant adipose tissue

Within our sample population, some samples were infants. As described in the literature (12), the samples acquired from the infant population had the highest levels of UCP1 staining and multilocular lipid presence in the epigastric and visceral regions, indicative of cBAT (Appendix Figure 2.6). Although gene expression in the visceral fat of infant patient 1 was negative for *Ucp1* expression, IHC displayed increased UCP1 staining (Appendix Figure 2.6C,E)

Lap band removal

To determine whether epigastric adipose tissue after significant weight loss from an adjustable banding procedure induced increased BAT detection, we acquired epigastric and visceral samples from an individual undergoing band removal. Both visceral and epigastric samples were negligible for *Ucp1* and BAT markers (Appendix Figure 2.7).

Discrepancies in the data

Appendix tables 2.2 and 2.3 represent a population of samples that either resulted in good correlation between gene expression of BAT and IHC for UCP1, or poor correlation between the two. From our findings, gene expression and UCP1 staining did not consistently match within a given sample, exemplifying heterogeneity of the tissue samples. The inconsistencies found between gene expression and histological staining could be attributed to: 1) heterogeneity of the sample, thus splitting the sample in two for both histological and expression analysis does not result in two equal pieces of tissue, or

2) samples could have been two distinct samples acquired from the patient, but collect from the same general region.

Mitochondrial structure from adipose samples

To determine whether mitochondrial structure was distorted in the obese patients, we sent samples for electron microscopy (EM). From the EM data we hoped to A) identify mitochondria within the fat depots deemed as "brown fat", and B) determine whether mitochondria from obese subjects differ in structure compared to mitochondria from lean subjects. Unfortunately, we were unable to detect mitochondria in our samples, possibly due to the sample heterogeneity. As discussed previously, the samples acquired contain a mixed population of brown and white adipose tissue, contributing to the difficulty of finding mitochondria in a diluted environment.

DISCUSSION

From this small study, we have determined that it is possible to acquire BAT in the epigastric region in obese and lean adolescent individuals. Although we are able to acquire BAT, this is an area of heterogeneity and therefore it is difficult to only acquire BAT. Further sample analysis must be performed using reliable markers of beige, WAT and BAT, to determine the origin of fat recovered.

To determine whether obesity distorts mitochondrial structure in humans, a mitochondrial isolation/purification step should be performed on each sample prior to EM. This method will ensure that a population of BAT mitochondria is acquired for analysis. This data

will elucidate whether the mitochondria in obese patients are distorted compared to the mitochondria of lean patients, and if overall structure can predict success to surgery. Additionally, having the ability to follow patients out longitudinally and acquire samples during gastric banding, as well as during band removal, will elucidate whether mitochondrial structure can be fixed in these depots after weight loss in humans (as we have seen in rodent models). Although we did acquire tissue from one patient who received band removal, it is clear that we did not receive BAT positive tissue from this patient (Appendix Figure 2.7).

FUTURE DIRECTIONS

It is important to note that we used epigastric fat acquired from lean individuals undergoing laparoscopic appendectomy as a calibrator for the gene expression data. For future studies, it will be important to acquire a reliable calibrator for the gene expression. Additionally, more tissue samples from lean (control) subjects need to be acquired and analyzed. We found many promising samples that stained positive for UCP1, yet negative on qPCR. Future studies looking at the macrophage marker, CD68, will need to be performed to elucidate whether the UCP1 IHC is an indicator of non-specific staining of macrophages. Lastly, as mentioned above, future studies involving mitochondrial isolation must be performed to elucidate whether mitochondrial structure in brown adipose tissue in obese subjects morphologically differ from those of lean individuals.

FIGURES AND TABLES

Gender	Weight Status	Average Age	N	Average BMI	Notes
Male	Obese (Class II, III)	15	1	50.9	
Female	Obese (Class II, III)	16.6	11	45.75	
Male	Class I Obese	14	1	31.2	Collected initially as a control lean
Female	Overweight	22	1	29.8	Lap Band Removal
Male	Lean	17.5	1	20.4	
Female	Lean		0		
Child	Lean	6.5	2	N/A	
Male & Female Baby	N/A	26 days	2	N/A	

Appendix Table 2.1: Demographic of patient population. Only a representative sample of gene expression data are shown in graphs below.

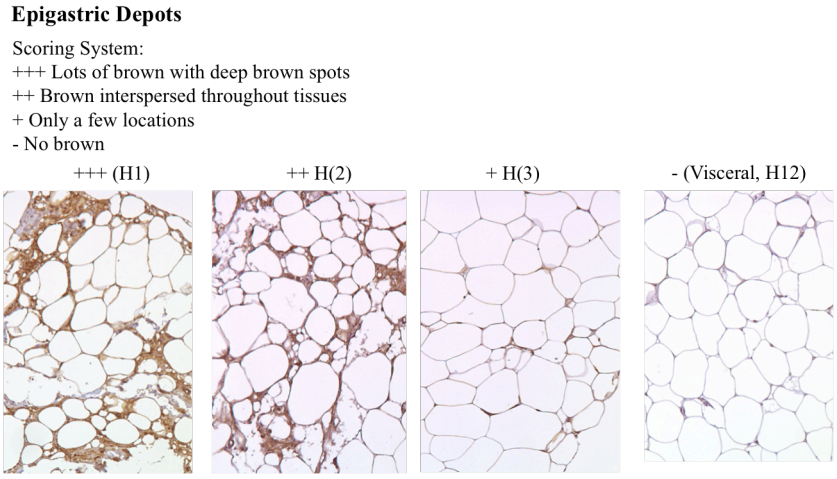

Scoring system for immunohistochemistry staining of epigastric adipose tissue, and negative control (visceral) tissue staining. Key was used to identify correlation between UCP1 staining and gene expression data within a given sample as identified in Appendix Table 2.2, 2.3.

Patient ID	Status	Location	Gender	Age (yr)	IHC	qPCR
Obese Patient 1; H1	Obese	Epigastric anterior approach	Male	15	+++	+++
Obese Patient 1; H2	Obese	Epigastric posterior approach	Male	15	+	++
Obese Patient 4; H17	Obese	Epigastric	Female	17	+	+
Obese Patient 6; H21	Obese	Epigastric	Female	15.1	++	+
Lean Patient 1; H7	Lean	Visceral	Male	17.5	++	+
Lean Child 1; H10	Lean	Epigastric	Male	8	+	+
Lean Child 1; H11	Lean	Falciform Ligament	Male	8	++	+

Appendix Table 2.2. Good correlation between gene expression and UCP1 IHC within samples. Samples from obese patients are represented in purple, samples from lean patients are represented in green.

Patient ID	Location	Status	Gender	Age (yr)	IHC	qPCR
Obese Patient 2; H4	Epigastric anterior approach	Obese	Female	16.9	+++	+
Obese Patient 3; H13	Epigastric	Obese	Female	17.5	++	Neg
Obese Patient 3; H14	Falciform Ligament	Obese	Female	17.5	Neg	++
Obese Patient 5; H20	Visceral	Obese	Female	15.6	+++	Neg
Lean Patient 1; H5	Falciform	Lean	Male	17.5	++	Neg
Lean Child 2; H15	Epigastric	Lean	Male	5	+	Neg

Appendix Table 2.3. Poor correlation between gene expression and UCP1 IHC within samples. Samples from obese patients are represented in purple, samples from lean patients are represented in green.

FIGURES

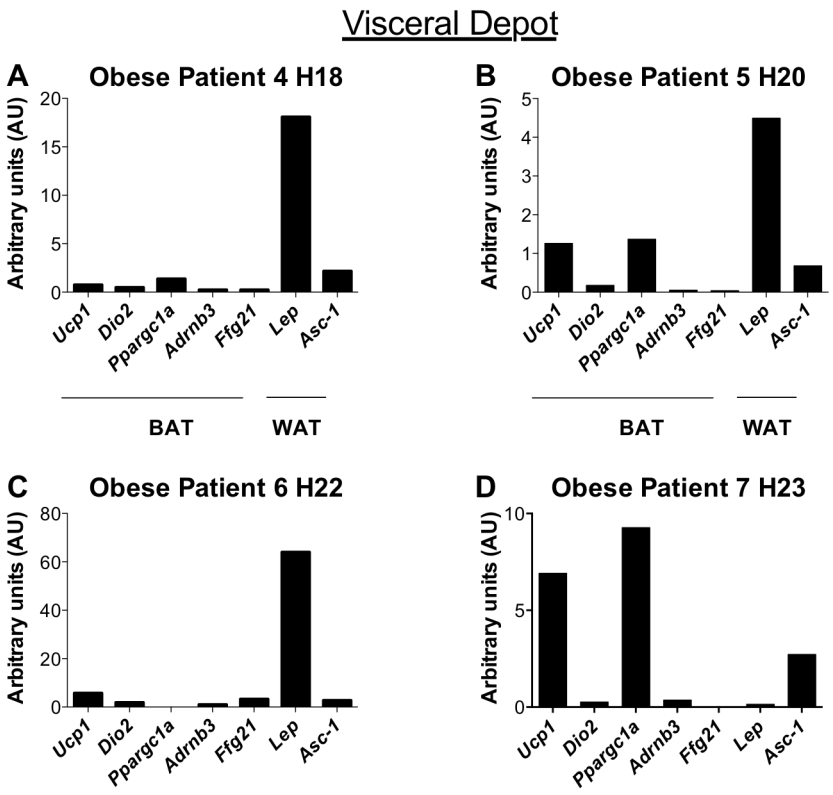

Appendix Figure 2.1. Gene expression analysis of visceral adipose tissue from obese patients. Relative expression was normalized to the epigastric sample of the lean patient.

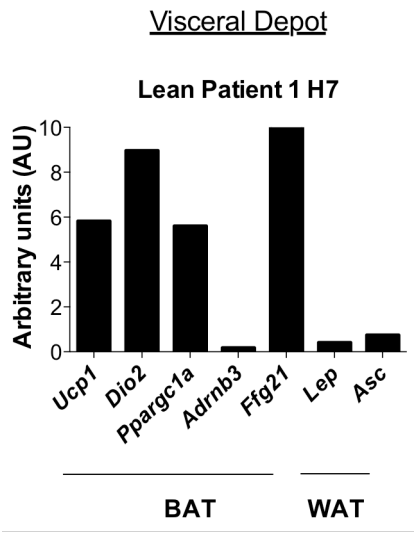

Appendix Figure 2.2: Gene expression analysis of visceral adipose tissue from a lean patient. Relative gene expression was normalized to the epigastric sample of the lean patient.

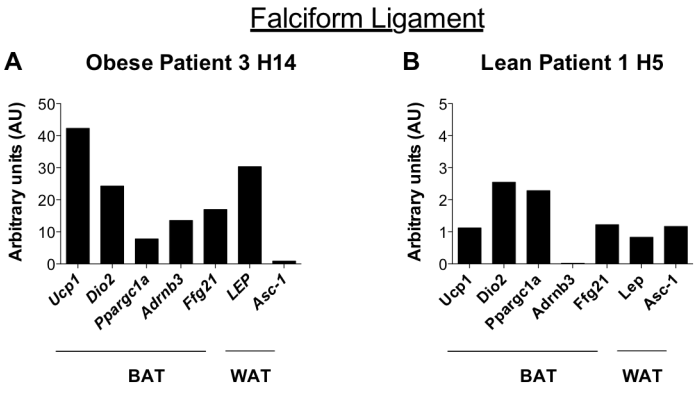

Appendix Figure 2.3. Gene expression analysis of the falciform ligament from both an obese and lean patient. Relative expression was normalized to epigastric sample of the lean patient.

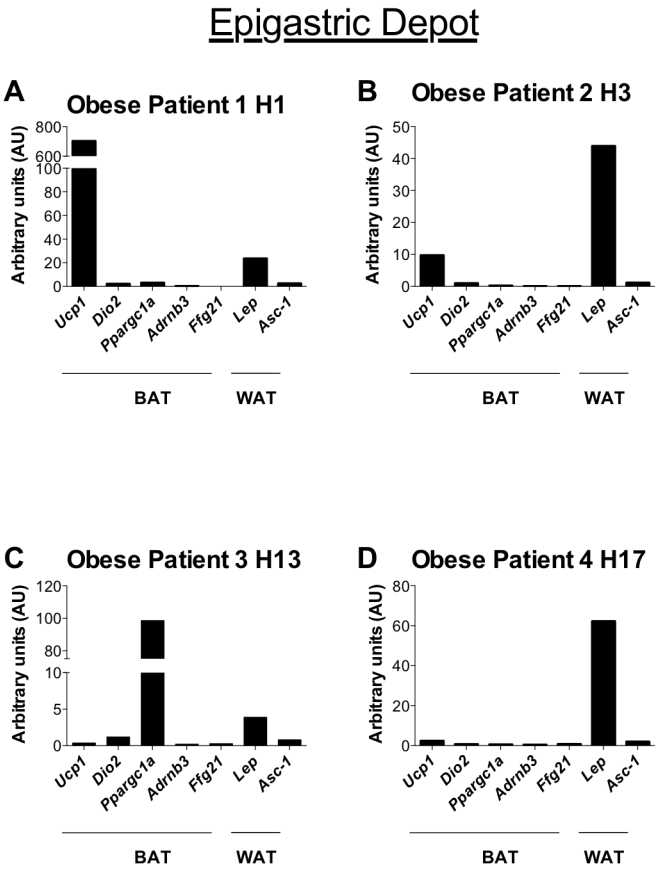

Appendix Figure 2.4. Gene expression analysis of the epigastric depot from obese patients. Relative expression was normalized to the epigastric sample of the lean patient.

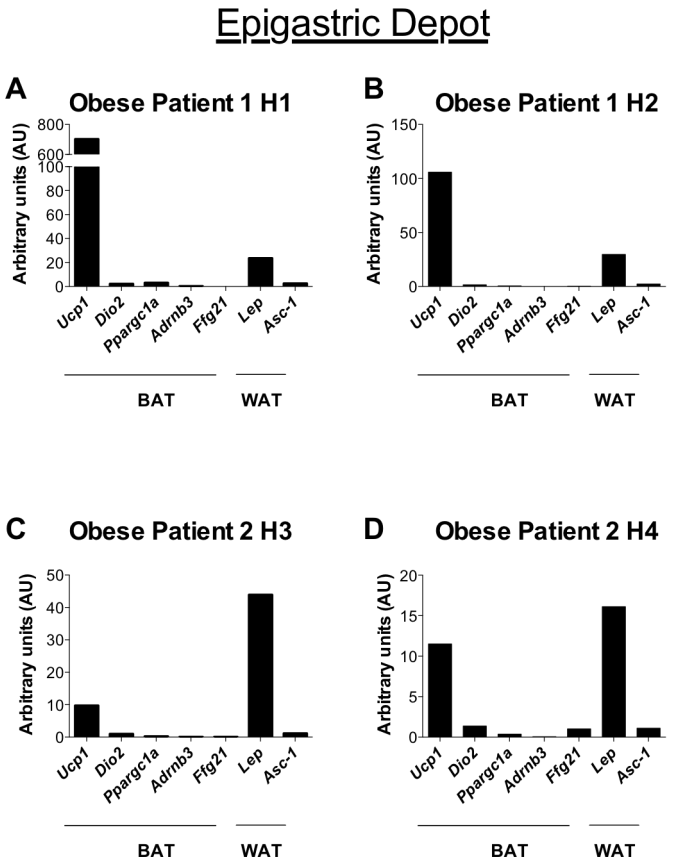

Appendix Figure 2.5. Intra-patient variation in gene expression analysis of epigastric tissue. (A,B) Epigastric depot acquired from obese patient 1. (A) Sample acquired from the anterior approach, (B) sample acquired from the posterior approach. (C,D) Epigastric depot acquired from obese patient 2. (C) Sample acquired from the posterior approach, (D) sample acquired from the anterior approach. Relative expression was normalized to epigastric sample of the lean patient.

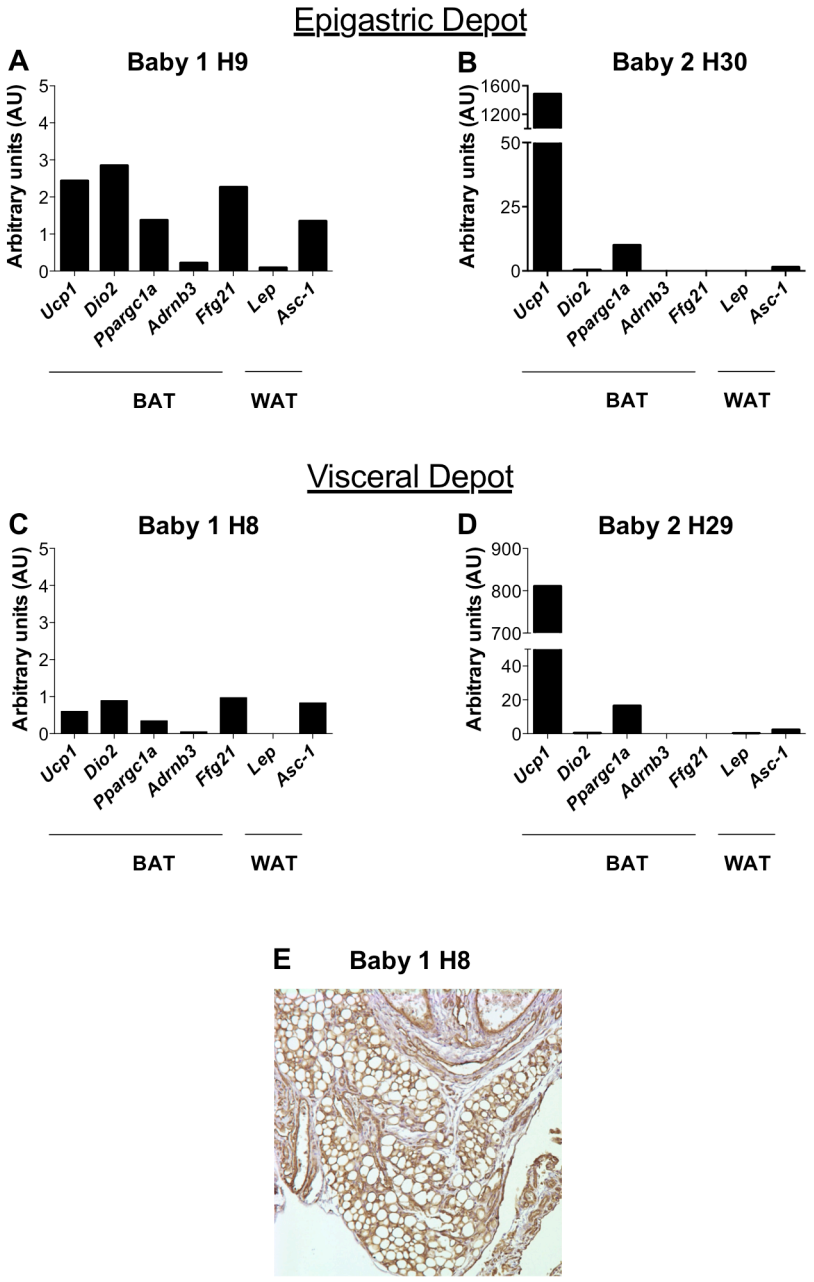

Appendix Figure 2.6. Gene expression analysis of the adipose depots from infants. (A,B) Epigastric gene expression data. (C,D) Visceral gene expression data. (E) UCP1 IHC staining in visceral adipose tissue. Relative expression was normalized to epigastric sample of the lean patient.

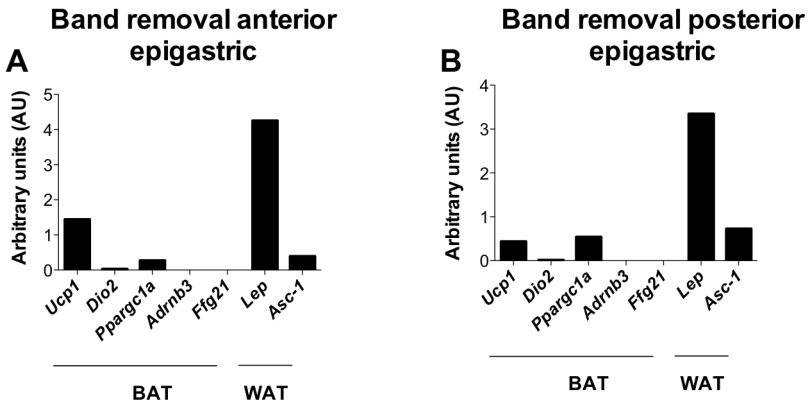

Appendix Figure 2.7. Gene expression from epigastric adipose depot after laparoscopic band removal. Relative expression was normalized to epigastric sample of the lean patient.

REFERENCES

1. Skinner AC, Skelton JA. Prevalence and trends in obesity and severe obesity among children in the United States, 1999-2012. JAMA Pediatr. 2014;168(6):561-6.

2. Ogden CL, Carroll MD, Kit BK, Flegal KM. Prevalence of childhood and adult obesity in the United States, 2011-2012. JAMA. 2014;311(8):806-14.

3. Michalsky M, Kramer RE, Fullmer MA, Polfuss M, Porter R, Ward-Begnoche W, et al. Developing criteria for pediatric/adolescent bariatric surgery programs. Pediatrics. 2011;128(Suppl 2):S65-S70.

4. Inge TH, Zeller MH, Lawson ML, Daniels SR. A critical appraisal of evidence supporting a bariatric surgical approach to weight management for adolescents. J Pediatr. 2005;147(1):10-9.

5. Inge TH, Prigeon RL, Elder DA, Jenkins TM, Cohen RM, Xanthakos SA, et al. Insulin Sensitivity and β-Cell Function Improve after Gastric Bypass in Severely Obese Adolescents. J Pediatr. 2015;167(5):1042-8.

6. Virtanen KA, Lidell ME, Orava J, Heglind M, Westergren R, Niemi T, et al. Functional brown adipose tissue in healthy adults. New England Journal of Medicine. 2009;360(15):1518-25.

7. Yeung HW, Grewal RK, Gonen M, Schöder H, Larson SM. Patterns of (18)F-FDG uptake in adipose tissue and muscle: a potential source of false-positives for PET. J Nucl Med. 2003;44(11):1789-96.

8. Lidell ME, Betz MJ, Dahlqvist Leinhard O, Heglind M, Elander L, Slawik M, et al. Evidence for two types of brown adipose tissue in humans. Nat Med. 2013;19(5):631-4.

9. Sidossis L, Kajimura S. Brown and beige fat in humans: thermogenic adipocytes that control energy and glucose homeostasis. J Clin Invest. 2015;125(2):478-86.

10. Sharp LZ, Shinoda K, Ohno H, Scheel DW, Tomoda E, Ruiz L, et al. Human BAT possesses molecular signatures that resemble beige/brite cells. PLoS One [Internet]. 2012; 7(11):[e49452 p.].

11. Svensson PA, Lindberg K, Hoffmann JM, Taube M, Pereira MJ, Mohsen-Kanson T, et al. Characterization of brown adipose tissue in the human perirenal depot. Obesity (Silver Spring). 2014;22(8):1830-7.

12. Tanuma Y, Tamamoto M, Ito T, Yokochi C. The occurrence of brown adipose tissue in perirenal fat in Japanese. Arch Histol Jpn. 1975;38(1):43-70.

13. Cypess AM, White AP, Vernochet C, Schulz TJ, Xue R, Sass CA, et al. Anatomical localization, gene expression profiling and functional characterization of adult human neck brown fat. Nat Med. 2013;19(5):635-9.

14. Heaton JM. The distribution of brown adipose tissue in the human. J Anat. 1972;112(Pt 1):35-9.

15. Ussar S, Lee KY, Dankel SN, Boucher J, Haering MF, Kleinridders A, et al. ASC-1, PAT2, and P2RX5 are cell surface markers for white, beige, and brown adipocytes. Sci Transl Med. 2014;6(247):PMCID: PMC4356008.